MASS SPECTROMETRIC ASSAYS OF BIOMOLECULAR INTERACTIONS

APPLICATION OF MAGNETIC "FISHING" AND MASS SPECTROMETRY FOR FUNCTION-BASED ASSAYS OF BIOMOLECULAR INTERACTIONS

by

MEGHAN J. McFADDEN, H.B.Sc., M.S.

A Thesis Submitted to the School of Graduate Studies in Partial Fulfillment of the

Requirements for the Degree Doctor of Philosophy

McMaster University
Hamilton, Ontario

DOCTOR OF PHILOSOPHY (2013)

Chemical Biology

TITLE: Application of Magnetic "Fishing" and Mass Spectrometry for Function-based Assays of Biomolecular Interactions

AUTHOR: Meghan J. McFadden, H.B.Sc. (Toronto), M.S. (John Jay College, CUNY)

SUPERVISORS: John D. Brennan
Murray S. Junop

NUMBER OF PAGES: x, 129

Abstract

The human interactome presents a goldmine of potentially powerful therapeutic targets, yet very few small molecule modulators of protein-protein interactions (PPI) have been identified. PPI pose a particular challenge for drug discovery, and one of the major obstacles to fully exploiting these interactions is a lack of appropriate technologies to screen for modulating compounds. This thesis aims to address the need for function-based approaches that target PPI by using magnetic beads (MB) and mass spectrometry (MS) to develop efficient assays to monitor these interactions and their modulation by small molecules. The work begins with the validation of a novel magnetic "fishing" assay, which uses affinity-capture MB to isolate intact complexes of a "bait" protein from solution. By monitoring the recovery of the secondary binding partner, this assay was used to functionally screen a library of 1000 compounds for small molecule modulators of a calmodulin/melittin (CaM/Mel) model system. The versatility of magnetic "fishing" is clearly demonstrated during a study of a more relevant CaM-based system, which uncovered a novel mode of interaction for the CaM-binding domain of transcription factor SOX9. In addition to the MB-based approach, a simple MS-based competitive displacement assay is developed to identify minimal inhibitory fragments of a target complex as indicators of potential 'hot-spots'. The assay was used to probe a DNA repair complex of XRCC4/ligaseIV, and identified a short helix that can be used as a more defined target surface for future high-throughput screening and rational drug design. The functional MS-based assays herein are highly adaptable tools to monitor PPI, and will facilitate the study of these and other important biomolecular interactions.

Acknowledgements

I would like to thank my supervisors, Dr. John Brennan and Dr. Murray Junop, for their support and guidance during the course of my studies. Murray, your eternal optimism and philosophies on life are inspiring, and I thank you for your unwavering confidence in my abilities through the many ups and downs of research.

I would also like to thank all the present and past group members that have made my time at McMaster fun, even during the most frustrating of times. To Julie, Anne Marie, and Clemence, our time together in the lab was short-lived but our friendships will last a lifetime.

I am forever grateful to my family for their love and patience throughout my entire academic career. Erin, thank you for being my biggest fan, and I am so proud to have you as a sister and as a friend. Thomas, we have come a long way and it means the world to me to have your love and support. I thank my dad for always being there when I need him and for being a consistent source of strength in my life. Mom, your endless support made this thesis possible, and I thank you for giving so much of yourself to help me reach my goals. You are an amazing person and role model, and I would not be where I am without you.

Finally, I want to thank my *Superman* for his unconditional love and support. This thesis brought you in to my life, and for that I am truly grateful.

"Live as if you were to die tomorrow.
Learn as if you were to live forever."
– Mahatma Gandhi

TABLE OF CONTENTS

List of Figures and Tables

List of Abbreviations

ALIS	automated ligand identification system
AS-MS	affinity selection-mass spectrometry
APTES	(3-aminopropyl)-triethoxysilane
Bh	β-hairpin
BRCT	BRCA1 [breast cancer associated 1] C terminal domain
BSA	bovine serum albumin
C4ST	chondroitin 4-sulfotransferase
ca.	circa
CaM	calmodulin
CBG	CSPG biosynthetic gene
CNS	central nervous system
CPZ	chlorpromazine
CSPGs	chondroitin sulfate proteoglycans
DMSO	dimethyl sulfoxide
DNA	deoxyribonucleic acid
DNA-PK	DNA-dependent protein kinase
DSB	double stranded breaks
EC_{50}	half maximal effective concentration
ESI-MS/MS	electrospray ionization tandem mass spectrometry
FAC-MS	frontal-affinity chromatography-mass spectrometry
FPZ	fluphenazine
FRET	fluorescence resonance energy transfer
H1	helix 1
H2	helix 2
His_6	hexahistidine tag
HLH	helix-loop-helix
HMG box	high mobility group box
HPLC	high pressure liquid chromatography
HR	homologous recombination
HTS	high-throughput screening
IC_{50}	half maximal inhibitory concentration
K_D	dissociation constant
K_I	dissociation inhibitory constant
L	loop
LigIV	DNA ligase IV
LC	liquid chromatography
MB	magnetic beads
Mel	melittin
MS	mass spectrometry
NHEJ	non-homologous end joining
NLS	nuclear localization sequence

NMR	nuclear magnetic resonance
Ni-NTA	nickel-charged nitrilotriacetic acid
PBS	phosphate buffered saline
PDB	protein databank
PMMA	poly(methyl methacrylate)
PPI	protein-protein interaction
R24571	calmidazolium (compound R24571)
RNA	ribonucleic acid
SCI	spinal cord injury
SD	standard deviation
SOX	SRY-related HMG box protein
SOX-CAL	calmodulin binding domain of SOX9
SPR	surface plasmon resonance
SRY	sex-determining region Y protein
TFP	trifluoperazine
TOF	time-of-flight mass analyzer
Tris	tris(hydroxymethyl)aminomethane
v/v	volume to volume ratio
XIR	XRCC4-interacting region
XRCC4	X-ray cross-complementing protein 4
XT-I	xylosyltransferase-I
XT-II	xylosyltransferase-II

Chapter One: Introduction

1.1 Thesis Overview and Goals

Proteins are essential components of a cell, and while some function independently, the majority participate in intricate interaction networks. Protein-protein interactions (PPI) regulate activity, movement, production, and destruction of biomolecules, and are involved in most, if not all, biological pathways including signaling, genetic expression and maintenance, metabolism, immune response, and programmed cell death.[1-7] As a consequence, abnormal interactions underlie many of the cellular malfunctions that are linked to diseases, and PPI have emerged as desirable drug targets for modulation by small molecules.[8-14]

The human protein interactome has proven to be especially challenging for drug discovery and development, and less than 0.01% of the estimated 650,000 PPI have been targeted with small molecule modulators.[11, 15] Unlike enzymes that have well-defined binding pockets and natural occurring ligands that can act as templates for potential drug candidates, PPI contain large flat interfaces that make difficult targets for rational drug design and inhibitor screening.[10-14] Researchers have discovered the existence of 'hot spots' within interfaces that contribute essential amino acid residues for PPI,[16, 17] and although these smaller regions provide better targets for screening to identify modulators, there remains a lack of technologies with which to screen such interactions. One of the major obstacles preventing full exploitation of PPI as drug targets is a deficiency in appropriate assays to monitor these interactions and efficiently screen small molecule libraries for lead compounds.[8-12] A review of current modulators of PPI has revealed that

these compounds deviate from the typical "rule-of-five" that describes orally available drug-like molecules,[18-21] exacerbating the need for high-throughput screening (HTS) approaches that would allow exploration of a greater amount of chemical space. Novel assays that are specifically designed to monitor PPI are therefore needed to take full advantage of these valuable drug targets and to gain access to a powerful new generation of therapeutics.

The present research aims to develop assays to assist the discovery of bioactive compounds that modulate PPI by using magnetic separation and mass spectrometry (MS) to develop function-based assays targeting these important interactions. The first goal of this thesis is to design a magnetic "fishing" assay to monitor formation of protein complexes in solution, and using the calmodulin/melittin (CaM/Mel) model system, validate this assay as a high-throughput approach to screen small molecule mixtures for modulators of PPI. MS is an established tool for the study of proteins and their interactions, and therefore this work focuses on demonstrating the utility of magnetic beads (MB) as an HTS platform and an efficient alternative to traditional methods of analytical separation. The novel magnetic "fishing" assay is then extended to the more therapeutically relevant interaction between CaM and transcription factor SOX9. Given that initial assay development used a CaM model system, magnetic "fishing" is presented as a simple method to characterize CaM/SOX9 and its modulation by small molecules. The goal is to quantify the binding affinity of CaM and the CaM-binding domain of SOX9 (SOX-CAL), and to determine inhibitory constants for known antagonists that are under investigation as therapeutic leads for the treatment of spinal cord injury (SCI). The

second phase of this thesis shifts focus from identifying small molecule modulators of PPI to identifying vulnerable 'hot-spots' within the interface of especially challenging protein complexes. The final goal is to use MS in a simple competitive displacement assay to probe disruption of X-ray cross complimenting protein 4/XRCC4-interacting region of ligase IV (XRCC4/XIR) by a series of ligase IV (LigIV) peptide fragments. The minimal LigIV fragment that displaces its XIR from a complex with XRCC4 may indicate potential 'hot spots' within the interface of this high-affinity PPI, which can then be used to better guide future inhibitor screens to identify modulators as potential leads for anti-cancer pharmaceuticals. The collective findings of this research are intended to expand the use of MS into the realm of function-based assays of PPI, and satisfy a general need for efficient techniques to monitor modulation of these interactions.

1.2 Current Approaches to Identify Modulators of Protein-Protein Interactions

Many of the current small molecule modulators against PPI have been found using affinity-based methods that identify ligands that bind to one of the target proteins.[8-10, 13] Affinity-based screening has become a fundamental part of early drug discovery, yet it is inherently inefficient and requires additional rounds of testing to assess bioactivity. Inhibitor screening on the basis of affinity, while widely successful for enzymes, has an especially low success rate for PPI.[9, 22] The disproportionate size of a small molecule compared to a large flat interface means that ligand binding is often nonspecific or insufficient to disrupt the association of two proteins. Compounds that both bind to and modulate protein behaviour have increased value as therapeutic leads, and function-based

assays are not only more efficient, but also the most promising strategy for HTS to identify modulators of PPI.[14, 23]

A great deal of research has been dedicated to identifying novel protein-based interactions and a few of these methods have been successfully converted into screening approaches to identify modulators of PPI (Table 1.1). For example, *ex vivo* techniques designed to detect protein binding within cells, such as two-hybrid systems[24-29] and protein fragment complementation assays,[30-34] have been adapted for screening small molecule libraries against a target interaction. The advantages of cell-based methods for assessing permeability and toxicity are offset by the disadvantages of excluding valuable lead compounds that could be modified and optimized into potent modulators. The dense intracellular matrix contains a great number of interferences, and there is potential for false negatives due to compounds that may bind with higher-affinity to other proteins present in the cell. In addition, two-hybrid systems require nuclear import of fusion proteins, which can also lead to false negatives when using these approaches.[31] Fortunately, most disadvantages of cell-based assays can be overcome by using a more controlled environment, which is an inherent benefit of *in vitro* HTS methods.

Similar to *ex vivo* screens, current *in vitro* methods to identify small molecule modulators of PPI are typically derived from existing approaches used to study protein-based interactions, including surface plasmon resonance (SPR),[35-38] nuclear magnetic resonance (NMR),[39, 40] and most commonly, fluorescence polarization[41-46] or energy transfer (FRET or AlphaScreen®)[47-52] (Table 1.1). Fluorescence-based assays are popular

Table 1.1: Current screening approaches for modulators of protein-protein interactions

Assay Type	Principle	Advantages	Disadvantages
Cell-based			
Protein Fragment Complementation[31]	Fragments of reporter molecule (i.e. luciferase, GFP) are fused to each target protein. PPI results in complementation of reporter to produce signal	Cellular environment Assessment of permeability and toxicity	Interferences from cellular components or fusion of fragment False signal from self-association of reporter
Two-Hybrid System[24, 26]	Each target protein is fused to either the activation or binding domain of a transcription factor. PPI restores transcriptional activity resulting in expression of reporter gene	Cellular environment Assessment of Permeability and toxicity	Interferences from cellular components or fusion of fragment Requires nuclear import of fusion proteins
In Vitro			
Fluorescence Polarization[23, 45]	Uses plane polarized light to monitor the rotation of biomolecules. PPI is indicated by a slower rate of rotation for the complex relative to that for unbound protein	Low cost, simple Sensitive Homogeneous Easily automated	Label required on one target Spectral interferences Anomalous polarization from aggregates
FRET[23, 50]	Each target protein is labeled with either donor or acceptor fluorophore. PPI brings the fluorophores in proximity such that emission from donor will excite acceptor, or acceptor will quench donor	Low cost, simple Sensitive Homogeneous Easily automated	Label required on both targets Spectral interferences from compounds Donor-acceptor pair must be 10-100 Å apart
AlphaScreen®[23, 51]	Each target protein is captured onto either donor or acceptor beads. Donor beads are photosensitive and produce excited singlet oxygen. PPI brings beads in proximity allowing diffusion of singlet oxygen to the acceptor, which stimulates emission of a fluorescent signal	Sensitive No wash steps required Easily automated Efficient energy transfer across relatively large distance (~200 nm)	Expensive Light sensitive Temperature sensitive Requires special instrumentation for high- energy donor excitation
NMR[8, 23]	Magnetic properties of nuclei depend on their molecular environment. PPI alter the environment around nuclei of N-H or C-H bonds, producing observable chemical shifts	Label-free (ligand monitoring) Applicable to weak PPI ($K_D < 10$ mM)	Requires isotopic label for protein monitoring High concentrations of protein (1-500 μM) Moderate throughput
SPR[8, 23]	When polarized light irradiates a gold surface, intensity of reflected light is proportional to mass of immobilized protein. PPI alter the angle at which minimal reflectance occurs	Label-free Sensitive Real-time monitoring Multiplexing	Requires immobilization of one target onto gold surface Moderate throughput

choices for HTS because they offer highly sensitive detection and are easily automated; however, labeling of one or both proteins with a fluorophore can be tedious and risks interfering with proper folding or subsequent interactions. There are additional concerns regarding spectral interferences from test compounds, although this is mostly avoided by the use of fluorophores with longer absorption and emission wavelengths within the visible spectrum. SPR provides sensitive and label-free monitoring of PPI in real-time but requires immobilization of one of the targets onto a gold surface, which can interfere with protein conformation and activity. A label is not required for NMR spectroscopy when used for ligand monitoring, though approaches designed for target detection requires high concentrations of isotopically labeled protein.[8] Both SPR and NMR experiments can provide additional information regarding kinetics and binding site identification, respectively, however throughput of these approaches are lower relative to fluorescent-based affinity screens.[8]

A general approach to enhance any HTS platform is to pool several test compounds together into small molecule mixtures. Although secondary screening of active mixtures is typically required to isolate lead compounds from the many inactive ones, the ability to assess multiple small molecules simultaneously in a single assay greatly reduces the time and reagents needed to evaluate a large amount of chemical space. As a result, the overall gain in throughput and efficiency have made mixture screening a practical and necessary part of HTS.[53]

A great deal can be learned from the above-mentioned methods that target PPI, and development of novel assays should include their advantages and improve on their

many disadvantages. Given the difficulty of identifying modulators of PPI, the desire to produce lead compounds, even those that may be initially cell impermeable or toxic, favours using an *in vitro* approach. The ideal assay platform should provide the same sensitivity and efficiency of fluorescence spectroscopy while employing label-free detection similar to SPR and NMR. Furthermore, a valuable opportunity exists to add to the benefits of mixture screening by building in a method of mixture deconvolution in order to avoid costly secondary screening to isolate active compounds. The combination of these characteristics into a function-based *in vitro* assay to monitor PPI, and its development into an efficient HTS platform, would make a significant step forward to surmounting the technological obstacle that hinders full exploration of these elusive drug targets.

1.3 Mass Spectrometry for High-Throughput Screening

Mass spectrometry (MS) is established as one of the most diverse tools for the study of proteins and their interactions,[54-64] and has become indispensible for almost all stages of drug discovery.[65] MS-based assays have numerous advantages for development of HTS platforms, including selective and universal detection of proteins and test compounds, automation, and compatibility to run in-line with many other analytical technologies. The reliance of HTS on small molecule mixtures emphasizes the importance of this latter advantage, where coupling of MS to analytical separation technologies provides an elegant strategy for mixture deconvolution by isolating protein-bound compounds for identification by molecular weight.[66] This general approach, called

affinity-selection mass spectrometry (AS-MS),[67, 68] involves incubation of a target protein with a mixture of compounds in solution, followed by rapid separation of protein-ligand complexes by generic size-exclusion media through centrifugation,[69] ultrafiltration,[70-72] or high-pressure LC (Automated Ligand Identification System, ALIS),[66, 73] The isolated complex is then dissociated to release free ligand for identification by MS. An important advantage of these AS-MS approaches over solid-phase affinity-based assays, such as frontal-affinity chromatography (FAC-MS), is that binding reactions are carried out using free protein. In contrast, FAC-MS uses immobilized protein in a column to capture ligands out of a continuous infusion of small molecules, where affinity is indicated by delayed elution of that compound relative to a void marker.[74-77] Immobilization of a target can interfere with its native conformation and its ability to interact with other biomolecules, which is not a concern for solution-based assays. Furthermore, FAC-MS requires distinct MS signals for each compound in order to monitor its rate of elution, which limits the complexity of mixtures that can be screened.

The popularity of MS for affinity-based HTS highlights its many advantages, however there are two key areas for improvement to consider when developing new assays targeting PPI. The first improvement would be to design activity-based assays that directly monitor formation or disruption of protein complexes in the presence of test compounds. As previously discussed, affinity-based selection has a low rate of success for identifying modulators of PPI, thus assessing dual affinity and function is a more promising approach for drug discovery.[9, 14, 22, 23] AS-MS methods provide an efficient model for affinity capture of ligands and mixture deconvolution, however the addition of

the second protein binding partner prior to separation would incorporate a reporter molecule for monitoring activity of these ligands against the target PPI. Following dissociation of isolated protein complexes, the presence of a small molecule would indicate affinity of a compound for the target, but changes in the amount of the secondary protein would indicate its activity. MS is inherently suited for this purpose, and allows sensitive and selective detection of both proteins and small molecules simultaneously.

The second opportunity to improve on existing MS-based HTS is the choice of technology for analytical separation. LC currently dominates the field of MS, owing to its seamless integration into ionization sources and a diverse selection of columns that can be used in tandem to achieve separation and sample enrichment. MS-compatible solvents are rarely optimal for bioassays, thus approaches using size-exclusion chromatography or filtration are most often still coupled to LC/MS systems to remove buffer components (i.e. salts, detergents, blocking agents) and to concentrate samples prior to analyses. Additional chromatography steps for purification and concentration are time-consuming, and the need for continuous solvent flow remains a major drawback of LC. Separations using centrifugation have the advantage of providing sample enrichment, however these methods are difficult to automate, even in the microwell plate format. An alternative to LC, filtration, and centrifugation is the magnetic bead (MB) platform, which has gained recent popularity for analytical separations.[78-80] Magnetic separation is a multifaceted approach allowing ligand capture, isolation, and sample enrichment, while using a platform that is scalable, automatable, and one that functions independent of solvent flow. The combination of MB and MS would provide the desired characteristics for the

development of an efficient function-based assay to probe PPI and their modulation by small molecules.

1.4 The Magnetic Bead Platform

Functionalized microparticles (beads) have been used for many decades as a solid support for a wide range of medical, biochemical, and analytical applications.[81, 82] In contrast to a flat surface, a small spherical bead presents a greater surface area for target immobilization, thus maximizing sensitivity and resolution of analytical separations. This advantage is reflected in the frequent use of beads as media in modern LC columns, however the need for large solvent volumes and time-consuming protocols remain major disadvantages. Dispersion of beads in solution, rather than packed within a column, provides even greater accessibility to the particle surface for high-density immobilization, and allows direct evaluation of viscous samples that would normally clog chromatography systems. Isolation of polymer beads from solution requires centrifugation or filtration, leading to the development of microparticles containing a magnetic core. These magnetic beads (MB) are a convenient alternative, allowing an applied magnetic field to be used to simultaneously manipulate, isolate, and concentrate captured analytes. The multiple advantages of magnetic separation have inspired the design of MB-based approaches for rapid sensing, purification, and quantification of biomolecules in both scientific and clinical applications.[78-80, 82-88]

The benefits of magnetic separation for isolating proteins from complex mixtures are evident from the growing popularity of MB-based approaches to facilitate the study

of biomolecular interactions. Similar to chromatographic media, the MB surface can be functionalized for covalent linkage or affinity-capture of targets, and assays based on similar principles as LC/MS have been used for protein profiling[89-94] and to develop protein interaction networks.[95, 96] A notable feature of these MB-based assays is that, unlike LC/MS methods, beads can be added to impure cell lysates permitting direct analysis of biological samples. Following from the success of magnetic separations for identification of novel therapeutic targets, a potential role for MB as an HTS platform for lead identification has also been investigated. In what are referred to as magnetic "fishing" experiments (Figure 1.1), a target protein is presented on the MB surface as "bait" to screen for novel protein-ligand interactions within small molecule mixtures[97-100] or directly from plant extracts.[101-105] The utility of magnetic separations for recovery of protein-protein and protein-ligand complexes has been clearly demonstrated, although the combination of "protein fishing" and "ligand fishing" into a single assay has not yet been explored as the foundation for efficient function-based HTS for modulators of PPI.

As is the case with most affinity-based approaches, nonspecific binding is a persistent and universal problem for assays using the MB platform. This issue is likely the result of hydrophobic interactions with polymer coatings on bead surfaces, and a critical part of assay development to reduce nonspecific binding is optimization of MB volume and incubation time. Prior to elution, vigorous wash steps are essential to remove nonspecific contaminants, which are common elements of all bead-based approaches. Optimized binding reactions and washing are adequate to overcome nonspecific

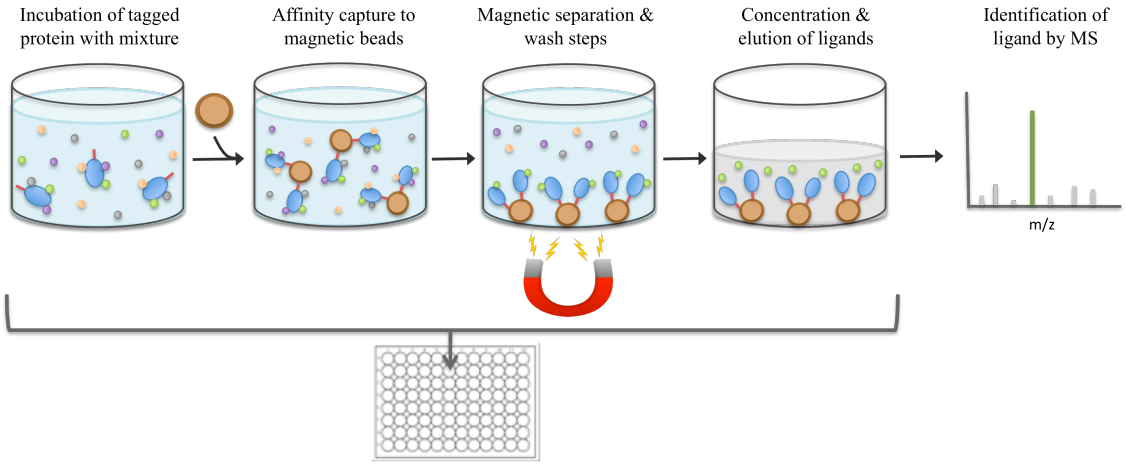

Figure 1.1: Magnetic "fishing" for protein-ligand interactions

interactions for qualitative applications, but the problem continues to limit the use of MB for quantitative studies. Development of MB into a reliable analytical platform requires further improvements in specificity to allow accurate and precise measurement of the amount of analyte bound to the immobilized target and not to the bead. Despite the difficulties associated with absolute quantification, MB remain an efficient way to assess relative amounts of analytes by careful comparison to control samples used to differentiate specific from nonspecific interactions.

1.5 Model Protein-Protein Interactions

Calmodulin/Melittin: A Classic Model System for Protein-Protein Interactions

Development and validation of a novel assay platform requires a well-characterized protein complex, and calmodulin/melittin (CaM/Mel) is among the most widely used PPI model systems.[106-111] CaM is a ubiquitous calcium-binding protein that regulates a variety of cellular pathways in eukaryotes, and Mel is a small 26-residue

peptide found in bee venom. In the presence of calcium, CaM undergoes a conformational change to bind a single molecule of Mel forming a high-affinity complex (K_d = 3 nM).[112-115] Several CaM antagonists of varying affinities have been identified, including chlorpromazine (CPZ, K_I = 5 μM)[116], trifluoperazine (TFP, K_I = 1-8 μM)[117-119], and the potent inhibitor, calmidazolium (R24571, K_I = 2-3 nM)[118].

In addition to its extensively studied behaviour, the CaM/Mel complex has other characteristics that make it an ideal model system for assay development. Intact Mel (2.8 kDa) is an appropriate size for direct analysis in low mass-range MS systems, and the signal for the peptide can therefore be used to monitor the interaction without the need for a secondary reporter ligand. To isolate the complex from solution, human recombinant CaM is commercially available with a N-terminal hexahistidine (His_6) tag for affinity capture to Ni^{2+}-charged MB. Lastly, a single tryptophan residue in Mel, and its absence in CaM, allow intrinsic fluorescence to be used as a secondary method to monitor and validate the interaction.[115, 120-122] The structural and spectroscopic properties of the CaM/Mel complex further increase its value as a model system, and made it an ideal choice for development of functional MB-based assays to monitor PPI.

Calmodulin/SOX9: Calcium-Mediated Nuclear Import of Transcription Factor SOX9

The CaM/Mel model system has many advantages for assay validation, but has limited physiological significance. To extend our work to a system that has a greater impact, we investigated the interaction between CaM and transcription factor SOX9. Recent studies using gene manipulation as a treatment strategy to improve neurological

function following spinal cord injury (SCI) have identified a group of regeneration-inhibiting genes that are collectively regulated by SOX9.[123, 124] Ablation of SOX9 in mice models has been shown to lead to improved motor performance after SCI[125]. Expressed in the cytosol, SOX9 enters the nucleus through interaction with CaM in a calcium-mediated nuclear import pathway, and known CaM antagonists are able to inhibit its transcriptional activity.[126] Key questions remain relating to the effect of disrupting the CaM/SOX9 interaction on SCI gene expression, and the potential use of anti-CaM compounds as therapeutics to enhance neural regeneration.

To study the CaM/SOX9 interaction, a peptide was synthesized corresponding to the CaM-binding domain of SOX9 (SOX-CAL). The SOX-CAL peptide is structurally similar to Mel, and contains a high number of hydrophobic residues and groupings of positively charged residues that are common features of CaM-binding domains.[127-130] Including a single tryptophan residue and small size (2.1 kDa), SOX-CAL shares in the many advantages of Mel for both MS and fluorescence-based studies. As a result, the magnetic "fishing" assay was determined to be an efficient approach to quantify the binding affinity of CaM/SOX-CAL, and to assess the potency of known CaM antagonists against this interaction.

XRCC4/Ligase IV: Non-Homologous End Joining DNA Repair

The third system under study is the high-affinity interaction between X-ray cross complimenting protein 4 (XRCC4) and DNA ligase IV (LigIV). Unlike the first two model systems, the focus is not on modulation of this interaction by small molecules, but

rather to demonstrate the use of MS for identifying 'hot-spots' within an interface[16, 17] that would be most susceptible to disruption by antagonists. The interaction surface has been isolated to the XRCC4-interacting region (XIR) of LigIV,[131-134] and given that the intact enzyme (104 kDa) is too large for direct MS analyses, a complex of XRCC4 and XIR (5.3 kDa) was chosen for inhibition studies. The approach is to screen smaller regions of XIR against an intact complex to determine the minimal fragment that is able to displace the peptide from its interaction with XRCC4. Delineation of the key surface required to maintain XRCC4/XIR interaction would provide a more defined target surface for rational inhibitor design and for HTS.

The XRCC4/LigIV interaction plays an essential role in non-homologous end joining (NHEJ) DNA repair, the predominant repair pathway for double-stranded breaks (DSB) in humans.[135-138] The process of DNA repair presents a paradox for cancer research, where maintenance of genetic integrity is vital to protect against the onset of cancer, yet these same repair pathways protect cancer cells from therapeutics that induce DNA damage. Consequently, DNA repair proteins have become desirable targets for small molecule modulators that can be developed into adjuvant compounds to improve the efficacy of anti-cancer treatments.[139-141] In addition, cancer cells develop from dysfunctional DNA repair and do not have access to the same redundancies in pathways as their healthy counterparts. Cancer cells consequently develop a preference for a particular repair pathway, which can be exploited as a synthetic lethality to more selectively target abnormal cells with DNA damaging agents.[141-143]

DSB are the most severe form of DNA damage, and clastogenic compounds and ionizing radiation that cause DSB are common anti-cancer therapies.[144] In human cells, most DSB are repaired through NHEJ,[136, 137] thus modulation of this pathway provides an opportunity to increase the efficacy of DSB-inducing agents. NHEJ involves seven proteins, of which LigIV carries out the final ligation step. Although inhibitors of LigIV catalytic activity have been shown to disrupt NHEJ, these compounds also inhibit one or both of the other human ligases.[145, 146] To avoid the promiscuity problem associated with targeting DNA binding activity, ligation by LigIV can be indirectly inhibited through modulation of its interaction with XRCC4. Formation of the XRCC4/LigIV complex is essential for NHEJ, and LigIV cannot function without XRCC4 as a structural counterpart.[147, 148] Therefore, targeting the XRCC4/LigIV interaction with small molecule modulators is a potential strategy for the development of novel anti-cancer therapeutics

1.6 Thesis Outline

In chapter two, magnetic separation and MS detection are combined into a magnetic "fishing" assay to functionally screen small molecule mixtures for modulators of PPI. Intact complexes are isolated from solution by affinity-capture to MB, and subsequently analyzed by MS in order to assess the degree of interaction and identify modulators by molecular weight. Assay validation is carried out using a library of 1000 compounds, doped with three known antagonists of the CaM/Mel model system. The ability to develop quantitative inhibition data is also demonstrated through dose-

dependent response curves and determination of inhibition constants (K_I) for two known anti-CaM compounds and a novel antagonist that is identified during primary screening.

Chapter three describes the application of magnetic "fishing" to study interaction of transcription factor SOX9 and CaM, which is a promising new target for the treatment of spinal cord injury. The binding constant for this interaction is determined using SOX-CAL as an antagonist of CaM/Mel by applying the magnetic "fishing" assay as described in chapter two. After modifying the assay to target CaM/SOX-CAL, an inhibition study using known antagonists leads to the identification of a novel mode of interaction. The versatility of magnetic fishing is shown through adaptation of the assay to monitor protein-protein and protein-ligand interactions during an investigation of this potentially novel low-affinity CaM/SOX-CAL complex.

The work in chapter four introduces an MS-based approach to probe the high-affinity complex of X-ray cross complimenting protein 4/ligase IV (XRCC4/LigIV), a desirable target for anti-cancer drug discovery. Preliminary work with XRCC4/XIR revealed that resistance of this high-affinity complex to typical denaturing conditions made it unsuitable for use with the magnetic "fishing" assay, which requires dissociation of the complex to assess the degree of interaction. The extreme affinity of XRCC4/XIR is turned from a challenge into an asset, when a simple competitive displacement assay is developed directly in MS-compatible solvents. Using this function-based assay, a series of LigIV peptides are screened for disruption of XRCC4/LigIV to identify the key interface for maintaining this tight interaction.

Conclusions and future directions of the research are summarized in chapter five. Following a summary of the thesis work, modifications to increase throughput and labour efficiency of the magnetic "fishing" assay are discussed, including automation, multiplexing, and the use of alternative MS instrumentation with wider mass ranges for the study of larger proteins. Possible applications of magnetic fishing for screening natural products is also presented, in addition to expansion of mass spectrometric assays to other biomolecular interactions.

1.7 References

1. Braun, P.; Gingras, A. C., *Proteomics* **2012,** *12* (10), 1478-98.
2. Good, M. C.; Zalatan, J. G.; Lim, W. A., *Science* **2011,** *332* (6030), 680-6.
3. Chari, A.; Fischer, U., *Trends Biochem. Sci.* **2010,** *35* (12), 676-83.
4. Peterson-Kaufman, K. J.; Carlson, C. D.; Rodriguez-Martinez, J. A.; Ansari, A. Z., *ChemBioChem* **2010,** *11* (14), 1955-62.
5. Keskin, O.; Gursoy, A.; Ma, B.; Nussinov, R., *Chem. Rev.* **2008,** *108* (4), 1225-44.
6. Stelzl, U.; Worm, U.; Lalowski, M.; Haenig, C.; Brembeck, F. H.; Goehler, H.; Stroedicke, M.; Zenkner, M.; Schoenherr, A.; Koeppen, S.; Timm, J.; Mintzlaff, S.; Abraham, C.; Bock, N.; Kietzmann, S.; Goedde, A.; Toksoz, E.; Droege, A.; Krobitsch, S.; Korn, B.; Birchmeier, W.; Lehrach, H.; Wanker, E. E., *Cell* **2005,** *122* (6), 957-68.
7. Nooren, I. M.; Thornton, J. M., *EMBO J.* **2003,** *22* (14), 3486-92.

8. Makley, L. N.; Gestwicki, J. E., *Chem. Biol. Drug Des.* **2013,** *81* (1), 22-32.

9. Mullard, A., *Nat. Rev. Drug Discov.* **2012,** *11* (3), 173-5.

10. Smith, M. C.; Gestwicki, J. E., *Expert Rev. Mol. Med.* **2012,** *14*, e16.

11. Thompson, A. D.; Dugan, A.; Gestwicki, J. E.; Mapp, A. K., *ACS Chem. Biol.* **2012,** *7* (8), 1311-20.

12. White, A. W.; Westwell, A. D.; Brahemi, G., *Expert Rev. Mol. Med.* **2008,** *10*, e8.

13. Wells, J. A.; McClendon, C. L., *Nature* **2007,** *450* (7172), 1001-9.

14. Arkin, M. R.; Wells, J. A., *Nat. Rev. Drug Discov.* **2004,** *3* (4), 301-17.

15. Stumpf, M. P.; Thorne, T.; de Silva, E.; Stewart, R.; An, H. J.; Lappe, M.; Wiuf, C., *PNAS* **2008,** *105* (19), 6959-64.

16. DeLano, W. L., *Curr. Opin. Struct. Biol.* **2002,** *12* (1), 14-20.

17. Bogan, A. A.; Thorn, K. S., *J. Mol. Biol.* **1998,** *280* (1), 1-9.

18. Morelli, X.; Bourgeas, R.; Roche, P., *Curr. Opin. Chem. Biol.* **2011,** *15* (4), 475-81.

19. Lipinski, C. A., *Drug Discov. Today Technol.* **2004,** *1* (4), 337-341.

20. Lipinski, C. A., *J. Pharmacol. Toxicol. Methods* **2000,** *44* (1), 235-49.

21. Lipinski, C. A.; Lombardo, F.; Dominy, B. W.; Feeney, P. J., *Adv. Drug Deliv. Rev.* **1997,** *23* (1-3), 3-25.

22. Spencer, R. W., *Biotechnol. Bioeng.* **1998,** *61* (1), 61-7.

23. Arkin, M. R.; Glicksman, M. A.; Fu, H.; Havel, J. J.; Du, Y., Inhibition of Protein-Protein Interactions: Non-Cellular Assay Formats. In *Assay Guidance Manual [Internet]*, 2012/05/04 ed.; Sittampalam, G.; Gal-Edd, N.; Arkin, M. R.;

al., e., Eds. Eli Lilly & Company and the National Center for Advancing Translational Sciences; 2004-: Bethesda, MD, 2012.

24. Lievens, S.; Caligiuri, M.; Kley, N.; Tavernier, J., *Methods* **2012,** *58* (4), 335-42.

25. Lin, Y.; Li, Y.; Zhu, Y.; Zhang, J.; Liu, X.; Jiang, W.; Yu, S.; You, X. F.; Xiao, C.; Hong, B.; Wang, Y.; Jiang, J. D.; Si, S., *PNAS* **2012,** *109* (43), 17412-7.

26. Lentze, N.; Auerbach, D., *Expert Opin. Ther. Targets* **2008,** *12* (4), 505-15.

27. Zhao, H. F.; Kiyota, T.; Chowdhury, S.; Purisima, E.; Banville, D.; Konishi, Y.; Shen, S. H., *Anal. Chem.* **2004,** *76* (10), 2922-7.

28. Kato-Stankiewicz, J.; Hakimi, I.; Zhi, G.; Zhang, J.; Serebriiskii, I.; Guo, L.; Edamatsu, H.; Koide, H.; Menon, S.; Eckl, R.; Sakamuri, S.; Lu, Y.; Chen, Q. Z.; Agarwal, S.; Baumbach, W. R.; Golemis, E. A.; Tamanoi, F.; Khazak, V., *PNAS* **2002,** *99* (22), 14398-403.

29. Young, K.; Lin, S.; Sun, L.; Lee, E.; Modi, M.; Hellings, S.; Husbands, M.; Ozenberger, B.; Franco, R., *Nat. Biotechnol.* **1998,** *16* (10), 946-50.

30. Chan, C. T.; Reeves, R. E.; Geller, R.; Yaghoubi, S. S.; Hoehne, A.; Solow-Cordero, D. E.; Chiosis, G.; Massoud, T. F.; Paulmurugan, R.; Gambhir, S. S., *PNAS* **2012,** *109* (37), E2476-85.

31. Morell, M.; Ventura, S.; Aviles, F. X., *FEBS Lett.* **2009,** *583* (11), 1684-91.

32. MacDonald, M. L.; Lamerdin, J.; Owens, S.; Keon, B. H.; Bilter, G. K.; Shang, Z.; Huang, Z.; Yu, H.; Dias, J.; Minami, T.; Michnick, S. W.; Westwick, J. K., *Nat. Chem. Biol.* **2006,** *2* (6), 329-37.

33. Remy, I.; Michnick, S. W., *Nat. Methods* **2006,** *3* (12), 977-9.

34. Galarneau, A.; Primeau, M.; Trudeau, L.; Michnick, S. W., *Nat. Biotechnol.* **2002,** *20*, 619-622.

35. Cheng, X. R.; Hung, V. W. S.; Scarano, S.; Mascini, M.; Minunni, M.; Kerman, K., *Anal. Methods* **2012,** *4*, 2228-2232.

36. Rich, R. L.; Myszka, D. G., *Anal. Biochem.* **2007,** *361* (1), 1-6.

37. Jung, S. O.; Ro, H. S.; Kho, B. H.; Shin, Y. B.; Kim, M. G.; Chung, B. H., *Proteomics* **2005,** *5* (17), 4427-31.

38. Vassilev, L. T.; Vu, B. T.; Graves, B.; Carvajal, D.; Podlaski, F.; Filipovic, Z.; Kong, N.; Kammlott, U.; Lukacs, C.; Klein, C.; Fotouhi, N.; Liu, E. A., *Science* **2004,** *303* (5659), 844-8.

39. Bista, M.; Kowalska, K.; Janczyk, W.; Domling, A.; Holak, T. A., *J. Am. Chem. Soc.* **2009,** *131* (22), 7500-1.

40. Rothweiler, U.; Czarna, A.; Weber, L.; Popowicz, G. M.; Brongel, K.; Kowalska, K.; Orth, M.; Stemmann, O.; Holak, T. A., *J. Med. Chem.* **2008,** *51* (16), 5035-42.

41. Shapiro, A. B.; Ross, P. L.; Gao, N.; Livchak, S.; Kern, G.; Yang, W.; Andrews, B.; Thresher, J., *J. Biomol. Screen.* **2013,** *18* (3), 341-7.

42. Tian, W.; Xu, Y.; Han, X.; Duggineni, S.; Huang, Z.; An, J., *J. Biomol. Screen.* **2012,** *17* (4), 530-4.

43. Zhai, D.; Godoi, P.; Sergienko, E.; Dahl, R.; Chan, X.; Brown, B.; Rascon, J.; Hurder, A.; Su, Y.; Chung, T. D.; Jin, C.; Diaz, P.; Reed, J. C., *J. Biomol. Screen.* **2012,** *17* (3), 350-60.

44. Zhang, M.; Huang, Z.; Yu, B.; Ji, H., *Anal. Biochem.* **2012,** *424* (1), 57-63.

45. Lea, W. A.; Simeonov, A., *Expert Opin. Drug Discov.* **2011,** *6* (1), 17-32.

46. Lokesh, G. L.; Rachamallu, A.; Kumar, G. D.; Natarajan, A., *Anal. Biochem.* **2006,** *352* (1), 135-41.

47. Cunningham, L.; Finckbeiner, S.; Hyde, R. K.; Southall, N.; Marugan, J.; Yedavalli, V. R.; Dehdashti, S. J.; Reinhold, W. C.; Alemu, L.; Zhao, L.; Yeh, J. R.; Sood, R.; Pommier, Y.; Austin, C. P.; Jeang, K. T.; Zheng, W.; Liu, P., *PNAS* **2012,** *109* (36), 14592-7.

48. Rogers, M. S.; Cryan, L. M.; Habeshian, K. A.; Bazinet, L.; Caldwell, T. P.; Ackroyd, P. C.; Christensen, K. A., *PLoS One* **2012,** *7* (6), e39911.

49. Mackie, D. I.; Roman, D. L., *J. Biomol. Screen.* **2011,** *16* (8), 869-77.

50. Alvarez-Curto, E.; Pediani, J. D.; Milligan, G., *Anal. Bioanal. Chem.* **2010,** *398* (1), 167-80.

51. Eglen, R. M.; Reisine, T.; Roby, P.; Rouleau, N.; Illy, C.; Bosse, R.; Bielefeld, M., *Curr. Chem. Genomics* **2008,** *1*, 2-10.

52. Glickman, J. F.; Wu, X.; Mercuri, R.; Illy, C.; Bowen, B. R.; He, Y.; Sills, M., *J. Biomol. Screen.* **2002,** *7* (1), 3-10.

53. Kainkaryam, R. M.; Woolf, P. J., *Curr. Opin. Drug Discov. Devel.* **2009,** *12* (3), 339-50.

54. Bantscheff, M.; Lemeer, S.; Savitski, M. M.; Kuster, B., *Anal. Bioanal. Chem.* **2012,** *404* (4), 939-65.

55. Dunham, W. H.; Mullin, M.; Gingras, A. C., *Proteomics* **2012,** *12* (10), 1576-90.

56. Pacholarz, K. J.; Garlish, R. A.; Taylor, R. J.; Barran, P. E., *Chem. Soc. Rev.* **2012,** *41* (11), 4335-55.

57. Pardo, M.; Choudhary, J. S., *J. Proteome Res.* **2012,** *11* (3), 1462-74.

58. Schirle, M.; Bantscheff, M.; Kuster, B., *Chem. Biol.* **2012,** *19* (1), 72-84.

59. Gavin, A. C.; Maeda, K.; Kuhner, S., *Curr. Opin. Biotechnol.* **2011,** *22* (1), 42-9.

60. Rinner, O.; Mueller, L. N.; Hubalek, M.; Muller, M.; Gstaiger, M.; Aebersold, R., *Nat. Biotechnol.* **2007,** *25* (3), 345-52.

61. Schermann, S. M.; Simmons, D. A.; Konermann, L., *Expert Rev. Proteomics* **2005,** *2* (4), 475-85.

62. Ong, S. E.; Mann, M., *Nat. Chem. Biol.* **2005,** *1* (5), 252-62.

63. Aebersold, R., *J. Am. Soc. Mass Spectrom.* **2003,** *14* (7), 685-95.

64. Aebersold, R.; Mann, M., *Nature* **2003,** *422* (6928), 198-207.

65. Geoghegan, K. F.; Kelly, M. A., *Mass Spectrom. Rev.* **2005,** *24* (3), 347-66.

66. Annis, D. A.; Anthanasopoulos, J.; Curran, P. J.; Felsch, J. S.; Kalghatgi, K.; Lee, W. H.; Nash, H. M.; Orminati, J.; Rosner, K. E.; Shipps, G. W., Jr.; Thaddupathy, G. R. A.; Tyler, A. N.; Vilenchik, L.; Wagner, C. R.; Wintner, E. A., *Int. J. Mass Spectrom.* **2004,** *238* (2), 77-83.

67. Jonker, N.; Kool, J.; Irth, H.; Niessen, W. M., *Anal. Bioanal. Chem.* **2011,** *399* (8), 2669-81.

68. Annis, D. A.; Nickbarg, E.; Yang, X.; Ziebell, M. R.; Whitehurst, C. E., *Curr. Opin. Chem. Biol.* **2007,** *11* (5), 518-26.

69. Muckenschnabel, I.; Falchetto, R.; Mayr, L. M.; Filipuzzi, I., *Anal. Biochem.* **2004,** *324* (2), 241-9.

70. Comess, K. M.; Schurdak, M. E.; Voorbach, M. J.; Coen, M.; Trumbull, J. D.; Yang, H.; Gao, L.; Tang, H.; Cheng, X.; Lerner, C. G.; McCall, J. O.; Burns, D. J.; Beutel, B. A., *J Biomol Screen* **2006,** *11* (7), 743-54.

71. van Breemen, R. B.; Huang, C. R.; Nikolic, D.; Woodbury, C. P.; Zhao, Y. Z.; Venton, D. L., *Anal. Chem.* **1997,** *69* (11), 2159-64.

72. Zhao, Y. Z.; van Breemen, R. B.; Nikolic, D.; Huang, C. R.; Woodbury, C. P.; Schilling, A.; Venton, D. L., *J. Med. Chem.* **1997,** *40* (25), 4006-12.

73. Kaur, S.; McGuire, L.; Tang, D.; Dollinger, G.; Huebner, V., *J. Protein Chem.* **1997,** *16* (5), 505-11.

74. Calleri, E.; Temporini, C.; Caccialanza, G.; Massolini, G., *ChemMedChem* **2009,** *4* (6), 905-16.

75. Ng, E. S.; Chan, N. W.; Lewis, D. F.; Hindsgaul, O.; Schriemer, D. C., *Nat. Protoc.* **2007,** *2* (8), 1907-17.

76. Slon-Usakiewicz, J. J.; Ng, W.; Dai, J. R.; Pasternak, A.; Redden, P. R., *Drug Discov. Today* **2005,** *10* (6), 409-16.

77. Schriemer, D. C.; Bundle, D. R.; Li, L.; Hindsgaul, O., *Angew. Chem. Int. Ed. Engl.* **1998,** *37* (24), 3383-3387.

78. de Moraes, M. C.; Vanzolini, L. K.; Cardoso, C. L.; Cass, Q. B., *J. Pharm. Biomed. Anal.* **2013,** *(In Press)*.

79. Pan, Y.; Du, X.; Zhao, F.; Xu, B., *Chem. Soc. Rev.* **2012,** *41* (7), 2912-42.

80. Beveridge, J. S.; Stephens, J. R.; Williams, M. E., *Annu. Rev. Anal. Chem.* **2011,** *4*, 251-73.

81. Cai, Y.; Chen, Y.; Hong, X.; Liu, Z.; Yuan, W., *Int. J. Nanomed.* **2013,** *8*, 1111-20.

82. Meza, M. B., *Drug Discov. Today* **2000,** *5*, 38-41.

83. Mok, H.; Zhang, M., *Expert Opin. Drug Deliv.* **2013,** *10* (1), 73-87.

84. Bitar, A.; Ahmad, N. M.; Fessi, H.; Elaissari, A., *Drug Discov. Today* **2012,** *17* (19-20), 1147-54.

85. Colombo, M.; Carregal-Romero, S.; Casula, M. F.; Gutierrez, L.; Morales, M. P.; Bohm, I. B.; Heverhagen, J. T.; Prosperi, D.; Parak, W. J., *Chem. Soc. Rev.* **2012,** *41* (11), 4306-34.

86. Reddy, L. H.; Arias, J. L.; Nicolas, J.; Couvreur, P., *Chem. Rev.* **2012,** *112* (11), 5818-78.

87. Gao, M.; Deng, C.; Zhang, X., *Expert Rev. Proteomics* **2011,** *8* (3), 379-90.

88. Marszall, M. P., *Pharm. Res.* **2011,** *28* (3), 480-3.

89. Ahn, Y. H.; Shin, P. M.; Ji, E. S.; Kim, H.; Yoo, J. S., *Anal. Bioanal. Chem.* **2012,** *402* (6), 2101-12.

90. Cheng, G.; Liu, Y. L.; Zhang, J. L.; Sun, D. H.; Ni, J. Z., *Anal. Bioanal. Chem.* **2012,** *404* (3), 763-70.

91. Razavi, M.; Frick, L. E.; LaMarr, W. A.; Pope, M. E.; Miller, C. A.; Anderson, N. L.; Pearson, T. W., *J. Proteome Res.* **2012,** *11* (12), 5642-9.

92. Choi, E.; Loo, D.; Dennis, J. W.; O'Leary, C. A.; Hill, M. M., *Electrophoresis* **2011,** *32* (24), 3564-75.

93. Whiteaker, J. R.; Zhao, L.; Anderson, L.; Paulovich, A. G., *Mol. Cell Proteomics* **2010,** *9* (1), 184-96.

94. Anderson, N. L.; Jackson, A.; Smith, D.; Hardie, D.; Borchers, C.; Pearson, T. W., *Mol. Cell Proteomics* **2009,** *8* (5), 995-1005.

95. Breitkreutz, A.; Choi, H.; Sharom, J. R.; Boucher, L.; Neduva, V.; Larsen, B.; Lin, Z. Y.; Breitkreutz, B. J.; Stark, C.; Liu, G.; Ahn, J.; Dewar-Darch, D.; Reguly, T.; Tang, X.; Almeida, R.; Qin, Z. S.; Pawson, T.; Gingras, A. C.; Nesvizhskii, A. I.; Tyers, M., *Science* **2011,** *328* (5981), 1043-6.

96. Hubner, N. C.; Bird, A. W.; Cox, J.; Splettstoesser, B.; Bandilla, P.; Poser, I.; Hyman, A.; Mann, M., *J. Cell Biol.* **2010,** *189* (4), 739-54.

97. Pochet, L.; Heus, F.; Jonker, N.; Lingeman, H.; Smit, A. B.; Niessen, W. M.; Kool, J., *J. Chromatogr. B Anal. Technol. Biomed. Life Sci.* **2011,** *879* (20), 1781-8.

98. Jonker, N.; Kretschmer, A.; Kool, J.; Fernandez, A.; Kloos, D.; Krabbe, J. G.; Lingeman, H.; Irth, H., *Anal. Chem.* **2009,** *81* (11), 4263-70.

99. Marszall, M. P.; Moaddel, R.; Kole, S.; Gandhari, M.; Bernier, M.; Wainer, I. W., *Anal. Chem.* **2008,** *80* (19), 7571-5.

100. Moaddel, R.; Marszall, M. P.; Bighi, F.; Yang, Q.; Duan, X.; Wainer, I. W., *Anal. Chem.* **2007,** *79* (14), 5414-7.

101. Tao, Y.; Zhang, Y.; Cheng, Y.; Wang, Y., *Biomed. Chromatogr.* **2013,** *27* (2), 148-55.

102. Qing, L. S.; Xue, Y.; Deng, W. L.; Liao, X.; Xu, X. M.; Li, B. G.; Liu, Y. M., *Anal. Bioanal. Chem.* **2011,** *399* (3), 1223-31.

103. Yasuda, M.; Wilson, D. R.; Fugmann, S. D.; Moaddel, R., *Anal. Chem.* **2011,** *83* (19), 7400-7.

104. Qing, L. S.; Shan, X. Q.; Xu, X. M.; Xue, Y.; Deng, W. L.; Li, B. G.; Wang, X. L.; Liao, X., *Rapid Commun. Mass Spectrom.* **2010,** *24* (22), 3335-9.

105. Qing, L. S.; Xue, Y.; Zheng, Y.; Xiong, J.; Liao, X.; Ding, L. S.; Li, B. G.; Liu, Y. M., *J. Chromatogr. A* **2010,** *1217* (28), 4663-8.

106. Zhang, H.; Gau, B. C.; Jones, L. M.; Vidavsky, I.; Gross, M. L., *Anal. Chem.* **2011,** *83* (1), 311-8.

107. Mathur, S.; Badertscher, M.; Scott, M.; Zenobi, R., *Phys. Chem. Chem. Phys.* **2007,** *9* (47), 6187-98.

108. Zhu, M. M.; Rempel, D. L.; Du, Z.; Gross, M. L., *J. Am. Chem. Soc.* **2003,** *125* (18), 5252-3.

109. Flora, K.; Keeling-Tucker, T.; Hogue, C. W.; Brennan, J. D., *Anal. Chim. Acta* **2002,** *470* (1), 19-28.

110. Wattenberg, A.; Sobott, F.; Barth, H. D.; Brutschy, B., *Int. J. Mass Spectrom.* **2000,** *203* (1), 49-57.

111. Steiner, R. F.; Albaugh, S.; Fenselau, C.; Murphy, C.; Vestling, M., *Anal. Biochem.* **1991,** *196* (1), 120-5.

112. Nemirovskiy, O. V.; Ramanathan, R.; Gross, M. L., *J. Am. Soc. Mass Spectrom.* **1997,** *8* (8), 809-812.

113. Kataoka, M.; Head, J. F.; Seaton, B. A.; Engelman, D. M., *PNAS* **1989,** *86* (18), 6944-6948.

114. Comte, M.; Maulet, Y.; Cox, J. A., *Biochem. J.* **1983,** *209* (1), 269-72.

115. Maulet, Y.; Cox, J. A., *Biochemistry* **1983,** *22* (24), 5680-6.

116. Weiss, B.; Prozialeck, W.; Cimino, M.; Barnette, M. S.; Wallace, T. L., *Ann. N. Y. Acad. Sci.* **1980,** *356*, 319-45.

117. Vandonselaar, M.; Hickie, R. A.; Quail, J. W.; Delbaere, L. T. J., *Nat. Struct. Biol.* **1994,** *1* (11), 795-801.

118. Johnson, J. D.; Wittenauer, L. A., *Biochem. J.* **1983,** *211* (2), 473-479.

119. Levin, R. M.; Weiss, B., *Mol. Pharmacol.* **1977,** *13* (4), 690-697.

120. Lukas, T. J.; Burgess, W. H.; Prendergast, F. G.; Lau, W.; Watterson, D. M., *Biochemistry* **1986,** *25* (6), 1458-64.

121. Blumenthal, D. K.; Takio, K.; Edelman, A. M.; Charbonneau, H.; Titani, K.; Walsh, K. A.; Krebs, E. G., *PNAS* **1985,** *82* (10), 3187-91.

122. Johnson, J. D.; Holroyde, M. J.; Crouch, T. H.; Solaro, R. J.; Potter, J. D., *J. Biol. Chem.* **1981,** *256* (23), 12194-8.

123. Gris, P.; Tighe, A.; Levin, D.; Sharma, R.; Brown, A., *Glia* **2007,** *55* (11), 1145-55.

124. Gris, P.; Murphy, S.; Jacob, J. E.; Atkinson, I.; Brown, A., *Mol. Cell. Neurosci.* **2003,** *24* (3), 555-67.

125. McKillop, W. M.; Dragan, M.; Schedl, A.; Brown, A., *Glia* **2013,** *61* (2), 164-77.

126. Argentaro, A.; Sim, H.; Kelly, S.; Preiss, S.; Clayton, A.; Jans, D. A.; Harley, V. R., *J. Biol. Chem.* **2003,** *278* (36), 33839-47.

127. Rhoads, A. R.; Friedberg, F., *FASEB J* **1997,** *11* (5), 331-40.

128. James, P.; Vorherr, T.; Carafoli, E., *Trends Biochem Sci* **1995,** *20* (1), 38-42.

129. O'Neil, K. T.; DeGrado, W. F., *Trends Biochem. Sci.* **1990,** *15* (2), 59-64.

130. Cox, J. A.; Comte, M.; Fitton, J. E.; DeGrado, W. F., *J. Biol. Chem.* **1985,** *260* (4), 2527-34.

131. Wu, P. Y.; Frit, P.; Meesala, S.; Dauvillier, S.; Modesti, M.; Andres, S. N.; Huang, Y.; Sekiguchi, J.; Calsou, P.; Salles, B.; Junop, M. S., *Mol. Cell. Biol.* **2009,** *29* (11), 3163-3172.

132. Modesti, M.; Junop, M. S.; Ghirlando, R.; van de Rakt, M.; Gellert, M.; Yang, W.; Kanaar, R., *J. Mol. Biol.* **2003,** *334* (2), 215-228.

133. Sibanda, B. L.; Critchlow, S. E.; Begun, J.; Pei, X. Y.; Jackson, S. P.; Blundell, T. L.; Pellegrini, L., *Nat. Struct. Biol.* **2001,** *8* (12), 1015-1019.

134. Grawunder, U.; Zimmer, D.; Lieber, M. R., *Curr. Biol.* **1998,** *8* (15), 873-876.

135. Weterings, E.; van Gent, D. C., *DNA Repair* **2004,** *3* (11), 1425-35.

136. Jackson, S. P., *Carcinogenesis* **2002,** *23* (5), 687-96.

137. Karran, P., *Curr. Opin. Genet. Dev.* **2000,** *10* (2), 144-50.

138. Kanaar, R.; Hoeijmakers, J. H.; van Gent, D. C., *Trends Cell. Biol.* **1998,** *8* (12), 483-9.

139. Furgason, J. M.; Bahassi el, M., *Pharmacol. Ther.* **2013,** *137* (3), 298-308.

140. Basu, B.; Yap, T. A.; Molife, L. R.; de Bono, J. S., *Curr. Opin. Oncol.* **2012,** *24* (3), 316-24.

141. Curtin, N. J., *Nat. Rev. Cancer* **2012,** *12* (12), 801-17.

142. Shaheen, M.; Allen, C.; Nickoloff, J. A.; Hromas, R., *Blood* **2011,** *117* (23), 6074-82.

143. Rassool, F. V.; Tomkinson, A. E., *Cell. Mol. Life Sci.* **2010,** *67* (21), 3699-710.

144. Fojo, T., *J. Natl. Cancer Inst.* **2001,** *93* (19), 1434-1436.

145. Srivastava, M.; Nambiar, M.; Sharma, S.; Karki, S. S.; Goldsmith, G.; Hegde, M.; Kumar, S.; Pandey, M.; Singh, R. K.; Ray, P.; Natarajan, R.; Kelkar, M.; De, A.; Choudhary, B.; Raghavan, S. C., *Cell* **2012,** *151* (7), 1474-87.

146. Chen, X.; Zhong, S. J.; Zhu, Y.; Dziegielewska, B.; Ellenberger, T.; Wilson, G. M.; MacKerell, A. D.; Tomkinson, A. E., *Cancer Res.* **2008,** *68* (9), 3169-3177.

147. Bryans, M.; Valenzano, M. C.; Stamato, T. D., *Mutation Res.* **1999,** *433* (1), 53-58.

148. Grawunder, U.; Zimmer, D.; Kulesza, P.; Lieber, M. R., *J. Biol. Chem.* **1998,** *273* (38), 24708-24714.

Chapter Two

Magnetic "Fishing" Assay To Screen Small Molecule Mixtures for Modulators of Protein-Protein Interactions

The following chapter was published in the journal *Analytical Chemistry*, under the citation:

McFadden, M.J.; Junop, M.S.; Brennan, J.D. **Magnetic "fishing" assay to screen small molecule mixtures for modulators of protein-protein interactions**. *Analytical Chemistry*, **2010**, 82, 9850-9857.

I developed all experimental protocols, completed all data collection and analysis, and prepared the first draft of the manuscript. Editorial input was given by Dr. Junop and Dr. Brennan to generate the final paper.

Chapter Two: Magnetic "Fishing" Assay To Screen Small Molecule Mixtures for Modulators of Protein-Protein Interactions

2.1 Abstract

Protein-protein interactions are an intricate part of biological pathways and have become important targets for drug discovery. Here we present a two-stage magnetic bead assay to functionally screen small-molecule mixtures for modulators of protein-based interactions, with simultaneous affinity-based isolation of active compounds and identification by mass spectrometry. Proteins of interest interact in solution prior to the addition of Ni(II)-functionalized magnetic beads to recover an intact protein-protein complex through affinity capture of a polyhistidine-tagged primary target ("protein-complex fishing"). Protein-complex fishing, utilizing His_6-tagged calmodulin (CaM) as the primary (bait) protein and melittin (Mel) as the target, was used to screen a mass-encoded library of 1000 bioactive compounds (50 mixtures, 20 compounds each) and successfully identified three known antagonists, three naturally occurring phenolic compounds previously reported to disrupt CaM-activated phosphodiesterase activity, and two newly identified modulators of the CaM-Mel interaction, methylbenzethonium and pempidine tartrate. The ability to produce quantitative inhibition data is also shown through the development of dose-dependent response curves and the determination of inhibition constants (K_I) for the novel compound methylbenzethonium (K_I = 14-49 nM) and two known antagonists, calmidazolium (K_I = 1.7-7.5 nM) and trifluoperazine (K_I = 1.2-3.0 μM), with the latter two values being in close agreement with literature values.

2.2 Introduction

Protein-protein interactions are an intricate part of biological pathways.[149] The interaction of proteins typically results in the activation or inhibition of one or more of the binding partners, thereby carefully regulating cellular functions ranging from replication to apoptosis. As a result, the disruption or enhancement of key interactions is frequently implicated in disease, and these protein complexes have become important targets for drug discovery.[150] Identified compounds that modulate these interactions, by enhancement or inhibition, have value as both novel chemical probes of cellular pathways and leads that could be developed into therapeutics.

A variety of methods have been used to screen for small molecule modulators that activate or inhibit protein-protein interactions. Success has been had in *silico* in producing lists of potential hits by applying specific druglike and pharmacoactive criteria[151] or making structure-based predictions of potential ligands based on analyses of the binding site on either protein target.[152-155] However, detailed information on protein structure and on the site of interaction is required, thus limiting the application for novel or poorly characterized targets. Cell-based approaches typically use a two-hybrid selection system utilizing fluorescent or luciferase-based reporters;[151, 156] however, such methods are limited by cell permeability, as well as toxicity, which may preclude identification of useful *in vitro* probes. Solution-based assays of protein-based interactions using fluorescence-based methods,[157, 158] nuclear magnetic resonance (NMR),[159, 160] surface plasmon resonance (SPR),[161] capillary electrophoresis,[162] or mass spectrometry (MS)[163-165] are commonly used, but these methods are limited either by the

requirement of moderate to high ligand and protein concentrations or by the need for extensive sample cleanup prior to analyses. Application of these *in vitro* methods for screening small molecule mixtures frequently requires multiple assays to first assess the affinity or activity of the library compounds against the target and then to isolate and identify the active ligand. As a result, the need exists for a single assay that combines low-level detection and isolation, while utilizing a format that is capable of functionally screening the state of protein complexes and identifying modulators of such interactions.

Magnetic beads (MBs) have rapidly gained popularity among researchers as a multifunctional assay platform, providing a facile method for the simultaneous isolation and enrichment of bound molecules.[166] Biomolecules are easily immobilized on the particle surface, by covalent linkage or by affinity-based interactions, leading MBs to be used as a platform to identify binding partners in both ligand and protein "fishing" experiments analyzed directly by MS[167, 168] or diverted into an LC/MS system.[169] For increased throughput of MB-based screens, attention has recently turned to automation[170] and toward online magnetic separation.[171] Immunoaffinity assays[172-177] and the purification of intact protein-protein complexes[178] using MBs demonstrate that protein-based interactions remain intact on the bead surface. However, the isolation of protein complexes has not yet been combined with ligand identification by affinity capture into an MB-based screening platform for modulators of protein-based interactions.

Here we present an efficient, MB-based assay that combines functional screening of the state of a protein-protein complex with affinity-based isolation and identification of small-molecule modulators of the interaction. Throughput is increased by screening

mixtures of mass-encoded small molecules from which bioactive ligands are isolated and identified by electrospray ionization tandem mass spectrometry (ESI-MS/MS).[179] The calmodulin-melittin (CaM/Mel) complex was chosen as the model system for assay development because it is a well-characterized interaction with several known antagonists of varying potency. CaM is an 18 kDa calcium-dependent protein that regulates a variety of cellular pathways. In the presence of Ca^{2+}, calmodulin undergoes a conformational change to bind a single molecule of Mel, a small 26-residue peptide, forming a high-affinity complex (K_D = 3 nM).[180] Several known antagonists are available, including calmidazolium (compound R24571), a potent Ca^{2+}-competitive inhibitor (K_I = 2-3 nM),[181] and lower affinity ligands, such as trifluoperazine (TFP; K_I = 1-8 μM)[182, 183] and fluphenazine (FPZ; $K_I \approx 10$ μM), which both compete for the hydrophobic binding pocket of CaM in a Ca^{2+}-dependent manner.

His_6-CaM and Mel are allowed to interact in solution prior to the addition of Ni(II)-functionalized MBs to recover the intact protein-protein complex by affinity capture, in what we refer to as "protein-complex fishing". Since untagged Mel is only recovered through interaction with the affinity-tagged CaM, the degree of interaction can be determined by quantitative ESI-MS/MS analyses of Mel concentration in the eluate after elution from the bead surface (Figure 2.1). During screening, CaM is preincubated with a mixture of small molecules before the addition of Mel (all steps are done under physiological pH and ionic strength to favor the monomeric form of Mel). The intact complex of CaM-Mel, or CaM-ligand in the presence of an active mixture, is isolated from solution using affinity capture and magnetic separation of Ni(II)-modified magnetic

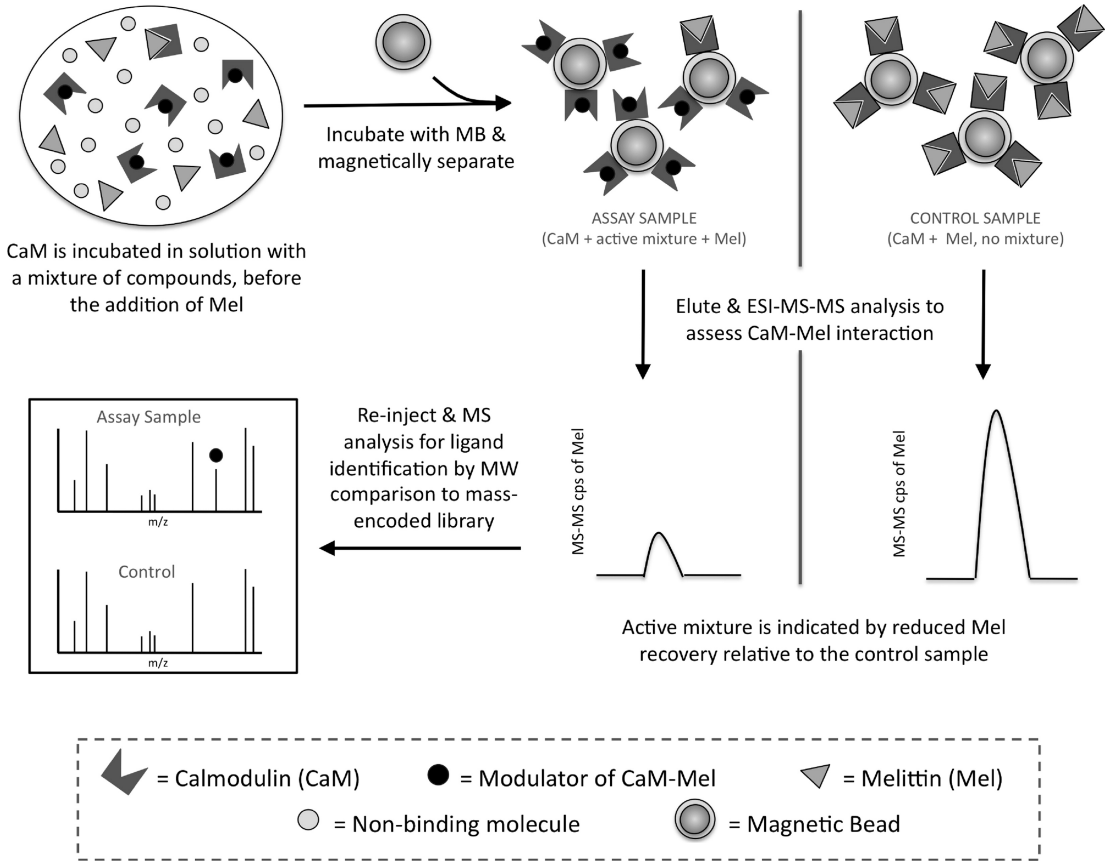

Figure 2.1: Schematic of the assay showing screening of a small-molecule mixture, in the specific case where an inhibitor is present, using a protein-complex fishing approach with magnetic beads and MS. After incubation of a polyhistidine-tagged primary target (CaM) with a mass-encoded mixture of compounds and the secondary protein (Mel), Ni(II)-coated magnetic beads are added to affinity capture the intact protein complex ("protein-complex fishing"). Following elution of bound molecules into an MS-compatible solvent, the magnitude of the protein-protein interaction is taken as the integrated peak area of the MS/MS chromatogram that follows a characteristic signal for the secondary target (Mel), which is only recovered through its interaction with the affinity-tagged primary protein. If decreased recovery is observed relative to a "no-inhibitor" control (<75%), a second injection is made to collect an MS spectrum to identify the active compound in the mixture by molecular mass.

beads. Disruption of the protein-protein interaction is indicated by reduced Mel recovery, relative to a control, following resuspension of the beads in an MS-compatible organic solvent to dissociate bound protein, followed by ESI-MS/MS analysis to quantify the Mel

content in the eluate. Mixtures that show a reduction in recovery of Mel are then further assessed by ESI-MS/MS to allow identification of modulators by molecular mass comparison to mass-encoded library data. Through the use of a magnetic bead assay platform, our approach efficiently screens small molecule mixtures in a significantly smaller volume than is required with traditional chromatographic separation. The ability to isolate and transfer magnetic beads under an applied magnetic field also allows the protein interaction assay to be performed under physiological conditions and then transferred to an ESI-compatible solvent. Furthermore, the design of the assay provides 2-fold assessment of the activity and the identity of potential modulators, eliminating the need for multiple time-consuming analyses.

2.3 Materials and Methods

Materials – PureProteome™ nickel magnetic beads (10 μm diameter, 0.2 g of MBs/mL in water) were purchased from Millipore (Billerica, MA) and were washed per the manufacturer's instructions prior to use. Magnetic separators were purchased from BioClone Inc. (San Diego, CA). Human recombinant calmodulin with an N-terminal 6×His-tag (His_6-CaM) and calmidazolium chloride (compound R24571) were purchased from Calbiochem (San Diego, CA). TFP (99+%) and FPZ (98%) were from Sigma-Aldrich (Oakville, ON, Canada). Polystyrene, 48-well, flat-bottom, microwell plates were purchased from BD Biosciences (Mississauga, ON, Canada). The bioactive small molecules were sourced from BIOMOL International, L.P. (Plymouth Meeting, PA), MicroSource Discovery Systems, Inc. (Gaylordsville, CT), Prestwick Chemical

(Plymouth Meeting, PA), and Sigma (Oakville, ON, Canada). HPLC-grade water was obtained from Caledon Laboratory Chemicals (Georgetown, ON, Canada), and all other reagents were of the highest available grade and used as received.

Protein-Complex Fishing – All fishing experiments were carried out in 48-well, polystyrene microwell plates. A solution of 1 μM CaM was prepared in each well using 50 μL of CaM (2 μM) with 50 μL of buffer (20 mM Tris-HCl, 1 mM $CaCl_2$, pH 7.5). To this solution was added 10 μL of Mel (10 μM) to provide each protein in a 1:1 molar ratio, and the resulting solution was incubated for 5 min before the addition of 40 μL of washed MB suspension (8 mg of beads). The plate was incubated on an orbital shaker for 15 min to allow affinity capture of the intact CaM-Mel complex (typically ~90% capture efficiency for His_6-CaM). The supernatant was removed, and the CaM-MBs were washed three times with 100 μL of buffer. The beads were subsequently incubated in 100 μL of 1% acetic acid in 1:1 (v/v) methanol/water for 30 min to remove bound CaM and Mel, and the eluate was collected and retained for analyses by ESI-MS/MS.

ESI-MS/MS Analysis of Eluates – Sample eluates were analyzed using a Thermo Scientific LCQ Fleet mass spectrometer fitted with a 10-μL sample loop of a 250 μm i.d. (3-aminopropyl)-triethoxysilane (APTES)-coated fused silica capillary. Note that the APTES-coated capillary was used for all connections in the MS system to reduce nonspecific binding of the highly cationic peptide. Using the online syringe pump, 0.5% acetic acid in 1:1 (v/v) methanol/water was delivered at a flow rate of 15 μL/min as 10 μL injections were made of each eluate sample, and the total MS/MS signal for the

fragmentation of the 712.5 m/z ($[M + 4H]^{4+}$) ion to four product ions, 863.0, 812.5, 703.5, and 542.5 m/z, was monitored over time. The total integrated peak area of each sample injection was compared to a calibration curve relating the signal to the Mel concentration and was used to determine the degree of interaction of Mel with CaM during the assay.

Reproducibility Study – The reproducibility of 10 protein-complex fishing assays was statistically assessed by applying the Z' test, which evaluates the ability to resolve a high control (HC) with no inhibitor and a low control (LC) sample with a high level of TFP, based on the differences in the Mel MS signals and the precision of the measurements. Before fishing, 50 μL of CaM (2 μM) was preincubated with 50 μL of TFP (10 mM) (LC), or 50 μL of buffer (HC), for a final concentration of 1 μM CaM in the presence of 5 mM TFP, to significantly disrupt the CaM-Mel interaction, or no TFP. After a 30 min incubation, Mel was added to achieve a 1:1 CaM:Mel molar ratio, incubated as described above, followed by addition of MBs, magnetic isolation, washing, elution, and ESI-MS/MS analyses of the Mel concentration in each high and low control as described above. These data were used to calculate the Z' factor using the formula[184]

$$Z' = 1 - \frac{\left(3\sigma_H + 3\sigma_L\right)}{\left|\mu_H - \mu_L\right|} \quad (1)$$

where σ_L is the standard deviation (SD) of the LC, σ_H is the SD of the HC, μ_H is the average signal of the HC, and μ_L is the average signal of the LC.

Primary Screen of a Bioactive Library of Mass-Encoded Mixtures – For screening, 997 bioactive compounds were selected from a subset of the Canadian Compound Collection obtained from the High Throughput Screening Lab at McMaster University (Hamilton, ON, Canada). The compounds were divided into 50 mass-encoded mixtures containing 20 compounds each, with R24571, FPZ, and TFP doped into mixtures 5, 10, and 26, respectively, as the 20th compound. All compounds were initially present as 1 mM stocks in DMSO and were mixed in batches of 20 compounds and diluted 2.5-fold with buffer to obtain a mixture containing a 20 μM concentration of each compound (400 μM total) in 40% DMSO (v/v). Assays were performed by preincubating 50 μL of CaM (2 μM) with 50 μL of each compound mixture or 50 μL of 40% (v/v) DMSO in buffer as a control, for a final concentration of 1 μM CaM in the presence of a 10 μM concentration of each bioactive molecule in 20% (v/v) DMSO. Note that this level of DMSO was not observed to affect the ratio of Mel from test samples relative to controls, although the absolute signal was decreased by ~40% in both. After a 30 min incubation, Mel was added to achieve a 1:1 CaM:Mel molar ratio, incubated as described above, followed by addition of MBs, magnetic isolation, washing, elution, and ESI-MS/MS analyses of the Mel concentration in each sample, as described above. The total peak area for each sample was normalized by letting the peak area for the "no-inhibitor" control correspond to a relative recovery of 100%. Active mixtures were identified as those resulting in less than 50% Mel recovery relative to the control, and mixtures showing 50-75% Mel recovery were considered to be low-potency hits and were selected for secondary screening and ligand identification.

Ligand Identification – Mixtures that were identified as "hits" were assayed a second time by directly injecting 10 μL of the original eluate and measuring the mass spectrum over the m/z range of 100-1000 relative to a control eluate that did not contain a compound mixture. Additional ion peaks present in the sample spectrum, but absent in the spectrum of the control, were compared to the list of mass-encoded compounds in the mixture to identify the ligand by molecular mass.

Secondary Screening of Discrete Bioactive Molecules – To further confirm the ligand identity, individual compounds that were identified as hits were rescreened using the complex fishing assay. In this case, 50 μL of CaM (2 μM) was preincubated with 50 μL of compound (20 μM), or 50 μL of 2% (v/v) DMSO in buffer as a control, for a final concentration of 1 μM CaM in the presence of a 10 μM concentration of bioactive molecule in 1% (v/v) DMSO. After a 30 min incubation, Mel was added to achieve a 1:1 CaM: Mel molar ratio, incubated as described above, followed by addition of MBs, magnetic isolation, washing, elution, and ESI-MS/MS analyses of the Mel concentration. The total peak area for each sample was normalized by letting the peak area for the no-inhibitor control correspond to a relative recovery of 100%.

Detection of Low-Affinity Ligands – Ten compounds were selected from the bioactive library for use in a modified screen for the identification of low-affinity ligands. In addition to TFP, FPZ, and five negative controls, three natural products (caffeic acid, (-)-epicatechin, and (±)-catechin) were chosen because they had been shown previously to

inhibit CaM-activated phosphodiesterase activity.[185] In these assays, 50 μL of CaM (2 μM) was preincubated with 50 μL of compound (40 μM), or 50 μL of 4% (v/v) DMSO in buffer as a control, for a final concentration of 1 μM CaM in the presence of a 20 μM concentration of each bioactive molecule in 2% (v/v) DMSO. After a 30 min incubation, 10 μL of 1 μM Mel was added to achieve a CaM:Mel molar ratio of 10:1, thus biasing the assay by using a higher ligand concentration and lower Mel concentration than in standard assays. Incubation, magnetic separation, washing, elution, and ESI-MS/MS analyses of Mel were done as described above. The total peak area for each sample was normalized by letting the peak area for the no-inhibitor control correspond to a relative recovery of 100%.

Determination of IC_{50} and K_I Values – Dose-dependent response curves were developed for the two known antagonists R24571 and TFP and a primary hit identified from mixture screening. A 50-μL volume of CaM (2 μM) was preincubated with 50 μL of compound (R24571, 100 nM to 50 μM; TFP, 10 μM to 500 mM; primary hit, 50 nM to 10 mM), or 50 μL of buffer as a control, for a final concentration of 1 μM CaM in the presence of 50 nM to 25 μM R24571, 5 μM to 250 mM TFP, or 25 nM to 5 mM lead compound. After a 30 min incubation, protein-complex fishing, using a 1:1 CaM:Mel molar ratio, and ESI-MS/MS analyses were carried out as described above. The total peak area for each sample was normalized by letting the peak area for the no-inhibitor control correspond to a relative recovery of 100%. A plot of relative signal versus log([inhibitor] (M)) was fitted with the four-parameter Hill equation using SigmaPlot 2000, and IC_{50} values were

taken as the concentration of compound that resulted in a relative Mel recovery midway between the maximum and the minimum levels achieved. Using the Cheng-Prusoff relationship,[186] the IC_{50} values derived from the dose-dependent response curves were converted to inhibition constants (K_I) for each of the antagonists:

$$K_I = \frac{IC_{50}}{1 + \frac{[L]}{K_D}} \quad (2)$$

where [L] is the concentration of ligand (Mel) and K_D is the dissociation constant between the target and ligand (CaM and Mel, respectively).

2.4 Results and Discussion

Assay Optimization – A number of factors were investigated as part of developing and optimizing the MB-based assay, with the goals of binding the maximum amount of CaM-associated Mel to the MBs in a specific manner with minimal nonspecific binding and maximizing the MS/MS signal level. These included (1) comparing the isolation of Mel using CaM-derivatized MBs relative to the isolation of the CaM-Mel complex using nickel(II)-nitrilotriacetic acid (NTA) or anti-histidine antibody-modified beads, (2) comparing Ni(II)NTA-hexahistidine and avidin-biotin immunoaffinity capture methods for binding CaM to the beads, (3) varying the total concentration of CaM and Mel and the molar ratio of CaM to Mel, (4) optimizing wash steps, and (5) optimizing the MS settings. Studies involving the isolation of Mel with CaM-MBs demonstrated that Mel bound only to a level of ~60% and showed relatively high nonspecific binding (ca. 30%) when CaM was not present. In comparison, isolation of the intact complex led to isolation

of up to 90% of Mel, with <10% of the signal arising from nonspecific binding, when using the His_6-CaM interaction with Ni(II)-derivatized beads to isolate the interaction complex (see the Supporting Information). Use of the avidin-biotin immobilization approach was not amenable to direct binding of CaM owing to the need to biotinylate the CaM protein, which could not be done selectively and thus resulted in loss of activity. Instead, the avidin-biotin method was used to immobilize an anti-hexahistidine antibody that then captured His_6-CaM. Unfortunately, CaM immobilized by this method was unable to selectively bind to Mel and demonstrated Mel recovery similar to that of control MBs that lacked CaM or antibody-CaM complexes. The immunoaffinity immobilization method also required multiple steps to build the biotin-avidin-biotin-antibody complex on the bead surface. As a result, all further studies were based on the isolation of CaM-Mel complexes using commercially available Ni(II)-charged magnetic beads.

Optimization of the protein concentration and CaM:Mel ratio led to the use of a 1 μM concentration of each protein (1:1 molar ratio) for the assay. This concentration led to good recovery of Mel and a high MS/MS signal level. Washing steps were optimized to minimize nonspecific binding. The key step for reducing the background signal from Mel was to transfer MBs to a clean well after the complex fishing step and prior to the elution step to prevent desorption of any adsorbed Mel from the original microwells. Finally, use of an acidic methanol solution was found to produce the highest Mel signal in ESI-MS/MS experiments, as the solution was suitable for removal of bound proteins from MBs, produced highly protonated Mel, and was ESI-MS compatible.

Assay Reproducibility – The reproducibility of the protein-complex fishing approach to screen for antagonists of protein-based interactions was assessed using the statistical measure of the Z′ factor. The Z′ value evaluates the quality of a high-throughput assay by considering the difference between sample means as well as the variability in replicate experiments for high and low controls. Ten protein-complex fishing experiments were carried out in the presence (low control) or absence (high control) of 5 mM TFP, and the peak areas for each sample were used to calculate the average and standard deviation within each data set (± TFP). The mean peak area and standard deviation were 70767 ± 8614 and 6370 ± 1715 for the high and low control samples, respectively (Figure 2.2). The corresponding Z′ value was determined to be 0.52, representing the ratio of the screening window to the dynamic range of the assay. Zhang et al.[184] in their presentation of the statistical parameter Z′ described an "excellent assay" as one that provides

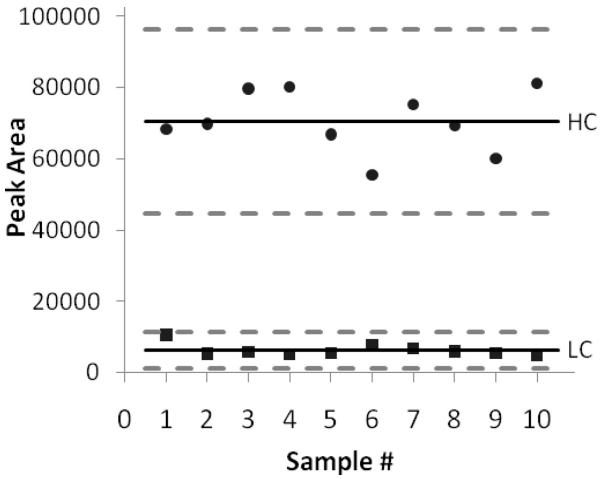

Figure 2.2: Z' plot of the protein-complex fishing approach to screen modulators of the CaM-Mel interaction in the presence (low control, ■) and absence (high control, ●) of 5mM trifluoperazine. Solid lines denote sample means for high and low controls, and broken lines denote 3 standard deviations from the mean for each experimental condition.

sufficient sensitivity, reproducibility, and accuracy to differentiate a large number of compounds across a range of activities and is reflected in a Z′ value between 0.5 and 1. Our Z′ value of 0.52 is within the range for an excellent assay and shows our approach has sufficient accuracy and reproducibility to identify active compounds, thus validating it as a method for screening small-molecule mixtures.

Mixture Screening – The application of protein-complex fishing to screening of small-molecule mixtures was demonstrated through a duplicate screen of 1000 mass-encoded compounds. The 1000 bioactive molecules, including the known inhibitors R24571 (mixture 3), FPZ (mixture 10), and TFP (mixture 26), were screened as 50 mass-encoded mixtures of 20 compounds each, in two independent screens using the complex fishing method. Mel recovery following incubation with each mixture was normalized to that of a control, where no compounds were present, and normalized data from both screens were plotted against each other in a duplicate plot (Figure 2.3A). Active mixtures were indicated as those showing at least 50% reduction in Mel recovery; however, a second threshold between 50% and 75% was established to select lower potency mixtures for secondary screening of discrete compounds.

Although known CaM inhibitors were present in mixtures 5, 10, and 26, only mixture 5 containing the potent antagonist R24571 showed <50% Mel recovery, with recoveries of 30% and 31% in each of the replicate screens (Figure 2.3A). However, Figure 2.3A also shows that two additional mixtures, mixtures 3 and 4, produced a moderate reduction in Mel recovery, showing recoveries of 59% and 72% (mixture 3)

and 64% and 62% (mixture 4) for the replicate screens, respectively. Because these were not previously doped with known bioactive compounds, the samples from mixtures 3 and 4 were chosen for subsequent ligand identification experiments and secondary screening. Mixtures 10 and 26, which were known to contain FPZ and TFP, respectively, were not detected under the assay conditions used in the primary screen (1:1 molar ratio of CaM to Mel), as they showed Mel recovery equivalent to that of the control in the replicate screens, suggesting that the assay conditions needed to be adjusted to allow for identification of low-affinity modulators (see below).

Ligand Identification by MS – Mixture deconvolution following a primary hit during screening can be a tedious process, and many current approaches require multiple or separate assays to identify hits. Using protein-complex fishing for screening mixtures, a compound showing affinity for the bait protein (CaM) is isolated from solution upon addition of the MBs and is thus recovered from solution through its interaction with CaM. Ligands present in solution may bind to CaM, but only those with activity will block the CaM-Mel interaction, indicated by a decrease in relative Mel recovery. The combination of an activity-based screen with affinity-based pull-down of ligands allows for mixture deconvolution and identification of antagonists by evaluation of the mass spectrum of the eluate and comparison to molecular mass data compiled for the active mixture.

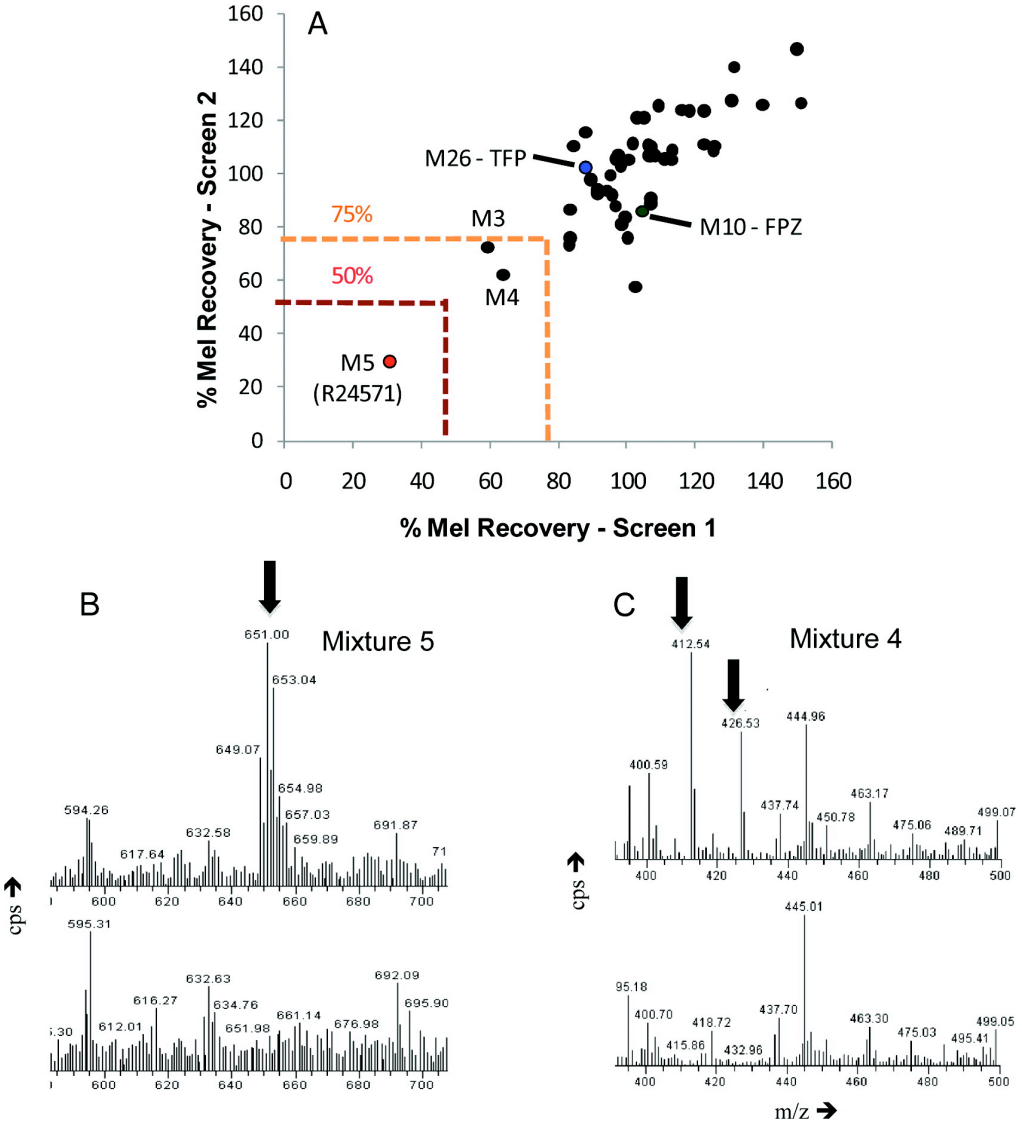

Figure 2.3: Mixture screening and hit identification by mass spectrometric analysis of sample eluates. (A) Duplicate plots of relative Mel recovery for two compound screens using protein-complex fishing for small-molecule modulators of the CaM-Mel interaction. Two independent mixture screens were performed on 1000 bioactive molecules, screened as 50 mass-encoded mixtures of 20 compounds each. M3, M4, and M5 refer to mixtures 3, 4, and 5, respectively. Data points for mixtures containing FPZ (mixture 10) and TFP (mixture 26) are also shown. (B) Identification of ligands from the mass-encoded library using MS analyses of the sample eluate from mixture 5. One additional peak at *m*/*z* 651 is seen in the sample for mixture 5 (top), which corresponds to R24571 (650 Da). (C) Identification of the ligand from mixture 4 shows two additional peaks, *m*/*z* 426.5 and 412.5 (top spectrum), which correspond to the molecular masses of the singly charged methylbenzethonium, 426.5 Da, and of the demethylated fragment of methylbenzethonium, 412.5 Da.

As noted above, the mixture screen of the mass-encoded library indicated one highly active mixture (mixture 5) and two moderately potent mixtures (mixtures 3 and 4). To identify the active compounds, a second injection was made of the original eluate and the mass spectrum was observed between 100 m/z and 1000 m/z and compared to that of a positive control where no compounds were present during preincubation. Figure 2.3B shows the test and control mass spectra obtained from mixture 5, while Figure 2.3C shows the test and control spectra for mixture 4. Test and control spectra for mixture 3 (the least potent hit) were identical, making it impossible to identify the active compound using the MS method directly. This result could be due to synergistic effects within the mixture of compounds or similar molecular masses for the ligand and a contaminant or could indicate affinity of the active compound for Mel rather than CaM.

As shown in Figure 2.3B,C, many peaks are observed at similar m/z values for both samples, which are likely contaminants that elute from the bead surface. However, in Figure 2.3B mixture 5 (top) clearly showed an additional peak at m/z 651 that was not present in the control (bottom). On the basis of molecular mass data for the compounds present in this mixture, R24571 (650 Da) was the only feasible candidate for the active compound. Comparison of the eluate from mixture 4 to the control (Figure 2.3C) revealed two additional peaks in the mass spectrum at m/z 426.5 and 412.5, which when compared to molecular mass data for that mixture indicated methylbenzethonium (426.5 Da) and benzethonium (412.5 Da), respectively, as potentially active compounds. As described below, further evaluation of the activity of these molecules, through secondary screening of individual compounds, revealed that the active compound was

methylbenzethonium (426.5 m/z), while the benzethonium was inactive. Thus, the peak at m/z 412.5 is a fragment of the methylated compound. This situation highlights the need to carefully select compounds for mass-encoded mixtures to avoid cases where one compound could have the same m/z as a fragment ion of a different compound.

Secondary Screening of Discrete Bioactive Molecules – An alternative method for identifying the bioactive compound within a mixture is to individually screen each compound to see which ones result in a reduction in the recovery of Mel. This approach was used to screen the 20 compounds in mixture 5, which contained the potent modulator R24571, the 20 compounds in mixture 3, for which no compound could be identified directly by MS, and both methylbenzethonium and benzethonium from mixture 4. Figure 2.4 shows the duplicate plot and indicated one compound that reduced Mel recovery by over 50% (compound R24571) and two that reduced Mel recovery by more than 25%. These two compounds corresponded to methylbenzothonium (triangles) and the newly identified modulator pempidine tartrate (open squares), corresponding to the bioactive compound in mixture 3.

The results above demonstrate that a combination of deconvolution methods may be needed to ultimately identify bioactive compounds in mixtures. Ligand identification by MS is applicable for moderately to highly active compounds that bind to the primary target. On the other hand, mixture deconvolution by functional screening of discrete molecules is more universal, though it is also more time-consuming and requires

additional reagent costs. A combination of both methods allows identification of ligands that bind to either protein partner.

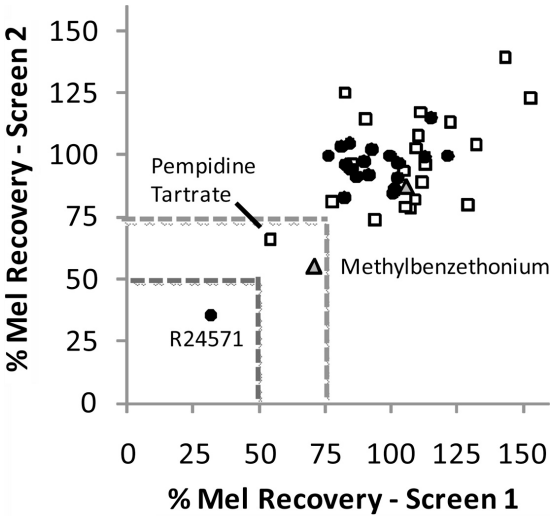

Figure 2.4: Secondary screening of discrete compounds from active mixtures identified in the primary screen, including all compounds in mixture 5 (●), containing the known antagonist R24571, all compounds in mixture 3 (□), which contained pempidine tartrate, and methylbenzethonium from mixture 4 (▲).

Detection of Low-Affinity Ligands – The inability to identify the two lower affinity ligands FPZ (mixture 10) and TFP (mixture 26) in the primary mixture screen is a consequence of both the strong affinity of Mel for CaM (K_D = 3 nM)[180] and the high concentration of Mel present during the assay (1 μM, 1:1 CaM: Mel ratio). Under these conditions, the assay is biased toward the identification of high-potency ligands with dissociation constants in the nanomolar range. To demonstrate that the screen could be used for the detection of lower potency ligands, 10 bioactive compounds were chosen for screening as discrete compounds at 2 times the compound concentration (20 μM) against

1/10 of the original concentration of Mel (100 nM) used in the primary screen (10:1 CaM: Mel molar ratio). Selected compounds included the known ligands TFP and FPZ, three potential ligands, caffeic acid (mixture 11), (-)-epicatechin (mixture 2), and (±)-catechin (mixture 18), and five negative control compounds from the original bioactive library. Inclusion of caffeic acid, (-)-epicatechin, and (±)-catechin in the new screen was based on a previous report that these natural products inhibited CaM-activated phosphodiesterase activity, although their mechanism of action was not determined.[185] Caffeic acid and the two flavonoids were not identified as hits in the initial mixture screen, suggesting they are of low potency and may be detected in a modified screen using a higher compound concentration against a lower concentration of Mel.

Using the modified conditions of higher compound and lower Mel concentration, both known antagonists, TFP and FPZ, were clearly indicated as active, showing 21% and 11%, and 45% and 20% relative signals, respectively (Figure 2.5). The three phenolic compounds were also detected, each showing over 70% reduction in relative Mel recovery, supporting the previous report of their inhibitory properties and suggesting each binds to CaM when inhibiting CaM-activated phosphodiesterase activity. No significant change in Mel recovery was observed in the presence of any of the five negative control compounds. These findings demonstrate that the MB-based protein-complex fishing approach can be adapted to selectively identify potent modulators (R24571, methylbenzethonium), or those of a lower potency, as was the case with TFP, FPZ, caffeic acid, and the flavonoids. Attempts were made to screen mass-encoded mixtures against the lower concentration of Mel; however, disruption of the target interaction due

to the high DMSO content compounded the signal loss resulting from lowering the protein concentration, decreasing the ESI-MS/MS signal to an unusable level. Removal of DMSO from mixtures prior to the fishing step, or use of methanol in place of DMSO, may help to alleviate this situation.

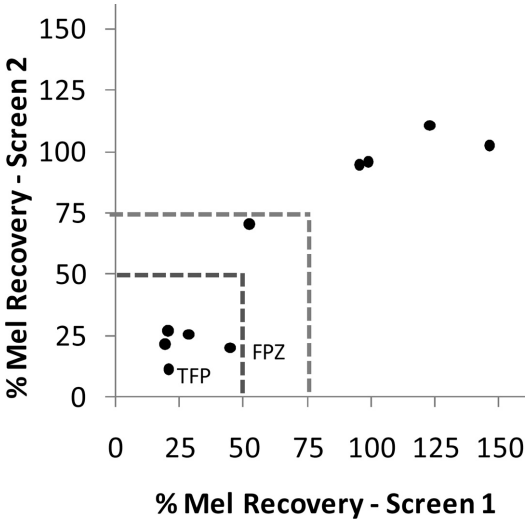

Figure 2.5: Duplicate plot of relative Mel recovery for two independent protein-complex fishing assays of 10 bioactive molecules as discrete compounds, using 2 times the concentration of compound and 1/10 of the concentration of Mel relative to the primary mixture screen. TFP and FPZ are shown, both of which are identified as hits using the modified assay.

Determination of IC_{50} and K_I Values – To demonstrate the use of protein-complex fishing for quantitative determination of inhibition constants, dose-dependent response curves were produced for the known antagonists R24571 and TFP, as well as the newly identified modulator methylbenzethonium. Protein-complex fishing was carried out using a 1:1 CaM:Mel ratio in the absence and presence of increasing amounts of R24571 (50 nM to 25 μM), TFP (5 μM to 250 mM), or methylbenzethonium (25 nM to 5 mM) to

evaluate the recovery of Mel as a function of the inhibitor concentration. As shown in Figure 2.6, a plot of relative Mel recovery versus log([inhibitor] (M)) produced a sigmoidal curve for each compound, as would be expected for dose-dependent inhibition. Upon fitting to a four-parameter Hill equation, the IC_{50} value for each antagonist was determined as the concentration that gives a signal at the midpoint between the maximum and minimum signal levels. Under our experimental conditions, IC_{50} values for R24571, TFP, and methylbenzethonium were 0.57-2.5 μM, 0.41-0.98 mM, and 4.7-16 μM, respectively. The highest concentration at which R24571 could be assayed was limited by its solubility, and as a result the response curve for this compound does not go below 20% relative Mel recovery.

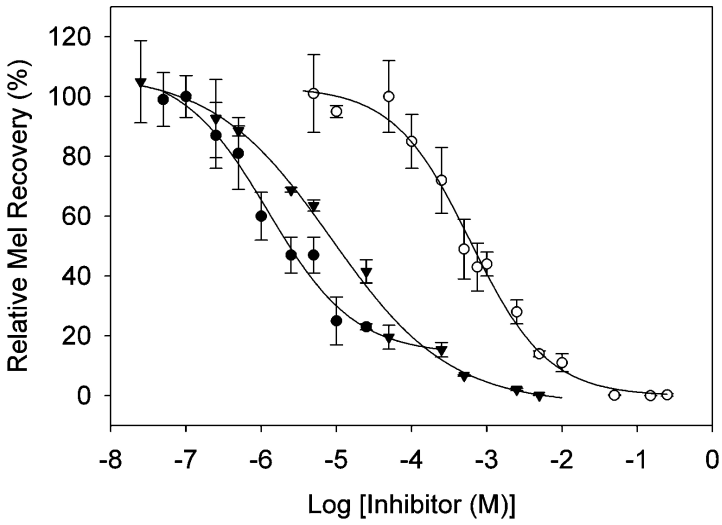

Figure 2.6: Dose-dependent inhibition of the CaM-Mel complex by R24571 (●), TFP (○), and the newly identified antagonist methylbenzethonium (▼).

For a valid comparison to literature values, each IC_{50} value was converted to an inhibitory constant (K_I) using the Cheng-Prusoff relationship, giving a K_I of 1.7-7.5 nM, 1.2-3.0 μM, and 14-49 nM for R24571, TFP, and methylbenzethonium, respectively. Comparison of experimental and literature K_I values for R24571 and TFP showed good agreement between those developed through protein-complex fishing and previous assays based on fluorescence[181] or nuclear magnetic resonance.[182] The large range of values for R24571 and the elevated upper limit of that range when compared to literature values (2-3 nM)[181] are likely the result of the incomplete curve due to solubility limits. The K_I values for TFP developed using protein-complex fishing is entirely within the range previously observed for this antagonist (1-8 μM).[182, 183] The IC_{50} value for methylbenzethonium suggests that it is a relatively potent CaM antagonist, though further study is needed to evaluate its action *in vivo*.

2.5 Conclusions

A novel screening platform combining magnetic beads and mass spectrometry is presented for the identification of ligands that modulate protein-protein interactions. A primary screen of 1000 bioactive compounds as mass-encoded mixtures, including three known CaM antagonists, successfully identified the active mixture that contained the most potent inhibitor, R24571, as well as two bioactive mixtures containing novel antagonists of the CaM-Mel interaction (methylbenzethonium and pempidine tartrate). For relatively potent ligands that bind CaM, the activity-based screening approach can be followed by affinity pull-down of bound ligands, allowing identification of ligands from

mass- encoded mixtures by MS analysis based on comparison to molecular mass data. Alternatively, secondary functional screening of individual compounds can identify less potent modulators or compounds that may bind to the soluble secondary protein (Mel in this assay). Modifications to assay conditions allowed detection of two lower affinity ligands, TFP and FPZ, along with three other suspected modulators, demonstrating that the protein-complex fishing approach can be adapted for selective recovery of high- or low-potency antagonists. The utility of this assay for quantitative inhibition studies was demonstrated through the development of dose-dependent response curves and calculation of K_I values for the novel compound methylbenzethonium and the two known antagonists R24571 and TFP, the latter two values being in close agreement with literature values previously reported. The dual capabilities of mixture screening and deconvolution, and the development of quantitative inhibition data, demonstrate that this assay could be a powerful tool for screening small-molecule mixtures for modulators of biomolecular interactions.

2.6 Acknowledgement

We thank the Natural Sciences and Engineering Research Council of Canada, the Canada Foundation for Innovation, and the Ministry of Research and Innovation (Ontario) for funding of this work. This work was also supported in part by a grant (MOP 89903) from the Canadian Institutes of Health Research to M.S.J. Sam Scozzaro is thanked for his help with the ESI-MS-MS analyses. J.D.B. holds the Canada Research Chair in Bioanalytical Chemistry.

2.7 References

149. Keskin, Z.; Gursoy, A.; Ma, B.; Nussinov, R., Chem. Rev. 2008, 108 (4), 1225-1244.

150. Arkin, M. R.; Wells, J. A., Nat. Rev. Drug Discov. 2004, 3 (4), 301-317.

151. Betzi, S.; Restouin, A.; Opi, S.; Arold, S. T.; Parrot, I.; Guerlesquin, F.; Morelli, X.; Collette, Y., Proc. Natl. Acad. Sci. U. S. A. 2007, 104 (49), 19256-19261.

152. Dickerson, T. J.; Beuscher, A. E.; Hixon, M. S.; Yamamoto, N.; Xu, Y.; Olson, A. J.; Janda, K. D., Biochemistry 2005, 44 (45), 14845-14853.

153. Rush, T. S.; Grant, J. A.; Mosyak, L.; Nicholls, A., J. Med. Chem. 2005, 48 (5), 1489-1495.

154. Huang, N.; Nagarsekar, A.; Xia, G. J.; Hayashi, J.; MacKerell, A. D., J. Med. Chem. 2004, 47 (14), 3502-3511.

155. Li, S.; Gao, J. M.; Satoh, T.; Friedman, T. M.; Edling, A. E.; Koch, U.; Choksi, S.; Han, X. B.; Korngold, R.; Huang, Z. W., Proc. Natl. Acad. Sci. U. S. A. 1997, 94 (1), 73-78.

156. Zhao, H. F.; Kiyota, T.; Chowdhury, S.; Purisima, E.; Banville, D.; Konishi, Y.; Shen, S. H., Anal. Chem. 2004, 76 (10), 2922-2927.

157. Roehrl, M. H. A.; Wang, J. Y.; Wagner, G., Biochemistry 2004, 43 (51), 16067-16075.

158. Peterson, J. R.; Lokey, R. S.; Mitchison, T. J.; Kirschner, M. W., Proc. Natl. Acad. Sci. U. S. A. 2001, 98 (19), 10624-10629.

159. Rothweiler, U.; Czarna, A.; Weber, L.; Popowicz, G. M.; Brongel, K.; Kowalska, K.; Orth, M.; Stemmann, O.; Holak, T. A., J. Med. Chem. 2008, 51 (16), 5035-5042.

160. Best, J. L.; Amezcua, C. A.; Mayr, B.; Flechner, L.; Murawsky, C. M.; Emerson, B.; Zor, T.; Gardner, K. H.; Montminy, M., Proc. Natl. Acad. Sci. U. S. A. 2004, 101 (51), 17622-17627.

161. Yoshida, T.; Sato, M.; Ozawa, T.; Umezawa, Y., Anal. Chem. 2000, 72 (1), 6-11.

162. Yang, P. L.; Whelan, R. J.; Mao, Y. W.; Lee, A. W. M.; Carter-Su, C.; Kennedy, R. T., Anal. Chem. 2007, 79 (4), 1690-1695.

163. Pan, J. X.; Konermann, L., Biochemistry 2010, 49 (16), 3477-3486.

164. Davidson, W.; Hopkins, J. L.; Jeanfavre, D. D.; Barney, K. L.; Kelly, T. A.; Grygon, C. A., J. Am. Soc. Mass Spectrom. 2003, 14 (1), 8-13.

165. Keetch, C. A.; Hernandez, H.; Sterling, A.; Baumert, M.; Allen, M. H.; Robinson, C. V., Anal. Chem. 2003, 75 (18), 4937-4941.

166. Smith, J. E.; Wang, L.; Tan, W., Trends Anal. Chem. 2006, 25 (9), 848-855.

167. Hu, F.; Zhang, H.; Lin, H.; Deng, C.; Zhang, X., J. Am. Soc. Mass Spectrom. 2008, 19 (6), 865-73.

168. Marszall, M. P.; Moaddel, R.; Kole, S.; Gandhari, M.; Bernier, M.; Wainer, I. W., Anal. Chem. 2008, 80 (19), 7571-7575.

169. Choi, Y.; van Breemen, R. B., Comb. Chem. & High Throughput Screen. 2008, 11 (1), 1-6.

170. Moaddel, R.; Marszall, M. P.; Bighi, F.; Yang, Q.; Duan, X.; Wainer, I. W., Anal. Chem. 2007, 79 (14), 5414-5417.

171. Jonker, N.; Kretschmer, A.; Kool, J.; Fernandez, A.; Kloos, D.; Krabbe, J. G.; Lingeman, H.; Irth, H., Anal. Chem. 2009, 81 (11), 4263-4270.

172. Raverot, V.; Lopez, J.; Grenot, C.; Pugeat, M.; Dechaud, H., Anal. Chim. Acta 2010, 658 (1), 87-90.

173. Zhu, X. S.; Duan, D. Y.; Publicover, N. G., Analyst 2010, 135 (2), 381-389.

174. Fukuda, N.; Ishii, J.; Tanaka, T.; Fukuda, H.; Ohnishi, N.; Kondo, A., Biotechnol. Prog. 2008, 24 (2), 352-357.

175. Wang, K. Y.; Chuang, S. A.; Lin, P. C.; Huang, L. S.; Chen, S. H.; Ouarda, S.; Pan, W. H.; Lee, P. Y.; Lin, C. C.; Chen, Y. J., Anal. Chem. 2008, 80 (16), 6159-6167.

176. Tsai, H. Y.; Hsu, C. F.; Chiu, I. W.; Fuh, C. B., Anal. Chem. 2007, 79 (21), 8416-8419.

177. Chou, P. H.; Chen, S. H.; Liao, H. K.; Lin, P. C.; Her, G. R.; Lai, A. C. Y.; Chen, J. H.; Lin, C. C.; Chen, Y. J., Anal. Chem. 2005, 77 (18), 5990-5997.

178. Li, J. S.; Ge, J. P.; Yin, Y. D.; Zhong, W. W., Anal. Chem. 2008, 80 (18), 7068-7074.

179. Annis, D. A.; Athanasopoulos, J.; Curran, P. J.; Felsch, J. S.; Kalghatgi, K.; Lee, W. H.; Nash, H. M.; Orminati, J. P. A.; Rosner, K. E.; Shipps, G. W.; Thaddupathy, G. R. A.; Tyler, A. N.; Vilenchik, L.; Wagner, C. R.; Wintner, E. A., Int. J. Mass Spectrom. 2004, 238 (2), 77-83.

180. Comte, M.; Maulet, Y.; Cox, J., Biochem. J. 1983, 209 (1), 269-72.

181. Johnson, J. D.; Wittenauer, L., Biochem. J. 1983, 211 (2), 473-479.

182. Vandonselaar, M.; Hickie, R.; Quail, J. W.; Delbaere, L. T. J., Nat. Struct. Biol. 1994, 1 (11), 795-801.

183. Levin, R.; Weiss, B., Mol. Pharmacol. 1977, 13 (4), 690-697.

184. Zhang, J. H.; Chung, T. D. Y.; Oldenburg, K. R., J. Biomol. Screen. 1999, 4 (2), 67-73.

185. Paliyath, G.; Poovaiah, B. W., Plant Cell Physiol. 1985, 26 (1), 201-9.

186. Cheng, Y.; Prusoff, W. H., Biochem. Pharmacol. 1973, 22 (23), 3099-3108.

2.8 Appendix

Supporting Information – Experimental

All assays were conducted in 48-well, polystyrene, microwell plates. Prior to use, the magnetic beads (MB) were washed as per manufacturer's instructions. Briefly, the supernatant was removed from a 200 μL aliquot of stock suspension, and the MB were washed twice in 500 μL of wash buffer (50 mM sodium phosphate, 300 mM NaCl, 10 mM imidazole) and resuspended to a total volume of 200 μL in assay buffer (20 mM Tris-HCl, 1 mM $CaCl_2$, pH 7.5).

For protein-fishing, the CaM-conjugated MB were made by incubating 100 pmol of CaM (1.8 μg) with 12 μL of washed MB suspension (2.4 mg of beads) in a total volume of 100 μL of assay buffer for 15 minutes at room temperature. The beads were washed three times with 100 μL of assay buffer before pre-incubating the CaM-MB with the

known inhibitor, R24571 (100 μL of 10 μM compound) or with assay buffer (100 μL), as the control. To this solution, 10 μL of Mel (5, 10, 20, or 30 μM) was added to provide each protein in a 2:1, 1:1, 1:2, or 1:3 CaM:Mel molar ratio, respectively. The plate was incubated on an orbital shaker for 15 min to allow affinity capture of Mel, before the supernatant was removed and the CaM-MB were washed three times with 100 μL of buffer. The beads were subsequently incubated in 100 μL of 1% acetic acid in 1:1 (v:v) methanol:water for 30 min to remove bound CaM and Mel, and the eluate was collected and retained for analyses by ESI-MS/MS.

Protein-complex fishing was completed by pre-incubating 100 pmol of CaM (1.8 μg) for 30 minutes with the known inhibitor R24571 (100 μL of 10 μM compound) or assay buffer (100 μL) as the control. To this solution, 10 μL of Mel (5, 10, 20, 30 μM) was added to provide each protein in a 2:1, 1:1, 1:2, or 1:3 CaM:Mel molar ratio, respectively. The plate was incubated on an orbital shaker for 15 min to allow affinity capture of the intact CaM-Mel complex. The supernatant was removed and the CaM-MB were washed three times with 100 μL of buffer. The beads were subsequently incubated in 100 μL of 1% acetic acid in 1:1 (v:v) methanol:water for 30 min to remove bound CaM and Mel, and the eluate was collected and retained for analyses by ESI-MS/MS.

Supporting Information – Results and Discussion

Data obtained during optimization of the assay are shown in Figure S2.1. Figure S2.1A shows a comparison of absolute Mel recovery between the two approaches, indicating that protein fishing is more efficient as more Mel is recovered using a lesser volume of

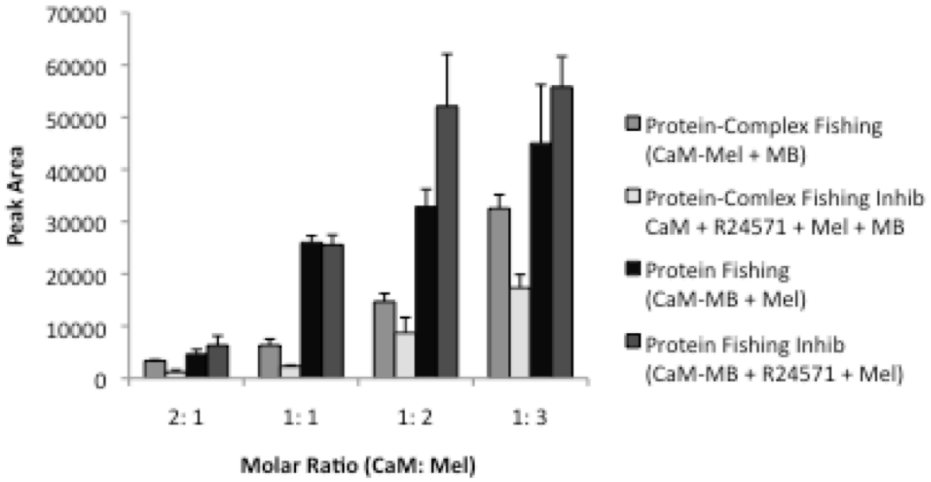

A)

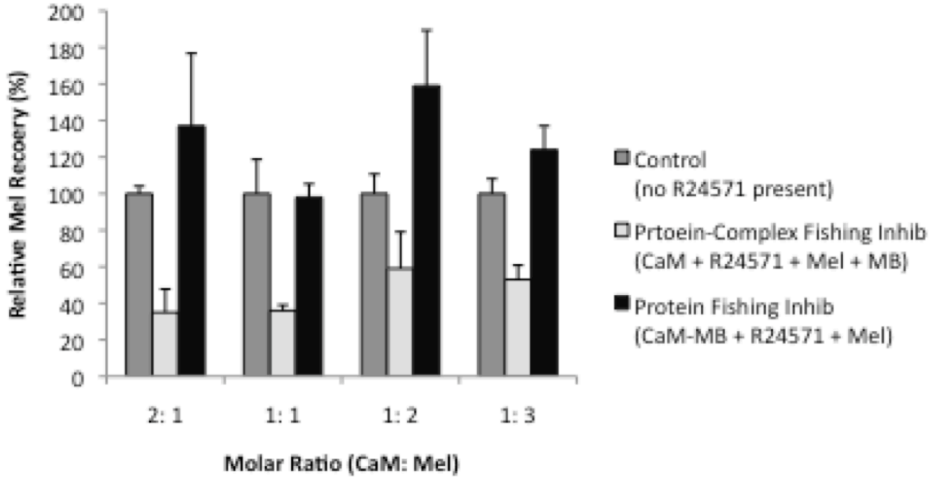

B)

Figure S2.1: Comparison of melittin (Mel) recovery with protein-complex fishing versus protein fishing. A) Comparison of absolute Mel recovery between the two approaches shows that protein fishing is more efficient and more Mel is recovered using a lesser volume of MB. The decreased efficiency of complex fishing is likely due to reduced accessibility of the polyhistidine-tag to the Ni(II) on the MB surface within the intact complex. B) Normalized data for Mel recovery shows inhibition of the CaM-Mel interaction with protein-complex fishing, but not with protein fishing. Reduced Mel recovery in the presence of R24571, a Ca^{2+}-competitive inhibitor, was not observed with protein fishing likely due to obstructed access to calcium binding sites when CaM is pre-bound to the magnetic bead. Furthermore, a 1:1 CaM:Mel molar ratio gave the largest difference between the control and inhibited sample.

MB. The decreased efficiency of complex fishing is likely due to reduced accessibility of the polyhistidine-tag to the Ni(II) on the MB surface within the intact complex. Figure S2.1B shows the normalized data for Mel recovery upon inhibition of the CaM-Mel interaction with protein-complex fishing and protein fishing. Reduced Mel recovery in the presence of R24571, a Ca^{2+}-competitive inhibitor, was observed for protein-complex fishing, but was not observed with protein fishing likely due to obstructed access to calcium binding sites when CaM is pre-bound to the magnetic bead. The data also demonstrate that a 1:1 CaM:Mel molar ratio gave the largest difference between the control and inhibited sample.

Mass Encoded Libraries and Activity Data

Table S2.1 summarizes the activity, and the active compound, if applicable, for each mixture that was assayed. The identity of all compounds in each mixture is available upon request from the corresponding author.

Table S2.1: Activity of Small Molecule Mixtures

Mixture	Activity/Modulator	Known/Spiked/Discovered
1	Inactive	–
2[b]	Active - (-)-Epicatechin	Known
3[c]	Active - Pempidine Tartrate	Discovered
4[c]	Active - Methylbenzethonium	Discovered
5[a]	Active - R24571	Spiked
6	Inactive	–
7	Inactive	–
8	Inactive	–
9	Inactive	–
10[a]	Active - Fluphenazine	Spiked

11[b]	Active - Caffeic Acid	Known
12	Inactive	–
13	Inactive	–
14	Inactive	–
15	Inactive	–
16	Inactive	–
17	Inactive	–
18[b]	Active - (+/-)-Catechin	Known
19	Inactive	–
20	Inactive	–
21	Inactive	–
22	Inactive	–
23	Inactive	–
24	Inactive	–
25	Inactive	–
26[a]	Active - Trifluoperazine	Spiked
27	Inactive	–
28	Inactive	–
29	Inactive	–
30	Inactive	–
31	Inactive	–
32	Inactive	–
33	Inactive	–
34	Inactive	–
35	Inactive	–
36	Inactive	–
37	Inactive	–
38	Inactive	–
39	Inactive	–
40	Inactive	–
41	Inactive	–
42	Inactive	–
43	Inactive	–
44	Inactive	–
45	Inactive	–
46	Inactive	–
47	Inactive	–
48	Inactive	–
49	Inactive	–
50	Inactive	–

a – Mixtures spiked with a known modulator
b – Mixtures containing a naturally occurring modulator that was already within the bioactive library
c – Newly discovered modulator that was found during the mixture screen of 1000 bioactives

Chapter Three

Magnetic "Fishing" to Study Calmodulin/SOX9

The following chapter is intended to be submitted as a full article to the journal *ChemBioChem*, under the authorship of Meghan J. McFadden, Todd Hryciw, Arthur Brown, Murray S. Junop, and John D. Brennan. I developed all experimental protocols, completed all data collection and analysis, and prepared the first draft of the manuscript. Editorial input was given by Dr. Junop and Dr. Brennan to generate the final paper. The work was initiated through collaboration with Dr. Hryciw and Dr. Brown from Robarts Research Institute, Western University.

Chapter Three: Magnetic "Fishing" to Study Calmodulin/SOX9

3.1 Abstract

The CaM/SOX9 interaction is a promising new target for the treatment of spinal cord injuries. Disruption of CaM/SOX9 by known anti-CaM compounds has been demonstrated *in vivo*, but there have not yet been quantitative studies to characterize this interaction and its modulation by small molecule antagonists. A magnetic "fishing" assay was previously developed using a CaM-based model system, and therefore presents an efficient way to determine the binding affinity for interaction of CaM with the CaM-binding domain of SOX9 (SOX-CAL), and to assess the potency of known anti-CaM compounds. Using SOX-CAL as an antagonist of the original CaM/Mel model system, the binding affinity of CaM/SOX-CAL was determined to be 27 ± 9 nM, indicating high affinity interaction via CaM's traditional hydrophobic channel. An inhibition study involving three known CaM antagonists against CaM/SOX-CAL led to the observation of two distinct types of complex; one formed through high-affinity interaction, and a second lower affinity complex. The results of magnetic fishing experiments are complimented with fluorescence spectroscopy data to provide evidence for a low-affinity binding site for SOX-CAL interaction with CaM. Future investigations of this novel interaction *in vivo* will be essential to determining if low-affinity binding occurs as an artifact of *in vitro* conditions, or is an important missing piece of information to understanding CaM-mediated nuclear import of transcription factor SOX9.

3.2 Introduction

Damage to the central nervous system (CNS) severely impacts quality of life and can lead to permanent deficits in cognition and motor function. The severity and irreversibility of symptoms following CNS injury result from loss of intricate and specific neural connections that are created and refined during embryonic growth. Following CNS damage, such as spinal cord injury (SCI), there is an immediate glial cellular response to protect affected neurons from further damage;[187, 188] however, persistence of this scar tissue is a major impediment for the axonal regeneration that is necessary for recovery of function. Consequently, various approaches to modulate the pathways involved in glial scar formation are being investigated and could potentially be developed into novel treatment strategies to reduce the adverse effects of SCI.[187, 189]

The glial scar at the site of SCI is composed primarily of reactive astrocytes and chondroitin sulfate proteoglycans (CSPGs).[190-193] CSPGs are especially detrimental to neural regeneration by both repelling axonal outgrowth and by inhibiting growth promoting molecules.[194-198] As a result, an emerging strategy to enhance neural regeneration is to reduce levels of CSPGs by inhibiting expression of the essential proteins and enzymes used in proteoglycan biosynthesis. Glial scar CSPGs require chondroitin 4-sulfotransferase (C4ST)[199] and xylosyltransferase-I and –II (XT-1 and XT-II)[200, 201] to synthesize and add the chondroitin sulfate side chains to the protein core. These enzymes and core proteins are all part of the same CSPG biosynthetic gene (CBG) battery, which is regulated by the SOX9 transcription factor.[202-204] Since many genes required for CSPG production are under the control of this single transcription factor,

reduction in the activity of SOX9 indirectly, but efficiently, disrupts CSPG biosynthesis. Recent work has demonstrated that following SCI, SOX9 conditional knockout mice show decreased levels of CSPG at the lesion site and improved recovery of hind limb motor function,[202] thus validating SOX9 as a target for SCI therapies.

SOX9 is expressed in the cytosol and requires translocation to the nucleus. Nuclear import of SOX9 is mediated by two nuclear localization sequences (NLS) that flank a high mobility group DNA binding domain (HMG box), where the N-terminal NLS binds calmodulin (CaM)[205-207] and the C-terminal NLS interacts with importin-β[208, 209]. The CaM-binding domain is highly conserved within the SRY-related HMG box (SOX) family of transcription factors and their namesake, sex-determining region Y protein (SRY).[205, 207, 210] Although redundant nuclear import mechanisms exist, the importance of the calcium-dependent CaM-mediated pathway is highlighted by a significant decrease in nuclear localization and transcriptional activity of SRY and SOX9 in the presence of known anti-CaM compounds, calmidazolium (R24571) and W7.[205, 206, 211, 212] The ability to use small molecules to modulate gene expression regulated by SOX9 provides a way of controlling the expression of CSPG proteins in a temporary and dose-dependent manner, which is advantageous for development of a therapeutic approach.

Current data from *in vivo* research indicates CaM/SOX9 to be a potentially powerful therapeutic target for the treatment of SCI, however there is a lack of quantitative *in vitro* studies to characterize this interaction and its disruption by small molecule modulators. We previously reported a magnetic "fishing" assay to monitor protein-protein interactions and validated the method with a CaM-based model system

(Figure 2.1).[213] In addition to high-throughput screening to identify small molecule modulators, magnetic "fishing" was used to determine dissociation inhibitory constants (K_I) for a selection of known antagonists against interaction of CaM with melittin (Mel). The structural features of the Mel peptide, a short 26-residue basic amphiphilic helix, are shared among CaM-binding domains of many proteins, including that of SOX9. Given the structural similarities between Mel and SOX9, magnetic fishing was therefore thought to be an ideal approach to carry out quantitative studies of CaM/SOX9 and modulation of this interaction by small molecule antagonists.

In the present study, the magnetic "fishing" assay was applied to characterize the interaction of CaM with transcription factor SOX9, represented by a synthetic 17-residue peptide corresponding to its CaM-binding domain (SOX-CAL). Using the original design of the assay,[213] the binding affinity of SOX-CAL was determined through dose-dependent inhibition of CaM/Mel, indicating high-affinity CaM/SOX-CAL interaction. However, substitution of SOX-CAL as the bait protein for magnetic fishing revealed a novel interaction between the target peptide and CaM, which is investigated using a combination of magnetic fishing and intrinsic fluorescence spectroscopy.

3.3 Materials and Methods

Materials – PureProteome™ Nickel Magnetic Beads (10 mm diameter, 0.2 g MB/mL) and human recombinant calmodulin with an N-terminal hexahistidine tag (His_6-CaM) were purchased from EMD Millipore (Billerica, MA). Human recombinant calmodulin was purchased from Cedarlane (Burlington, ON). A peptide corresponding to the CaM-

binding domain of SOX9 (residues 106-122, SOX-CAL) was synthesized with an N-terminal acetyl group and a C-terminal amide group by EZBiolab (Carmel, IN). Chlorpromazine hydrochloride (CPZ), calmidazolium chloride (R24571), melittin from honeybee venom (Mel), and methylbenzethonium chloride were purchased from Sigma-Aldrich (Oakville, ON). All other reagents were of the highest available grade and used as received.

Determination of the Dissociation Constant for CaM/SOX-CAL – A dose-dependent response curve for disruption of the calmodulin-melittin (CaM/Mel) complex (K_D = 3 nM)[214, 215] by the SOX-CAL peptide was developed using a magnetic "fishing" assay. Application of the magnetic "fishing" assay to determine IC_{50} and K_I values is described elsewhere.[213] In brief, 100 μL solutions of 1 μM His_6-CaM were pre-incubated with increasing concentrations of SOX-CAL (2.5 to 250 μM) or buffer (20 mM Tris, 1 mM $CaCl_2$, pH 7.5) to use as a control. Following a 30-minute incubation, Mel (1 μM) was added to each solution (1:1 CaM:Mel mol ratio) and incubated for 5 min before the addition of 40 μL of Ni(II)-charged magnetic beads. Solutions were placed on an orbital shaker for 15 minutes to allow affinity-capture of protein complexes. The magnetic beads were washed three times for 1 min each with 100 μL of buffer, before incubation in 100 μL of 1% acetic acid in 1:1 (v/v) methanol/water for 30 min to elute bound protein for analysis by electrospray ionization tandem mass spectrometry (ESI-MS/MS). Injections of 10 μL of each sample were made at 15 μL/min (0.5% acetic acid in 1:1 (v/v) methanol/water) and the total MS/MS signal for the fragmentation of 570.5 m/z

([Mel+5H]$^{5+}$) to three product ions 563.0, 665.5, and 670.0 m/z was monitored over time. The total integrated peak area of each sample was normalized by letting the peak area for the buffer control correspond to 100% Mel recovery. A plot of relative signal versus log([SOX-CAL (M)]) was fitted with a four-parameter Hill equation using SigmaPlot 12, and the IC_{50} value was taken as the concentration of SOX-CAL that resulted in 50% relative Mel recovery. Using the Cheng-Prusoff relationship,[216] the IC_{50} value was converted to the inhibitory dissociation constant (K_I) for CaM/SOX-CAL.

Magnetic "Fishing" for CaM/SOX-CAL – Binding reactions (100 μL) were prepared using 1 μM SOX-CAL in 20 mM Tris, 1 mM $CaCl_2$, pH 7.5 in the presence of increasing amounts of His_6-CaM (100 nM to 2 μM) or a non-binding control protein, His_6-XRCC4. Following a 15-min incubation, magnetic fishing was carried out as described above, except the volume of magnetic beads was reduced to 15 μL, and the wash steps were increased to 15 min. For ESI-MS/MS analyses, the fragmentation of three SOX-CAL ions ([M+3H]$^{3+}$: 711.5 m/z to 697.0, 705.5, 889.0, and 967.0 m/z; [M+4H]$^{4+}$: 534.0 m/z to 543.0, 573.5, 608.5, 666.5, 682.0, and 751.0 m/z; and [M+5H]$^{5+}$: 427.5 m/z to 329.5, 458.5, 493.5, 524.0, and 573.5 m/z) were monitored concurrently over time, and the sum of the integrated peak areas was used to represent the total SOX-CAL signal for each sample.

Development of Dose-Dependent Response Curves for Anti-CaM Compounds – Dose-dependent response curves were developed for the disruption of CaM/SOX-CAL by

known CaM antagonists, CPZ, R24571, and Mel. Solutions of His_6-CaM (1 μM) were incubated for 30 min with increasing amounts of CPZ (500 nM to 500 μM), R24571 (100 nM to 125 μM), or Mel (100 nM to 100 μM), in addition to two control compounds, caffeine (500 nM to 500 μM) or benzamidine (500 nM to 500 μM), in 2.5% (v/v) DMSO in buffer. As a protein control, CPZ (500 nM to 500 μM) was also incubated with His_6-XRCC4 (1 μM). SOX-CAL (1 μM) was added to each solution and allowed to bind for 5 min before magnetic fishing and ESI-MS/MS analyses were carried out as described above for CaM/SOX-CAL complex. In the case of Mel, the MS/MS signal for $[SOX\text{-}CAL+3H]^{3+}$ (711.5 m/z) was ignored due to interferences from $[Mel+4H]^{4+}$ (712.5 m/z). The total SOX-CAL signal for each sample was normalized by letting the value for the no-compound control correspond to 100%, and these values were plotted versus log([compound (M)]).

Tryptophan Fluorescence Polarization Measurements – To assess the effect of CPZ on CaM/SOX-CAL interaction, samples containing 100 nM SOX-CAL in 20 mM Tris, 1 mM $CaCl_2$, pH 7.5 were titrated with human recombinant CaM (50 nM to 1 μM) in the presence or absence of 50 μM CPZ while polarization measurements were collected on a Cary Eclipse Fluorescence Spectrophotometer using a 1-cm pathlength quartz cell. The single tryptophan residue in SOX-CAL was probed at room temperature (20 ± 1 °C) using excitation and emission wavelengths of 295 nm and 355 nm, respectively. The signal was integrated for 2 sec with excitation and emission band pass widths of 10 nm.

Collection of Tryptophan Emission Spectra – Self-association of Mel and SOX-CAL were assessed by intrinsic fluorescence to monitor changes in maximum emission wavelength upon titration with salt. All fluorescence spectra were collected at room temperature (20 ± 1 °C) on a Cary Eclipse Fluorescence Spectrophotometer using a 1-cm pathlength quartz cell. The single tryptophan residue in Mel or SOX-CAL (1 μM in 20mM Tris, 1 mM $CaCl_2$, pH 7.5) was excited at 280 nm and emission spectra collected from 320 to 400 nm as each sample was titrated with NaCl (0.25 to 2 M). Spectra were measured in 1-nm increments with excitation and emission band pass widths of 5 nm. All spectra were background corrected using those collected for the titration of buffer with equal amounts of NaCl, and normalized to maximum intensity observed for each sample.

3.4 Results and Discussion

Determination of the Dissociation Constant for CaM/SOX-CAL – The magnetic "fishing" assay was previously validated through the determination of dissociation constants for known anti-CaM compounds against a complex of CaM/Mel, thus using SOX-CAL as an antagonist of this model system provides a simple method to characterize its interaction with CaM. Magnetic fishing for CaM/Mel was carried out in the presence of increasing concentrations of SOX-CAL, and the relative amount of Mel recovery in each sample was determined by ESI-MS/MS. Greater amounts of SOX-CAL resulted in decreased recovery of Mel, and a plot of relative signal versus log([SOX-CAL] (M)) shows dose-dependent modulation of CaM/Mel by SOX-CAL (Figure 3.1). The data was fit with a 4-

parameter Hill equation and the concentration of SOX-CAL that resulted in 50% relative Mel signal (IC_{50}) was determined to be 9.2 ± 2.8 μM, and subsequently converted to a inhibitory dissociation constant (K_I) of 27 ± 9 nM. These results indicate a specific, high-affinity interaction between SOX-CAL and CaM.

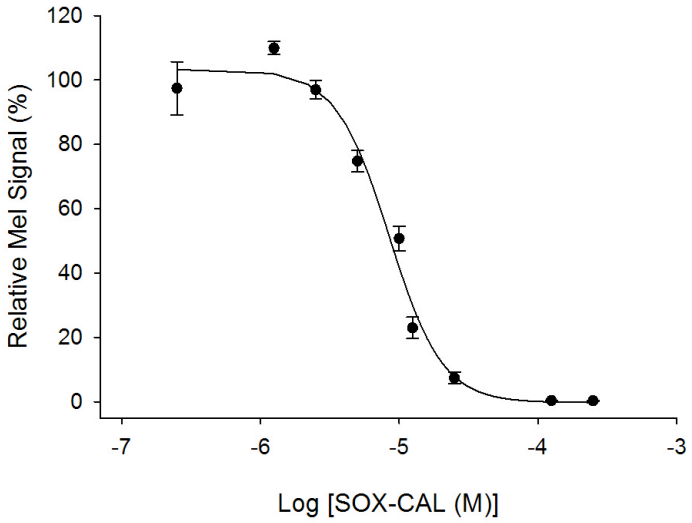

Figure 3.1: Dose-dependent response curve for the disruption of CaM/Mel by SOX-CAL. A magnetic "fishing" assay was used to recover CaM/Mel in the presence of increasing concentrations of SOX-CAL. The resulting IC_{50} value (9.2 ± 2.8 μM) was subsequently converted to the inhibitory dissociation constant for SOX-CAL (K_I = 27 ± 9 nM).

The binding of CaM to HMG-containing proteins, such as SRY and SOX9, is well established, yet few analytical studies have been conducted to quantify the affinity of these interactions. Dissociation constants have been reported for interaction of CaM with the HMG box from SRY that range from 0.43 ± 0.07 nM[212] to 75 ± 10 nM[205], suggesting that this class of proteins displays strong affinity for CaM. Although no data

is available for CaM/SOX9, the value determined by magnetic fishing is within the range of literature values reported for the closely related SRY protein.

A helical structure consisting of basic and hydrophobic amino acids is highly conserved between Mel and other CaM-binding domains,[217-219] and most undergo a common mode of interaction, where the target helix is engulfed within a hydrophobic channel between two globular lobes of Ca^{2+}-activated CaM.[214, 215, 220-225] SOX-CAL, the CaM-binding domain of SOX9, has these same structural features and is expected to interact with CaM in the typical fashion described in the literature. Dose-dependent displacement of Mel observed during the assay, with a nanomolar affinity constant, further supports that the high-affinity SOX-CAL interaction is occurring within the main hydrophobic channel of CaM.

Magnetic "Fishing" for CaM/SOX-CAL – Despite many structural similarities, the direct substitution of SOX-CAL for Mel in the original "fishing" assay was unsuccessful and adaptation of magnetic fishing for CaM/SOX-CAL required further optimization. Preliminary work showed that decreasing the volume of magnetic beads from 40 to 15 μL, and increasing each wash step from 1 to 15 min, significantly improved the specificity and reproducibility of SOX-CAL recovery. With these modifications, increasing amounts of His_6-CaM or His_6-XRCC4 control protein were used to recover SOX-CAL from solution by magnetic fishing. The MS/MS signal for SOX-CAL increases with increasing amount of His_6-CaM used in the assay before reaching a plateau around 1:1 mol ratio of CaM:SOX-CAL (Figure 3.2A). The data reveal a

moderate amount of nonspecific binding, where SOX-CAL is recovered in the absence of either His_6-protein (~ 20% of max signal), or by fishing with His_6-XRCC4, which shows ~ 35−45% SOX-CAL signal compared to that for an equal amount of CaM. In an attempt to more closely examine the signal change resulting from specific CaM/SOX-CAL interaction, the peak area for XRCC4 was subtracted from that for CaM for each concentration. The corrected SOX-CAL signal was plotted against concentration of His_6-CaM and fitted with a one-site ligand binding equation (Figure 3.2B), giving an apparent dissociation constant ($K_{D,app}$) for CaM/SOX-CAL of 400 ± 160 nM. It is important to note that the $K_{D,app}$ from this data would over-estimate the true value because the

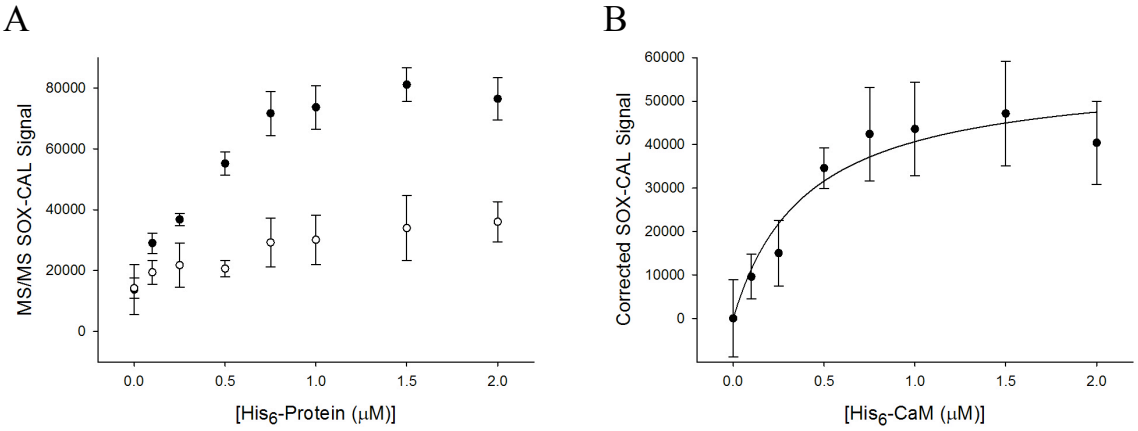

Figure 3.2: Magnetic "fishing" for CaM/SOX-CAL. A) Magnetic fishing was used to recover SOX-CAL from solution using increasing amounts of His_6-CaM (●), or His_6-XRCC4 (○) as a non-binding control. B) A binding curve was developed by subtracting the signal for XRCC4 from each equivalent point for CaM to correct for nonspecific interactions, giving an apparent binding affinity for CaM/SOX-CAL of 400 ± 160 nM.

concentrations of protein used in the assay are well in excess of the estimated binding affinity (Figure 3.1). Even though accurate determination of the dissociation constant is

not possible, the clear hyperbolic trend to peptide recovery with apparent nanomolar binding affinity is consistent with formation of a specific high-affinity complex of CaM/SOX-CAL.

Modulation of CaM/SOX-CAL with Known CaM Antagonists – Small molecule modulation of the CaM/SOX9 interaction is a promising new treatment strategy for SCI, and previous *in vivo* studies have shown that known anti-CaM compounds, such as calmidazolium (R24571)[206] and chlorpromazine (CPZ),[226] are able to inhibit SOX9 nuclear localization and transcription activity. Both CPZ (K_I = 5 μM),[227, 228] a phenothiazine-derived drug that makes multiple contacts within the hydrophobic channel of CaM, and R24571 (K_I = 2−3 nM),[224, 229, 230] a potent inhibitor that binds to its calcium-binding domains, and are established antagonists of CaM-based interactions; however, quantitative inhibition data has yet to be developed for interaction with SOX9 in particular. Therefore R24571 and CPZ, putative high and low affinity modulators, were chosen along with Mel (K_I = 3 nM)[215] as antagonists for modulation studies using magnetic fishing for CaM/SOX-CAL.

Prior to magnetic fishing, His_6-CaM was incubated with increasing concentrations of the three antagonists, in addition to two control compounds, caffeine and benzamidine. Surprisingly, a plot of relative signal versus log([compound (M)]) does not display dose-dependent inhibition, with the SOX-CAL signal initially increasing in the presence of R24571, CPZ, and Mel (Figure 3.3). After reaching a maximum, higher concentrations of Mel and CPZ show a reduction in SOX-CAL recovery; however, the maximum

R24571 concentration that could be used in the assay was limited by its solubility and the curve does not extend far enough to view this trend with this compound. The change in SOX-CAL signal is dose-dependent for each antagonist, with half-maximum signal occurring at different concentrations for R24571 (~ 5 μM), Mel (~ 2 μM), and CPZ (~ 35 μM). No significant effect was observed for either control compound, or for assays using the XRCC4 control protein, suggesting that the signal enhancements observed for R24571, Mel, and CPZ reflect specific changes to CaM/SOX-CAL interaction. Although magnetic fishing is detecting modulation of the target interaction, it is not yet known why

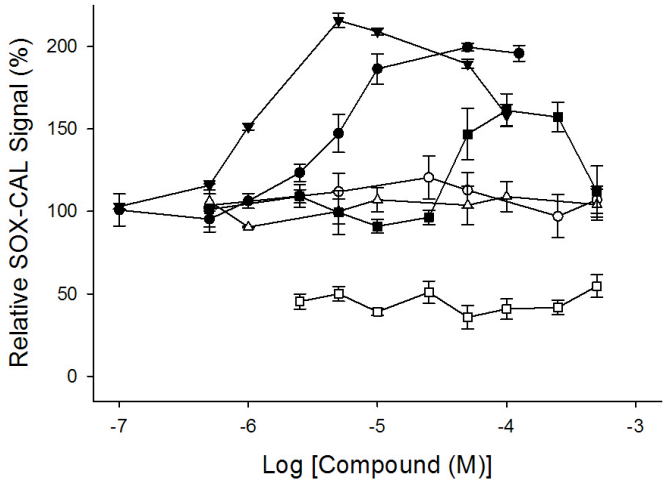

Figure 3.3: Modulation of CaM/SOX-CAL by known CaM antagonists. Prior to magnetic fishing, His_6-CaM was incubated with increasing concentrations of known CaM antagonists, R24571 (●), Mel (▼), and CPZ (■), and two control compounds, caffeine (○) and benzamidine (△). As a protein control, CPZ was also assayed against His_6-XRCC4 (□, relative signal as compared to no-compound CaM control). Although CaM antagonists would be expected to decrease SOX-CAL recovery, the SOX-CAL signal increases in a dose-dependent manner for R24571 (half-maximum ~ 5 μM), Mel (half-maximum ~ 2 μM), and CPZ (half-maximum ~ 35 μM).

SOX-CAL recovery appears to increase, rather than decrease, in the presence of low concentrations of known CaM antagonists.

To confirm that the interaction and recovery of CaM/antagonist complexes during the assay were not artifacts, magnetic fishing for CaM/SOX-CAL was repeated in the presence of CPZ and caffeine, while monitoring MS/MS signals for both SOX-CAL and the respective compound concurrently (CPZ: 319.0 m/z to 239, 246, and 274 m/z; or caffeine: 195.0 m/z to 138.0 m/z). XRCC4 was also used as a protein control for the CPZ interaction. As shown in Figure 3.4, the signal for CPZ increases proportionately with original concentration of compound assayed, during which the signal for SOX-CAL increased (data not shown). In contrast, significantly less CPZ is recovered using the

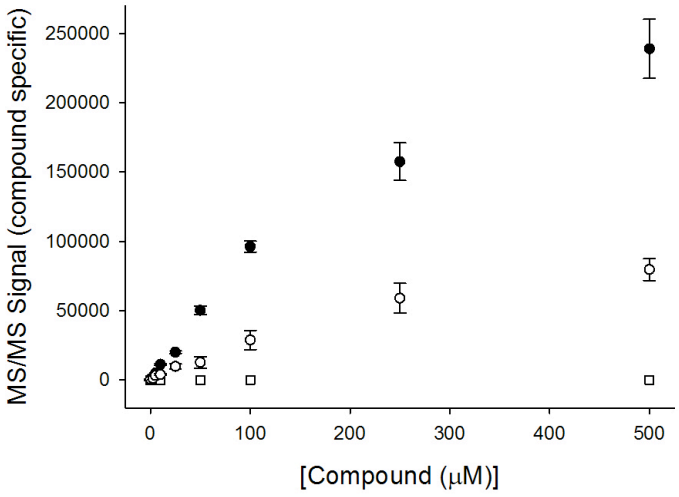

Figure 3.4: Monitoring CaM/antagonist interactions. CaM was incubated with the known antagonist, CPZ (●), and caffeine as a control compound (□), before the addition of SOX-CAL. XRCC4 was also included as a nonbinding protein control for CPZ (○). Following magnetic fishing, the amount of CPZ or caffeine recovered during the assay was determined using specific MS/MS signals for each compound.

nonbinding control protein, and no detectable level of caffeine is recovered by CaM. Ionization efficiencies of the two compounds would obviously differ, but given that the signal for caffeine remains below the limit of detection for the analysis software, the data provides strong evidence for a specific CaM/CPZ interaction.

The modulation study using magnetic fishing reveals that known CaM antagonists are able to specifically bind CaM and, in some way, modulate its interaction with SOX-CAL. If CaM/antagonist complexes are forming as described in the literature, then it is reasonable to conclude that peptide interactions with CaM via the high-affinity binding site would be disrupted by R24571, CPZ, and Mel.[215, 224, 227-234] Recovery of SOX-CAL by magnetic fishing, in spite of blocking access to the primary hydrophobic channel of CaM, therefore suggests that an alternative interaction must be occurring. Analysis of standard solutions of SOX-CAL with increasing amounts of CPZ showed a consistent signal for the peptide, and therefore ionization efficiency is unchanged by the presence of antagonist (data not shown). Nonspecific binding is a recurring issue for protein interaction studies, however control samples did not show the same signal increase, and the addition of salt to the assay buffer to mitigate electrostatic interactions had no appreciable effect on SOX-CAL recovery. Further support of a specific, albeit atypical, CaM/SOX-CAL interaction is the apparent dose-dependence to the signal increase, in order of relative antagonist affinity.

The classic CaM/peptide complex presents a single Ca^{2+}-loaded CaM collapsed around a basic amphiphilic target helix that is thread through a hydrophobic channel.[214, 215, 221-225] Unconventional interactions of CaM with target peptides can be found in the

literature,[235-242] including modes of CaM/Mel binding involving inverted conformations of Mel[243] and the formation of a low-affinity complex in the absence of calcium.[215, 244] This apo-CaM/Mel complex showed increased susceptibility to denaturants, and was able to bind multiple Mel per molecule of CaM at high concentrations of peptide.[244] Phenothiazine class drugs are also known to bind CaM at two distinct binding sites, one high affinity (K_D = 1 – 30 μM) and one low affinity (K_D = 130 – 500 μM),[227, 228, 245] demonstrating that even model ligands can form atypical CaM-complexes.

The results shown in Figure 3.3 and Figure 3.4 imply that upon disruption of high-affinity interactions by known antagonists, an alternative CaM/SOX-CAL interaction occurs that consequently leads to an apparent increase in SOX-CAL recovery. The underlying cause of the greater SOX-CAL signal produced by this alternative CaM/SOX-CAL interaction is not clear, and several possibilities were considered (Figure 3.5). The first is that CaM/SOX-CAL forms a low-affinity complex, either from incomplete disruption of binding within the hydrophobic channel, or through a distinct secondary binding site similar to those reported for phenothiazines[228, 245, 246] and apo-CaM/Mel.[215, 244] Decreased affinity of CaM/SOX-CAL could result in more extensive denaturation of the complex in the elution solvent compared to its high-affinity counterpart, thereby producing a greater signal for free peptide. A second possibility is that signal enhancement could reflect the low-affinity binding of multiple SOX-CAL peptides to each molecule of CaM, since both phenothiazines and Mel show increased stoichiometry in their low-affinity forms. A third possibility is that increased SOX-CAL recovery could be explained by a change in the oligomeric state of the peptide in the

presence of antagonist. Self-association of SOX-CAL is under consideration because Mel is known to form a tetramer in solution,[247-251] however this behaviour has not been observed for other calmodulin binding peptides. The fourth and final possibility is an inverse antagonist effect causing improved binding affinity, but this represents the least likely option given that R24571, CPZ, and Mel have been solely documented as disruptors of CaM-based interactions.

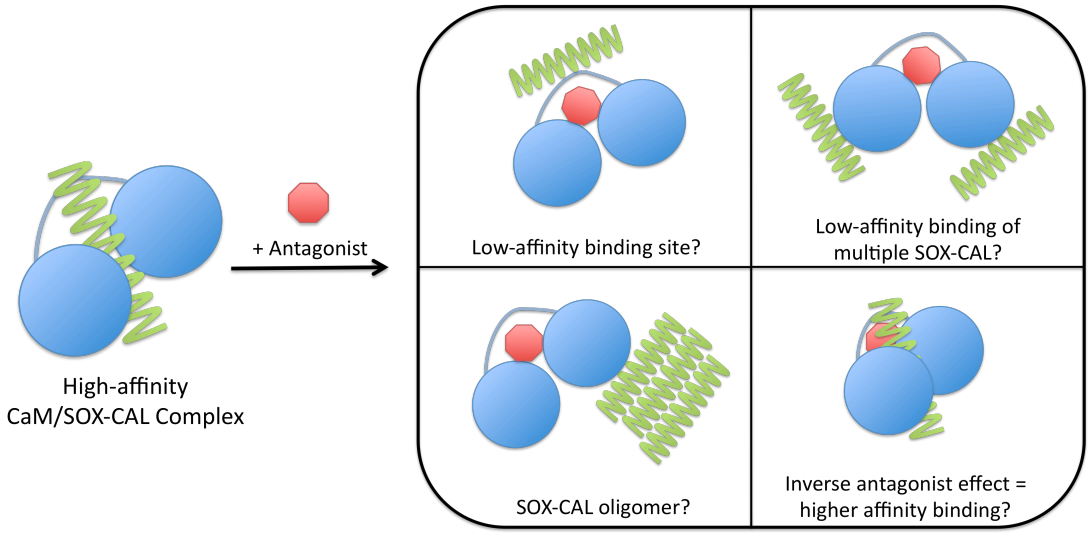

Figure 3.5: Schematic showing possible explanations for increased SOX-CAL recovery observed during the modulation study of known CaM antagonists. Cartoon representation of CaM is shown in blue, the SOX-CAL peptide in green, and an anti-CaM compound in red.

Effect of CPZ on CaM/SOX-CAL Interaction Using Tryptophan Fluorescence Polarization – Two of the proposed explanations for enhanced SOX-CAL recovery by magnetic fishing involve a change in binding affinity, thus it was desirable to examine the effect of CPZ on the CaM/SOX-CAL interaction using a secondary method. A single tryptophan residue in SOX-CAL allowed the use of fluorescence polarization to monitor

its interaction with CaM in the presence and absence of CPZ, and without the use of magnetic beads. Upon titration with CaM, the polarization of SOX-CAL increases from 64 ± 11 mP to 145 ± 7 mP in the absence of CPZ and from 54 ± 12 mP to 135 ± 16 mP with 50 μM CPZ present (Figure 3.6). Although similar changes are observed for both conditions, the initial slope is considerably reduced in the presence of CPZ, which is a clear indication of a weaker interaction. The high protein concentrations used in the assay do not permit calculation of accurate binding constants, but it is clear that the affinity of CaM/SOX-CAL is lower in the presence of CPZ. These findings show that CPZ is disrupting the high-affinity CaM/SOX-CAL interaction, and therefore excludes the possibility that the higher SOX-CAL signal observed during the modulation study is due to a tighter interaction with CaM that allows better recovery of the peptide.

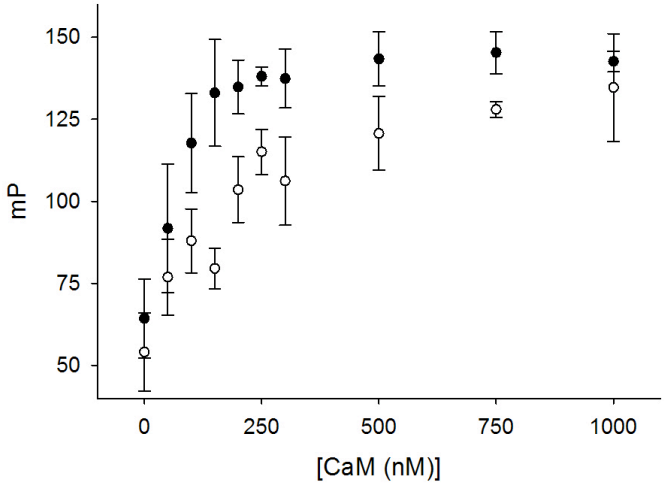

Figure 3.6: Monitoring CaM/SOX-CAL interaction by tryptophan fluorescence polarization. SOX-CAL was titrated with CaM in the absence (○) and presence (●) of 50 μM CPZ. Although similar maximum and minimum values were observed in both conditions, the initial slope is significantly decreased in the presence of antagonist, indicating that CPZ lowers the affinity of CaM/SOX-CAL interaction.

Tryptophan Emission Spectra to Monitor Self-Association of Peptides – Unbound Mel has a high propensity to form a tetramer, creating a woven structure that buries its hydrophobic residues and exposes its many positive charges to the aqueous environment.[247, 248] Self-association of this highly basic and amphiphilic peptide requires a delicate balance between electrostatic repulsion and hydrophobic adhesion, and is strongly influenced by ionic strength.[247-250, 252, 253] The single tryptophan residue of Mel is often used as a probe of peptide conformation by monitoring its large blue-shift in emission maximum from 354 ± 2 nm for the monomer to 339 ± 3 nm for the tetramer or membrane-bound state.[250, 253-257] Note that these values are derived from uncorrected emission spectra, which are acceptable for comparative studies of changes in fluorescence characteristics.[258] SOX-CAL also includes this single tryptophan that shifts emission maximum upon interaction with CaM or DNA,[206] making intrinsic fluorescence a straightforward method to compare self-association behaviour of these two peptides. Upon titration with salt, the emission maximum of Mel blue-shifted from 355 nm in 20 mM Tris, 1mM $CaCl_2$, pH 7.5 to 341 nm in the presence of 2M NaCl (Figure 3.7A). For clarity, only the spectra for 0 M and 2 M NaCl are shown. In contrast, the emission maximum for SOX-CAL remains unchanged at 356 nm after the addition of salt, indicating that solvent exposure of the tryptophan residue is unaffected by increasing ionic strength (Figure 3.7B). A change in SOX-CAL oligomeric state should be accompanied by a visible shift in the emission spectrum as a result of the changing environment, as is seen for the Mel tetramer. It is unlikely that such a small peptide could self-associate without altering the environment of its tryptophan, thus a change in the

oligomeric state of SOX-CAL is discounted as a possible cause for the signal increase during the modulation study with magnetic fishing.

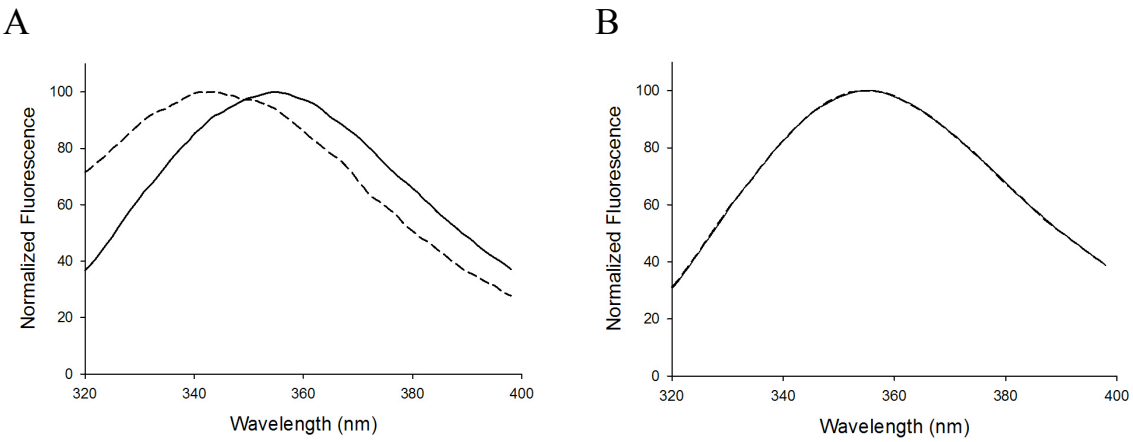

Figure 3.7: Effect of ionic strength on tryptophan emission spectra of Mel and SOX-CAL. A) Normalized emission spectra for 1 μM Mel in 20 mM Tris, 1 mM $CaCl_2$, pH 7.5 (—), and final titration to 2 M NaCl (---), showing a large shift in maximum wavelength from 355 nm to 341 nm, respectively. B) Normalized emission spectra for 1 μM SOX-CAL under same conditions, showing no shift in maximum wavelength.

CaM Interactions in the Presence of High Concentrations of SOX-CAL – Fluorescence-based studies have excluded either increased CaM/SOX-CAL affinity or self-association of the peptide as possible sources for the unexpected signal increase during modulation studies, leaving the possibility of a second low-affinity binding site on CaM for SOX-CAL interaction. Thus far, magnetic fishing experiments have used a constant amount of SOX-CAL with varying amounts of CaM, so it was desirable to investigate the inverse situation by observing CaM interaction in the presence of excess peptide. Complexes of His_6-CaM (1 μM) were isolated by magnetic fishing from binding reactions containing up to 75-fold molar excess of SOX-CAL (2.5 to 75 μM). Magnetic fishing with His_6-

XRCC4 was also run as a control protein to correct each corresponding sample of His_6-CaM for nonspecific binding. The resulting sigmoidal curve presented in Figure 3.8 suggests cooperative binding, where a primary high-affinity interaction assists SOX-CAL to bind at least one other site on CaM. Although structural or functional activation of a second binding site is possible, the data most likely reflect two independent non-identical sites that exist in competing equilibria. Conventional high-affinity binding in the hydrophobic pocket dominates until sufficiently high concentrations of peptide are present to permit the weaker CaM/SOX-CAL interaction to occur. Interaction of SOX-CAL at the low-affinity site would then indirectly depend on saturation of the primary binding pocket, leading to apparent cooperativity in the data. A comparable situation that

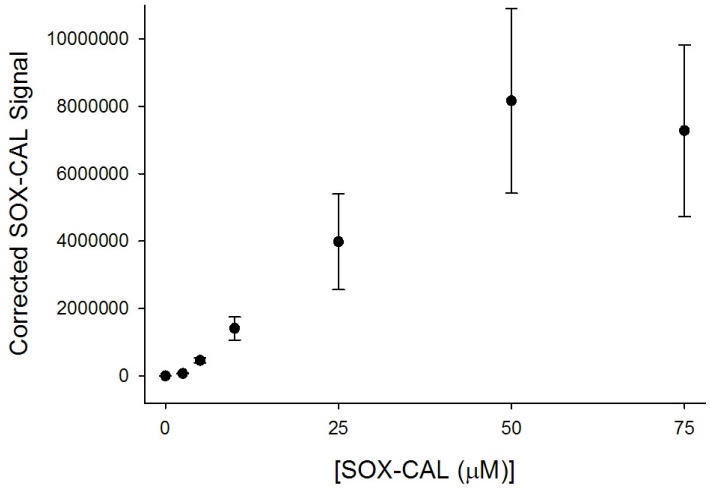

Figure 3.8: Saturation of CaM with high concentrations of SOX-CAL. Magnetic fishing was used to isolate His_6-CaM from solutions containing up to 75-fold molar excess of SOX-CAL. The sigmoid curve most likely reflects two independent and non-identical SOX-CAL binding sites on CaM, where the low-affinity site is only observed upon saturation of high affinity interaction within the primary hydrophobic channel, leading to apparent cooperativity in the data.

involves a shift to a weaker binding site could be occurring in the presence of antagonist, where the hydrophobic channel is occupied or inaccessible, causing magnetic fishing to recover low-affinity CaM/SOX-CAL. During the modulation study, the difference in maximum signal observed, and the concentration at which it occurs, reflect the potency of each antagonist and its ability to compete with SOX-CAL for high-affinity interaction within the primary binding pocket.

Taken together with the results from the fluorescence-based studies, magnetic fishing provides strong evidence for a second low-affinity binding site for interaction of SOX-CAL with CaM. This atypical CaM/SOX-CAL interaction was first evident during the modulation study, where a shift from a high to a low affinity complex produced a greater MS/MS signal for SOX-CAL. Magnetic fishing relies on the use of an organic solvent to dissociate the recovered complex and release free SOX-CAL for MS/MS detection, thus a weaker interaction may generate a higher signal simply as a result of the assay design. It is also possible that low affinity CaM/SOX-CAL complex may exhibit increased stoichiometry, and the SOX-CAL signal is greater owing to the recovery of multiple peptides per molecule of CaM. In the case of low affinity apo-CaM/Mel, up to 5 peptides were bound to each CaM protein.[244] Since both explanations are equally plausible at this time, closer examination will be required to establish the stoichiometry of this novel low-affinity CaM/SOX-CAL interaction.

3.5 Conclusions

The magnetic "fishing" assay has revealed an unexpected CaM/SOX-CAL interaction, and validation of this novel complex is essential. The existence of this novel low-affinity SOX-CAL binding site on CaM must be confirmed, and if so, determination of the stoichiometry and binding constant for interaction will be necessary. Fluorescence spectroscopy (i.e. polarization, FRET) and analytical centrifugation will be useful techniques, however the significance of these *in vitro* findings depends heavily on the physiological relevance of low-affinity CaM/SOX9 interaction. The proposed interaction may likely be an artifact of the *in vitro* assay, where the small size of synthetic peptide (17 residues) could permit interaction at artificial sites or in modified conformations that would not be available to full-length SOX9 (56 kDa). Similar structures and physical properties of CaM-binding peptides mean that SOX-CAL may be accessing a binding site that is intended for a different target. The preference of unbound Mel to form a tetramer[247-251] could provide protection from artificial interactions with CaM, and may also have contributed to the success of using Mel as a model protein for assay development. *In vivo* interaction studies will be essential to search for low-affinity CaM/SOX9 interaction within the context of a cell, and to examine the possibility that a secondary binding site could serve a biological purpose related to CaM-mediated nuclear import of this transcription factor.

Regardless of the mode of interaction, a very important finding from this study is that known CaM antagonists do cause significant modulation of the CaM/SOX-CAL interaction. When Mel, R24571, or CPZ is present, a specific signal change occurs in a

way that directly reflects the ranking of their K_I values. Although it is unknown if full-length SOX9 will participate in the novel low-affinity interaction observed for SOX-CAL, it is clearly shown that known CaM antagonists are able to modulate traditional high-affinity binding of the peptide. In light of previous *in vivo* data demonstrating SOX9 ablation led to improved recovery of function following SCI,[202] the use of small "drug-like" molecules to interfere with CaM-mediated nuclear import of the transcription factor has potential to be a powerful treatment strategy for these devastating injuries.

3.6 Acknowledgement

This work was supported by operating grants: Canadian Institutes of Health Research to MSJ (MOP 89903), Natural Sciences and Engineering Research Council of Canada to JDB. MJM was supported in part by an Ontario Graduate Student Fellowship. JDB holds a Canada Research Chair in Bioanalytical Chemistry and Biointerfaces.

3.7 References

[187] J. R. Faulkner, J. E. Herrmann, M. J. Woo, K. E. Tansey, N. B. Doan, M. V. Sofroniew, *J. Neurosci.* **2004**, *24*, 2143.

[188] T. G. Bush, N. Puvanachandra, C. H. Horner, A. Polito, T. Ostenfeld, C. N. Svendsen, L. Mucke, M. H. Johnson, M. V. Sofroniew, *Neuron.* **1999**, *23*, 297.

[189] J. Silver, J. H. Miller, *Nat. Rev. Neurosci.* **2004**, *5*, 146.

[190] L. L. Jones, R. U. Margolis, M. H. Tuszynski, *Exp. Neurol.* **2003**, *182*, 399.

[191] X. Tang, J. E. Davies, S. J. Davies, *J. Neurosci. Res.* **2003**, *71*, 427.

[192] L. L. Jones, Y. Yamaguchi, W. B. Stallcup, M. H. Tuszynski, *J. Neurosci.* **2002**, *22*, 2792.

[193] R. J. McKeon, M. J. Jurynec, C. R. Buck, *J. Neurosci.* **1999**, *19*, 10778.

[194] E. J. Fry, M. J. Chagnon, R. Lopez-Vales, M. L. Tremblay, S. David, *Glia* **2010**, *58*, 423.

[195] Y. Shen, A. P. Tenney, S. A. Busch, K. P. Horn, F. X. Cuascut, K. Liu, Z. He, J. Silver, J. G. Flanagan, *Science* **2009**, *326*, 592.

[196] S. J. Davies, M. T. Fitch, S. P. Memberg, A. K. Hall, G. Raisman, J. Silver, *Nature* **1997**, *390*, 680.

[197] C. L. Dou, J. M. Levine, *J. Neurosci.* **1994**, *14*, 7616.

[198] R. J. McKeon, R. C. Schreiber, J. S. Rudge, J. Silver, *J. Neurosci.* **1991**, *11*, 3398.

[199] V. Gallo, A. Bertolotto, *Exp. Cell Res.* **1990**, *187*, 211.

[200] C. Gotting, J. Kuhn, R. Zahn, T. Brinkmann, K. Kleesiek, *J. Mol. Biol.* **2000**, *304*, 517.

[201] A. E. Kearns, S. C. Campbell, J. Westley, N. B. Schwartz, *Biochemistry* **1991**, *30*, 7477.

[202] W. M. McKillop, M. Dragan, A. Schedl, A. Brown, *Glia* **2013**, *61*, 164.

[203] P. Gris, A. Tighe, D. Levin, R. Sharma, A. Brown, *Glia* **2007**, *55*, 1145.

[204] P. Gris, S. Murphy, J. E. Jacob, I. Atkinson, A. Brown, *Mol Cell Neurosci* **2003**, *24*, 555.

[205] H. Sim, K. Rimmer, S. Kelly, L. M. Ludbrook, A. H. Clayton, V. R. Harley, *Mol. Endocrinol.* **2005**, *19*, 1884.

[206] A. Argentaro, H. Sim, S. Kelly, S. Preiss, A. Clayton, D. A. Jans, V. R. Harley, *J. Biol. Chem.* **2003**, *278*, 33839.

[207] V. R. Harley, R. Lovell-Badge, P. N. Goodfellow, P. J. Hextall, *FEBS Lett.* **1996**, *391*, 24.

[208] J. K. Forwood, V. Harley, D. A. Jans, *J. Biol. Chem.* **2001**, *276*, 46575.

[209] S. Preiss, A. Argentaro, A. Clayton, A. John, D. A. Jans, T. Ogata, T. Nagai, I. Barroso, A. J. Schafer, V. R. Harley, *J. Biol. Chem.* **2001**, *276*, 27864.

[210] J. A. Hanover, D. C. Love, W. A. Prinz, *J. Biol. Chem.* **2009**, *284*, 12593.

[211] H. Sim, A. Argentaro, D. P. Czech, S. Bagheri-Fam, A. H. Sinclair, P. Koopman, B. Boizet-Bonhoure, F. Poulat, V. R. Harley, *Endocrinology* **2011**, *152*, 2883.

[212] G. Kaur, A. Delluc-Clavieres, I. K. Poon, J. K. Forwood, D. J. Glover, D. A. Jans, *Biochem. J.* **2010**, *430*, 39.

[213] M. J. McFadden, M. S. Junop, J. D. Brennan, *Anal. Chem.* **2010**, *82*, 9850.

[214] M. Kataoka, J. F. Head, B. A. Seaton, D. M. Engelman, *PNAS* **1989**, *86*, 6944.

[215] M. Comte, Y. Maulet, J. A. Cox, *Biochem. J.* **1983**, *209*, 269.

[216] Y. Cheng, W. H. Prusoff, *Biochem. Pharmacol.* **1973**, *22*, 3099.

[217] A. R. Rhoads, F. Friedberg, *FASEB J* **1997**, *11*, 331.

[218] P. James, T. Vorherr, E. Carafoli, *Trends Biochem Sci* **1995**, *20*, 38.

[219] K. T. ONeil, W. F. DeGrado, *Trends Biochem. Sci.* **1990**, *15*, 59.

[220] A. Crivici, M. Ikura, *Annu Rev Biophys Biomol Struct* **1995**, *24*, 85.

[221] G. M. Clore, A. Bax, M. Ikura, A. M. Gronenborn, *Curr. Opin. Struc. Biol.* **1993**, *3*, 838.

[222] M. Ikura, G. M. Clore, A. M. Gronenborn, G. Zhu, C. B. Klee, A. Bax, *Science* **1992**, *256*, 632.

[223] W. E. Meador, A. R. Means, F. A. Quiocho, *Science* **1992**, *257*, 1251.

[224] J. D. Johnson, L. A. Wittenauer, *Biochem. J.* **1983**, *211*, 473.

[225] T. Tanaka, H. Hidaka, *J. Biol. Chem.* **1980**, *255*, 11078.

[226] A. Brown, S. G. Vascotto, (Ed.: W. I. P. Organization), Canada, **2011**, p. 53.

[227] B. Weiss, W. Prozialeck, M. Cimino, M. S. Barnette, T. L. Wallace, *Ann. N. Y. Acad. Sci.* **1980**, *356*, 319.

[228] R. M. Levin, B. Weiss, *J. Pharmacol. Exp. Ther.* **1979**, *208*, 454.

[229] D. G. Reid, L. K. MacLachlan, K. Gajjar, M. Voyle, R. J. King, P. J. England, *J Biol Chem* **1990**, *265*, 9744.

[230] H. Van Belle, *Cell Calcium* **1981**, *2*, 483.

[231] M. Vandonselaar, R. A. Hickie, J. W. Quail, L. T. Delbaere, *Nat Struct Biol* **1994**, *1*, 795.

[232] S. H. Seeholzer, M. Cohn, J. A. Putkey, A. R. Means, H. L. Crespi, *Proc Natl Acad Sci U S A* **1986**, *83*, 3634.

[233] D. R. Marshak, T. J. Lukas, D. M. Watterson, *Biochemistry* **1985**, *24*, 144.

[234] M. S. Barnette, R. Daly, B. Weiss, *Biochem Pharmacol* **1983**, *32*, 2929.

[235] Q. Ye, H. Wang, J. Zheng, Q. Wei, Z. Jia, *Proteins* **2008**, *73*, 19.

[236] Y. Zhang, H. Tan, Z. Jia, G. Chen, *J Mol Recognit* **2008**, *21*, 267.

[237] Q. Ye, X. Li, A. Wong, Q. Wei, Z. Jia, *Biochemistry* **2006**, *45*, 738.

[238] A. P. Yamniuk, H. J. Vogel, *Mol Biotechnol* **2004**, *27*, 33.

[239] K. P. Hoeflich, M. Ikura, *Cell* **2002**, *108*, 739.

[240] M. A. Schumacher, A. F. Rivard, H. P. Bachinger, J. P. Adelman, *Nature* **2001**, *410*, 1120.

[241] B. Elshorst, M. Hennig, H. Forsterling, A. Diener, M. Maurer, P. Schulte, H. Schwalbe, C. Griesinger, J. Krebs, H. Schmid, T. Vorherr, E. Carafoli, *Biochemistry* **1999**, *38*, 12320.

[242] M. Kataoka, J. F. Head, T. Vorherr, J. Krebs, E. Carafoli, *Biochemistry* **1991**, *30*, 6247.

[243] D. M. Schulz, C. Ihling, G. M. Clore, A. Sinz, *Biochemistry* **2004**, *43*, 4703.

[244] Y. Maulet, J. A. Cox, *Biochemistry* **1983**, *22*, 5680.

[245] R. M. Levin, B. Weiss, *Biochim Biophys Acta* **1978**, *540*, 197.

[246] R. M. Levin, B. Weiss, *Mol Pharmacol* **1977**, *13*, 690.

[247] T. C. Terwilliger, D. Eisenberg, *J. Biol. Chem.* **1982**, *257*, 6010.

[248] T. C. Terwilliger, D. Eisenberg, *J. Biol. Chem.* **1982**, *257*, 6016.

[249] J. F. Faucon, J. Dufourcq, C. Lussan, *FEBS Lett.* **1979**, *102*, 187.

[250] J. C. Talbot, J. Dufourcq, J. de Bony, J. F. Faucon, C. Lussan, *FEBS Lett.* **1979**, *102*, 191.

[251] E. Habermann, *Science* **1972**, *177*, 314.

[252] W. Wilcox, D. Eisenberg, *Protein Sci* **1992**, *1*, 641.

[253] S. C. Quay, C. C. Condie, *Biochemistry* **1983**, *22*, 695.

[254] A. Andersson, H. Biverstahl, J. Nordin, J. Danielsson, E. Lindahl, L. Maler, *Biochim Biophys Acta* **2007**, *1768*, 115.

[255] A. K. Ghosh, R. Rukmini, A. Chattopadhyay, *Biochemistry* **1997**, *36*, 14291.

[256] M. van Veen, G. N. Georgiou, A. F. Drake, R. J. Cherry, *Biochem J* **1995**, *305 (Pt 3)*, 785.

[257] A. Chattopadhyay, R. Rukmini, *FEBS Lett* **1993**, *335*, 341.

[258] R. F. Chen, *J. Res. Nat. Bur. Stand. Sec. A: Phys. Chem.* **1972**, *72A*, 593.

Chapter Four

Delineation of Key XRCC4/LigaseIV Interfaces for Targeted Disruption of Non-Homologous End Joining DNA Repair

The following chapter is currently in press in the journal *Proteins: Structure, Function, and Bioinformatics*, under the citation:

McFadden, M.J.; Lee, W.K.; Brennan, J.D.; Junop, M.S. **Delineation of Key XRCC4/LigaseIV Interfaces for Targeted Disruption of Non-Homologous End Joining DNA Repair**. *Proteins*, **2013**, doi: 10.1002/prot.24349.

I developed all experimental protocols, completed all data collection and analysis, and prepared the first draft of the manuscript. Wilson Lee provided me with the purified recombinant XRCC4 protein that was required for the project. Editorial input was given by Dr. Brennan and Dr. Junop to generate the final paper.

Chapter Four: Delineation of Key XRCC4/LigaseIV Interfaces for Targeted Disruption of Non-Homologous End Joining DNA Repair

4.1 Abstract

Efficient DNA repair mechanisms frequently limit the effectiveness of chemotherapeutic agents that act through DNA damaging mechanisms. Consequently, proteins involved in DNA repair have increasingly become attractive targets of high-throughput screening initiatives to identify modulators of these pathways. Disruption of the XRCC4-Ligase IV interaction provides a novel means to efficiently halt repair of mammalian DNA double strand break repair, however the extreme affinity of these proteins presents a major obstacle for drug discovery. A better understanding of the interaction surfaces is needed to provide a more specific target for inhibitor studies. To clearly define key interface(s) of Ligase IV necessary for interaction with XRCC4, we developed a competitive displacement assay using ESI-MS/MS and determined the minimal inhibitory fragment of the XRCC4-interacting region (XIR) capable of disrupting a complex of XRCC4/XIR. Disruption of a single helix (helix 2) within the helix-loop-helix clamp of Ligase IV was sufficient to displace XIR from a pre-formed complex. Dose-dependent response curves for the disruption of the complex by either helix 2 or helix-loop-helix fragments revealed that potency of inhibition was greater for the larger helix-loop-helix peptide. Our results suggest a susceptibility to inhibition at the interface of helix 2 and future studies would benefit from targeting this surface of Ligase IV to identify modulators that disrupt its interaction with XRCC4. Furthermore, helix 1 and loop regions of the helix-loop-helix clamp provide secondary target surfaces to

identify adjuvant compounds that could be used in combination to more efficiently inhibit XRCC4/Ligase IV complex formation and DNA repair.

4.2 Introduction

Anticancer treatments inflict severe genetic damage through radiation or chemotherapeutics to induce cell death, however the ability of tumour cells to repair damaged DNA greatly decreases the effectiveness of these agents. As a result, compounds that can modulate DNA repair pathways have become highly desirable for their potential to significantly increase the cytotoxicity of anticancer therapies.[259-266] Cancer cells are often reliant on a particular pathway of DNA repair and lack access to redundant pathways that are available to their healthy counterparts. This restriction to specific repair pathways presents a potential to exploit synthetic lethality that can selectively target cancer cells.[259, 260, 267, 268] Modulators of DNA repair therefore have dual value as powerful adjuvant compounds to enhance both the efficacy and specificity of current anticancer treatment strategies.

Clastogens, such as alkylating agents (ex. cisplatin) and inhibitors of DNA topoisomerase I or II, are known to induce double stranded breaks (DSB), a lethal form of DNA damage.[266] Repair of DSB can progress through either the homologous recombination (HR) or non-homologous end joining (NHEJ) pathways, depending on the phase of the cell cycle.[269] HR repair of DSB is an error-free process carried out by the Rad52 group of proteins, which have been targeted to enhance tumour sensitivity to anti-cancer agents.[270-273] HR requires a sister chromatid to be used as a template strand, thus

limiting it to late S and G_2 phases of the cell cycle. As a result, the predominant repair pathway of DSB in human cells is NHEJ that functions independent of a template strand or terminal sequence homology. The repair of DSB by way of NHEJ requires at least seven proteins, most notably the Ku heterodimer (Ku70 and Ku80) that recognizes and binds to broken ends, DNA-dependent protein kinase (DNA-PK), and the complex of x-ray cross-complementing protein 4/DNA ligase IV (XRCC4/LigIV), which carries out the final ligation step. Radiosensitization of cells has been achieved through inhibition of Ku expression[274, 275] and DNA binding[276], but the most common NHEJ target has been DNA-PK and several inhibitors of this enzyme have been shown to increase toxicity of chemotherapeutics.[277-283] XRCC4/LigIV has yet to be targeted for inhibition despite being an essential complex for DSB repair in NHEJ.

XRCC4 exhibits no enzymatic activity but is a necessary structural counterpart to LigIV[284], which is nearly undetectable in cells lacking XRCC4.[285] Disrupting the protein-protein interaction, rather than the protein-DNA interaction, to prevent ligation reduces the risk of identifying promiscuous antagonists that are often found when targeting the catalytic activity of human ligases.[286, 287] Of the two small molecule inhibitors of LigIV that have been identified, SCR7 also prevents ligation of nicked substrates by LigIII,[286] and compound L189 blocks DNA binding of all three human ligases[287]. The XRCC4-LigIV interaction provides an opportunity to selectively inhibit LigIV without interfering with ligation functions of LigI or LigIII. Overexpression of XRCC4[288] or LigIV[289] fragments *in vivo* has been shown to sensitize cells to ionizing radiation, validating the XRCC4-LigIV interaction as a target for the modulation of the NHEJ pathway. A major

problem for drug discovery is the identification of a compound (small molecule or biomolecule) capable of disrupting a pre-assembled high-affinity complex (K_D < 50 nM)[290] that can withstand denaturing conditions of over 1 M salt[291, 292] and 7 M urea[293]. Despite these challenges, such high affinity interactions appear to be desirable for development of potent small molecule modulators.[294] Having a better understanding of the key interaction surfaces between XRCC4 and LigIV would be of great value and would provide a more specific target for guided screens of compound libraries and for rational design of modulators to disrupt this very strong interaction.

Biochemical and crystallographic studies have shown XRCC4 and LigIV form a 2:1 complex and the interaction occurs entirely between the extended helical tails of the XRCC4 homodimer and the C-terminal region of LigIV located between two tandem BRCT (BRCA1 [breast cancer associated 1] C terminal) domains (Figure 4.1A).[289, 290, 293, 295] This inter-BRCT linker is referred to as the XRCC4-interacting region (XIR) of LigIV. The crystal structure of $XRCC4^{1-203}$ (amino acids 1-203) and the tandem BRCT domains of $LigIV^{654-911}$ shows that XIR interacts asymmetrically with the XRCC4 homodimer through two clearly defined interaction surfaces: 1) a β-hairpin motif (residues 759-770); and 2) a helix-loop-helix clamp (residues 771-804) (Figure 4.1B).[289] Deletion analysis[295] and immunoprecipitation experiments[289] further demonstrated that XIR is required for XRCC4 binding, thus disruption of the interface in this region should prevent the association of these two proteins. The XIR region from LigIV represents a significant amount of the total interaction surface between LigIV and XRCC4, thus

further delineation of the key interface(s) within this region is needed to provide a more limited target for inhibition studies.

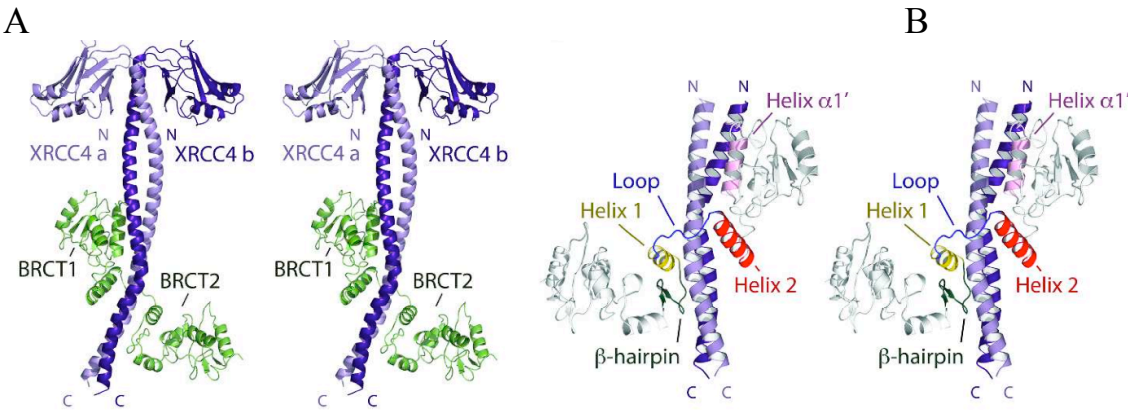

Figure 4.1: Structure of the human XRCC4/LigIV complex (PDB 3II6). A, Crystal structure of human XRCC4 homodimer (1-203) bound to the C-terminal tandem BRCT domains of Ligase IV (654-911); subunit A in light purple, subunit B in dark purple, Ligase IV interacting region in dark green with both BRCT1 and 2 labelled accordingly. B, Close-up view of the interaction of the XRCC4 homodimer (purple) and XIR region of Ligase IV; β-hairpin motif (dark green), helix 1 (yellow), loop region (blue), and helix 2 (red). Also indicated is helix α1' (pink) that is used as a negative control in competitive displacement assays.

In this study, we have used a competitive displacement assay based on electrospray ionization tandem mass spectrometry (ESI-MS/MS) to determine the minimal LigIV fragment capable of displacing XIR from a pre-formed complex with XRCC4. We identified the key interface within XIR that is sufficient to disrupt the XRCC4-XIR interaction, providing a narrow target surface for modulator design. Furthermore, we demonstrated that greater disruption of the XRCC4/XIR interaction is achieved when multiple interfaces within the helix-loop-helix clamp are targeted simultaneously.

4.3 Materials and Methods

Materials – Synthetic peptides corresponding to the C-terminal domain of LigIV –XIR and XIR with an N-terminal fluorescein label (D759 – S804), β-hairpin (D759 – D770), helix 1 (L771 – G780), loop (I781 – E790), helix 2 (E791 – Y803), helix-loop-helix (L771 – Y803), and helix α1' (G835 – H848) – were purchased at >95% purity from LifeTein (South Plainfield, NJ). HPLC grade water was obtained from Caledon Laboratory Chemicals (Georgetown, ON, Canada), and LC-MS grade acetic acid and HPLC grade methanol were purchased from Sigma-Aldrich (Oakville, ON, CA). All other reagents were of the highest available grade and used as received.

Expression and Purification of XRCC4 and Tandem BRCT Domains of LigIV – Expression and purification of full-length XRCC4 and the tandem BRCT domains of $LigIV^{654–911}$ were carried out as previously described.[290, 296]

Determination of the Dissociation Constant (K_D) for XRCC4/XIR – Binding reactions were prepared with XIR (10 nM) in 1% acetic acid in 1:1 (v/v) methanol/water in the presence of increasing amounts of XRCC4 (5 to 500 nM), or BSA as a control, and incubated at room temperature for 15 minutes. Samples were then analyzed by ESI-MS/MS using a Thermo Scientific LCQ Fleet 3D ion trap mass spectrometer fitted with a 10 μL sample loop. Using the online syringe pump, 0.5% acetic acid in 1:1 (v/v) acetonitrile/water was delivered at a flow rate of 15 μL/min as 10 μL injections were made of each sample and the total MS/MS signal for the fragmentation of 1329 m/z

(XIR, $[M+4H]^{4+}$) to 1683, 1576, 1303, and 1262 m/z product ions was monitored over time. The total integrated peak area of each sample injection was normalized by letting the peak area for the no-XRCC4 control represent 100% unbound XIR. A plot of % bound versus [XRCC4 (nM)] was fitted with a one-site ligand binding equation using SigmaPlot 12, and the K_D value was taken as the concentration of XRCC4 resulting in 50% bound XIR.

Competitive Displacement Assay – Samples containing XIR (50 nM) and XRCC4 (200 nM) in 1% acetic acid in 1:1 (v/v) methanol/water were incubated for 15 minutes at room temperature prior to addition of the XIR fragment (25 μM). Four XIR secondary structures – β-hairpin, helix 1, loop, and helix 2 – were screened as individual fragments and in combination, in addition to the tandem BRCT domains and helix α1' to function as positive and negative controls, respectively (Figure 4.1B). After incubating for 30 minutes, the amount of unbound XIR in each sample was determined by ESI-MS/MS as described above. The total integrated peak area for each sample was normalized by letting the peak area for the intact XRCC4/XIR control represent a relative signal of 1. Active XIR fragments were identified as those samples showing a minimum 1.5-fold increase in signal over that of the intact XRCC4/XIR control.

Dose-Dependent Response Curves – Dose-dependent response curves were developed for the displacement of XIR by either helix 2 or helix-loop-helix using the competitive displacement assay described above. Solutions containing XIR (50 nM) and XRCC4

(200 nM) were incubated for 15 minutes, before the addition of XIR fragment (helix 2, 1 nM to 500 μM; helix-loop-helix, 1 nM to 125 μM). Samples were incubated for 30 minutes, before ESI-MS/MS analysis was carried out as described above. The total integrated peak area for each sample was normalized by letting the peak area for the intact XRCC4/XIR control represent a relative signal of 1. A plot of relative signal versus log [Fragment (M)] was fitted with a 4-parameter Hill equation using SigmaPlot 12. The EC_{50} value was taken as the concentration of fragment that resulted in XIR displacement at a level midway between the maximum and minimum signal achieved.

Fluorescence Polarization Measurements – A single N-terminal fluorescein on XIR was probed at room temperature (20 ± 1 °C) on a Cary Eclipse Fluorescence Spectrophotometer in a 1-cm path length PMMA cuvette using excitation and emission wavelengths of 494 nm and 517 nm, respectively. The signal was integrated for 2 seconds with excitation and emission band pass widths of 5 nm. Polarization measurements of fluorescent XIR (100 nM in PBS buffer) were collected before and after the addition of XRCC4 (200 nM) or XRCC4 (200 nM) incubated with helix 2 (50 μM).

4.4 Results

Binding Affinity of the XRCC4-XIR Interaction – XRCC4 and XIR form a high affinity complex that is highly resistant to denaturing conditions thereby allowing direct analysis of protein complex formation by ESI-MS/MS. Using this approach the amount of free XIR was measured in the presence of increasing concentrations of XRCC4. The MS/MS

signal for free XIR decreased hyperbolically as the concentration of XRCC4 was increased, indicating a loss of free XIR from solution when XRCC4 is present (Figure 4.2A). In contrast, increasing the amount of a non-specific protein (BSA) had no significant effect (Figure 4.2A). These findings suggest that the reduction of free XIR observed in the presence of XRCC4 is due to a specific interaction and the formation of a complex of XRCC4/XIR. To quantify binding affinity, the MS/MS data was used to develop a plot of % bound XIR versus concentration of XRCC4. Binding data fit well with a single-site saturation model (Figure 4.2B), and the dissociation constant (K_D) for the interaction was determined to be 7.8 ± 4.2 nM. The observed K_D for the complex under these experimental conditions indicates a very strong interaction and is consistent with previous work showing XRCC4/XIR is extremely resistant to strong denaturing conditions.

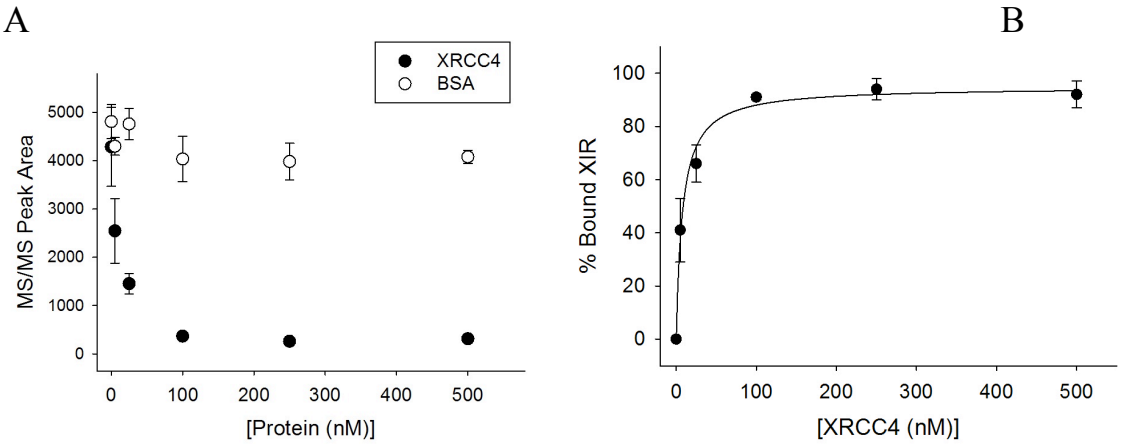

Figure 4.2: Binding study of XRCC4/XIR. A, Change in ESI-MS/MS signal for free XIR as a function of concentration of XRCC4 (l) or a non-specific protein, BSA (d). B, Saturation binding curve for the XRCC4/XIR interaction with an observed dissociation constant, K_D, of 7.8 ± 4.2 nM.

Competitive Displacement Assay to Identify Inhibitory XIR Fragments – The crystal structure of XRCC4 and the C-terminal BRCT domains of LigIV clearly shows a significant amount of interaction occurs along the entire XIR surface (Figure 4.1).[289] Although this region of LigIV is only 46 residues, it encompasses a large surface area (~2900 $Å^2$) making it difficult to target with a small molecule to disrupt its interaction with XRCC4. To more narrowly define the key interaction surface, we used a competitive displacement assay to screen XIR fragments for inhibitory activity against an intact complex of XRCC4/XIR. XIR fragments were selected based on secondary structure boundaries observed in the crystal structure. Each of these four fragments was shown to bind free XRCC4, as indicated by a loss of MS/MS signal for the peptide in the presence of one molar equivalent of XRCC4, but not of BSA (Supporting Information, Figure S4.1). Inhibitory activity of the fragments was then assessed by observing displacement of XIR from a pre-formed complex. Of the four fragments tested, only helix 2 (H2) showed activity, where the amount of unbound XIR was 2-times that of the intact XRCC4/XIR control (Figure 4.3, black bars). Furthermore, even when the non-active fragments were re-analyzed in combination, activity was only observed when H2 was present (Figure 4.3, grey bars). As well, the combination of H2 with any one of the inactive fragments did not alter the activity of H2. These results indicate that only the effect of blocking the region of helix 2 is severe enough on its own to interfere with the interaction of XIR and XRCC4.

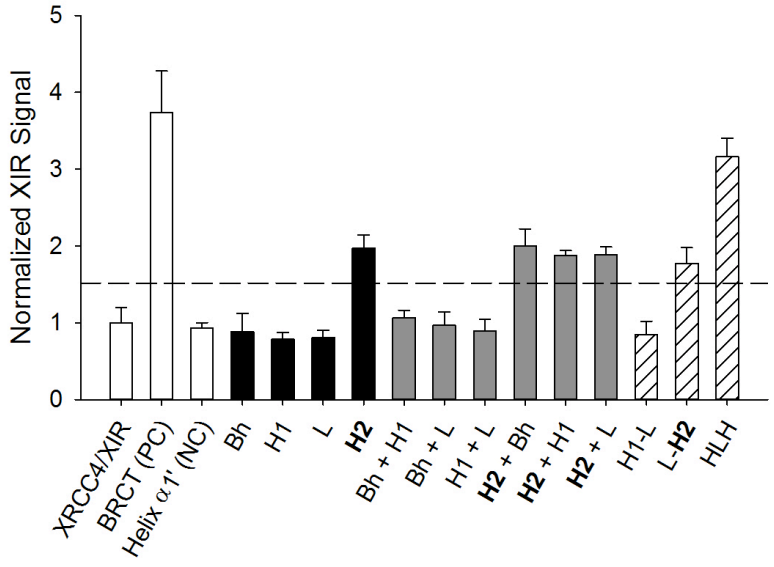

Figure 4.3: Competitive displacement assay to screen XIR fragments for displacement of XIR from a complex with XRCC4. Samples of XRCC4/XIR were incubated with the XIR fragments as indicated, and were analyzed by ESI-MS/MS to determine the amount of unbound XIR present. XIR fragments include the β-hairpin (Bh), helix 1 (H1), loop (L), helix 2 (H2), helix-loop-helix clamp (HLH), and the positive and negative controls, tandem BRCT domains and helix α1', respectively. The signal for each sample was normalized to that of the intact complex (XRCC4/XIR), and active fragments were identified as those showing a minimum 1.5-fold increase in signal. All active samples contained H2 (bold), with the greatest displacement of XIR observed for HLH.

Since helix 2 is present within XIR as part of an extended helix-loop-helix clamp, we also tested three larger fragments encompassing multiple secondary structures: helix 1-loop (H1-L), loop-helix 2 (L-H2), and helix 1-loop-helix 2 (HLH), in the same competitive displacement assay. No activity was observed for H1-L, and the data for L-H2 was similar to that for the discrete H2 fragment (Figure 4.3, lined bars). However, HLH showed increased displacement relative to all other fragments with a 3-fold increase in the amount of unbound XIR over that of the intact XRCC4/XIR control. Since no difference was observed between L-H2 and H2, this suggests that the enhanced activity

observed for HLH is not solely the result of increasing the size of the fragment. Considering earlier findings that combinations of H1 or L with H2 did not increase activity, the enhancement effect is likely due to disruption of both helix 1 and loop interfaces in addition to blocking helix 2. Although disruption of helix 2 appears sufficient to inhibit the interaction, XIR is more easily displaced from XRCC4 when all three interfaces of the helix-loop-helix clamp are targeted simultaneously.

Dose-Dependent Response Curves for H2 and HLH – To further assess the different inhibitory activities of H2 and HLH, we developed dose-dependent response curves for displacement of XIR from an intact complex with XRCC4 by each active fragment. Samples of XRCC4/XIR were incubated with increasing amounts of H2 or HLH, and the amount of unbound XIR in each solution was measured with ESI-MS/MS. Dose-dependent displacement of XIR from the XRCC4 complex was demonstrated by H2 (r^2 = 0.972, Hill slope = 1.95) and HLH (r^2 = 0.988, Hill slope = 3.28), with half-maximal effective concentrations (EC_{50}) of 56 ± 10 μM and 29 ± 3 μM, respectively (Figure 4.4). HLH is significantly more potent (p = 0.011), however the difference between maximum signal observed for H2 (max = 5.45 ± 0.68) and HLH (max = 6.53 ± 0.61) was not significant (p = 0.12). Our data suggest that blocking the helix 2 interface specifically inhibits the XRCC4-XIR interaction, and potency of this inhibitory effect can be improved by targeting additional surfaces in helix 1 and loop regions of XIR.

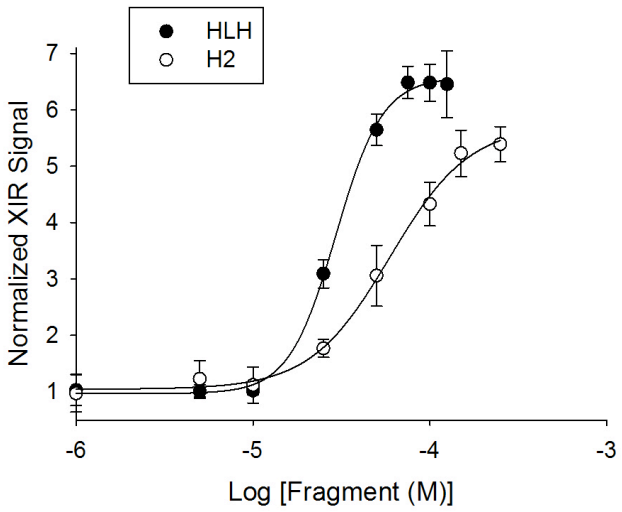

Figure 4.4: Dose-dependant displacement of XIR from XRCC4/XIR by fragment H2 (d) and HLH (l). H2 demonstrates specific inhibition of the XRCC4/XIR interaction (EC_{50} = 56 ± 10 μM), however greater potency and was observed for HLH (EC_{50} = 29 ± 3 μM).

Fluorescence Polarization – The ability of H2 to disrupt XRCC4/XIR was investigated using fluorescence polarization to allow the use of a more physiologically relevant buffer (i.e. PBS). The polarization of free fluorescein-labelled XIR (F-XIR) was 43.2 ± 0.7 mP and increased to 61.6 ± 1.2 mP upon the addition of XRCC4. Titration of XRCC4/F-XIR with H2 had no effect on the measured polarization, indicating that H2 was not able to displace F-XIR from a pre-formed complex with XRCC4. XRCC4 was also incubated with H2 before addition to F-XIR to assess the ability of H2 to interfere with formation of the complex. Under these conditions, a decreased polarization of 56.7 ± 1.1 mP was observed, suggesting a greater portion of F-XIR remains unbound. Although H2 is not sufficient to disrupt XRCC4/XIR, formation of the complex can be modulated if the surface of XRCC4 corresponding to the helix 2 interface is disrupted prior to its interaction with XIR.

4.5 Discussion

DNA repair proteins have become increasingly desirable targets to identify modulators of repair pathways that can be used as leads for anti-cancer therapeutics.[261-266] DNA double strand breaks represent the most cytotoxic form of DNA damage and are therefore one of the best sources of damage to induce tumor cell death. In humans, DNA double strand breaks are predominantly repaired through the NHEJ pathway. Essential to this pathway is the final ligation step carried out by the XRCC4-LigIV complex. Prior studies demonstrated that disruption of this complex using overexpression of interacting regions of either XRCC4 or LigIV was able to radiosensitize cells. Although this approach provides a way to efficiently and specifically prevent NHEJ DNA double strand break repair, small molecule modulators have not yet been identified. The extremely high-affinity of XRCC4 and LigIV[290-293] represents a major problem for drug design, thus a better understanding of the most susceptible target surfaces at the interface of these proteins would be of significant value. Previous studies of the XRCC4/LigIV complex have localized the interaction surface of LigIV to the XIR and have shown this region is required for the interaction of these two proteins.[289, 293, 295] To more narrowly define the key interface within XIR that is most vulnerable to a modulator, we developed a competitive displacement assay to determine the minimal fragment of XIR able to disrupt XRCC4/XIR complex.

Resistance of the interaction to strong chaotropic conditions, such as high salt[291, 292] or urea[293], has been previously documented, and our work revealed the XRCC4/XIR complex was also resistant to organic solvents. The extreme nature of the interaction

permitted sample preparation in MS-compatible solvents and direct analysis by ESI-MS/MS to determine the amount of free XIR present. Using this technique, we have demonstrated that XIR binds specifically to XRCC4 with a very high affinity reflected in the observed binding constant (K_D = 7.8 ± 4.2 nM). A K_D value in the low nanomolar range is not surprising given the large interaction surface that was observed between XRCC4 and XIR in crystal structures, and agrees with a previous estimate that the binding constant in solution is < 50 nM.[290] The low value observed for the K_D under harsh assay conditions suggests that the *in vivo* binding affinity would be significantly greater, possibly picomolar or femtomolar range.

The XIR region of LigIV is required for interaction with XRCC4[289, 295]. Further *in vivo* analysis involving expression of LigIV XIR regions suggests that disruption of the complex would be most effective within this region. To delineate the minimal portion of XIR mediating stable interaction between XRCC4 and LigIV we divided XIR into four smaller fragments that correspond to the β-hairpin motif and the helix 1, loop, and helix 2 of the C-terminal helix-loop-helix clamp (Figure 4.1B), and tested them for the ability to displace the intact complex. Previous studies have shown that small regions within XIR are sufficient for binding to XRCC4.[293, 295] In contrast, our approach determined the minimal region of XIR that is sufficient to modulate high-affinity XRCC4/XIR interaction. Ability to disrupt the XRCC4/XIR complex depends on formation of secondary structures within small peptides encompassing regions of XIR. It is unlikely that any of these peptides retain stable structure in the absence of XRCC4. A crystal structure, however, of XRCC4 bound to residues 748-784 of LigIV[293] (β-hairpin + helix

1) demonstrates that a shortened XIR peptide is able to retain proper folding in the presence of XRCC4. XRCC4 would therefore be expected to induce proper secondary structure of XIR fragments upon complex formation with XRCC4. Consistent with this interpretation, each of the four XIR fragment peptides was able to bind XRCC4 (Figure S4.1), suggesting the ability to adopt proper secondary structure in the presence of XRCC4. The data from our ESI-MS studies suggest that of the secondary structures present within XIR only helix 2 is sufficient to disrupt a preformed complex of XRCC4/XIR. This amphipathic helix makes extensive contacts (~800 $Å^2$) with hydrophobic surfaces on both tails of the XRCC4 homodimer and is important for the stable interaction of the larger helix-loop-helix clamp.[289] Although helix 1 and the loop portion of the clamp form hydrogen bonds with XRCC4, the loss of these interactions is not sufficient to displace XIR from the complex. In contrast, blocking the interface of helix 2 has a detrimental effect on the complex and consequently XIR is not able to maintain its interaction with XRCC4. Once the helix 2 interface of XIR has been disrupted, further loss of interaction may be achieved by also targeting helix 1 and loop surfaces simultaneously.

Further studies of the H2 peptide were carried out using fluorescence polarization to allow the use of non-volatile buffers that better represent physiological conditions. The H2 peptide failed to displace XIR from a complex with XRCC4, however our data show that the degree of interaction can be reduced if the XRCC4 interface is disrupted in this region prior to complex formation. The approach taken for the MS-based assays was directed toward identifying minimal XIR regions sufficient to disrupt preformed

XRCC4/LigIV complex; however, the ability to interfere with complex formation is also of value. Although prior *in vivo* studies clearly demonstrated that intact XIR region is able to radiosensitize cells,[289] it was not established if this was due to disruption or prevention of XRCC4/LigIV complex interaction. Efficacy *in vivo* of inhibitory peptides is expected to be dependent on the ability to both prevent and disrupt protein-protein interactions as XRCC4 is an abundant protein that exists in both LigIV-bound and unbound states. Our findings clearly identify helix 2 as a key interface for the XRCC4/LigIV interaction, and the data strongly suggest that future inhibition studies should focus on this defined surface.

Results of this study provide a more detailed understanding of key regions mediating high-affinity XRCC4/LigIV association. This knowledge will be particularly important to help guide future screens of compound libraries to more efficiently identify modulators of the XRCC4/LigIV interaction. Small molecule modulators or biomolecules capable of disrupting XRCC4/LigIV would prevent DNA double strand break repair and have the potential to be developed into powerful, novel anti-cancer therapeutics. In addition, this work has identified secondary target surfaces able to augment potency of disruption by helix 2. This knowledge could be further exploited to identify adjuvant compounds able to increase the effectiveness of helix 2 disrupting modulators. The implication of this possibility is that combination drug therapy could disrupt NHEJ DNA repair more effectively, and therefore maximize the value of these compounds as anti-cancer agents. Given the high-affinity of XRCC4/LigIV, disruption of this interaction using a small molecule modulator may not be feasible. To further validate key interaction

surfaces identified here, future *in vivo* studies will need to be conducted focusing on assessing competitive displacement of LigIV from XRCC4 by XIR fragments.[289]

4.6 Acknowledgement

This work was supported by operating grants: Canadian Institutes of Health Research to MSJ (MOP 89903), Natural Sciences and Engineering Research Council of Canada to JDB. MJM was supported in part by an Ontario Graduate Student Fellowship. JDB holds a Canada Research Chair in Bioanalytical Chemistry and Biointerfaces.

4.7 References

259. Furgason JM, Bahassi el M. Targeting DNA repair mechanisms in cancer. Pharmacol Ther 2013;137(3):298-308.

260. Curtin NJ. DNA repair dysregulation from cancer driver to therapeutic target. Nat Rev Cancer 2012;12(12):801-817.

261. Frosina G. DNA repair and resistance of gliomas to chemotherapy and radiotherapy. Mol Cancer Res 2009;7(7):989-999.

262. Zhu Y, Hu J, Hu Y, Liu W. Targeting DNA repair pathways: a novel approach to reduce cancer therapeutic resistance. Cancer Treat Rev 2009;35(7):590-596.

263. Helleday T, Petermann E, Lundin C, Hodgson B, Sharma RA. DNA repair pathways as targets for cancer therapy. Nat Rev Cancer 2008;8(3):193-204.

264. Madhusudan S, Hickson ID. DNA repair inhibition: a selective tumour targeting strategy. Trends Mol Med 2005;11(11):503-511.

265. Madhusudan S, Middleton MR. The emerging role of DNA repair proteins as predictive, prognostic and therapeutic targets in cancer. Cancer Treat Rev 2005;31(8):603-617.

266. Fojo T. Cancer, DNA Repair Mechanisms, and Resistance to Chemotherapy. J Natl Cancer Inst 2001;93(19):1434-1436.

267. Basu B, Yap TA, Molife LR, de Bono JS. Targeting the DNA damage response in oncology: past, present and future perspectives. Curr Opin Oncol 2012;24(3):316-324.

268. Shaheen M, Allen C, Nickoloff JA, Hromas R. Synthetic lethality: exploiting the addiction of cancer to DNA repair. Blood 2011;117(23):6074-6082.

269. Takata M, Sasaki MS, Sonoda E, Morrison C, Hashimoto M, Utsumi H, Yamaguchi-Iwai Y, Shinohara A, Takeda S. Homologous recombination and non-homologous end-joining pathways of DNA double-strand break repair have overlapping roles in the maintenance of chromosomal integrity in vertebrate cells. EMBO J 1998;17(18):5497-5508.

270. Arnbrosini G, Seehnan SL, Qin L, Schwartz GK. The cyclin-dependent kinase inhibitor flavopiridol potentiates the effects of topoisomerase I poisons by suppressing rad51 expression in a p53-dependent manner. Cancer Res 2008;68(7):2312-2320.

271. Yu D, Sekine E, Fujimori A, Ochiya T, Okayasu R. Down regulation of BRCA2 causes radio-sensitization of human tumor cells in vitro and in vivo. Cancer Sci 2008;99(4):810-815.

272. Bristow RG, Ozcelik H, Jalali F, Chan N, Vesprini D. Homologous recombination and prostate cancer: a model for novel DNA repair targets and therapies. Radiother Oncol 2007;83(3):220-230.

273. Hansen LT, Lundin C, Spang-Thomsen M, Petersen LN, Helleday T. The role of RAD51 in etoposide (VP16) resistance in small cell lung cancer. Int J Cancer 2003;105(4):472-479.

274. Vandersickel V, Mancini M, Slabbert J, Marras E, Thierens H, Perletti G, Vral A. The radiosensitizing effect of Ku70/80 knockdown in MCF10A cells irradiated with X-rays and p(66)+Be(40) neutrons. Radiat Oncol 2010;5:30.

275. Ayene IS, Ford LP, Koch CJ. Ku protein targeting by Ku70 small interfering RNA enhances human cancer cell response to topoisomerase II inhibitor and gamma radiation. Mol Cancer Ther 2005;4(4):529-536.

276. Castore R, Hughes C, Debeaux A, Sun J, Zeng C, Wang SY, Tatchell K, Shi R, Lee KJ, Chen DJ, Harrison L. Mycobacterium tuberculosis Ku can bind to nuclear DNA damage and sensitize mammalian cells to bleomycin sulfate. Mutagenesis 2011;26(6):795-803.

277. Munck JM, Batey MA, Zhao Y, Jenkins H, Richardson CJ, Cano C, Tavecchio M, Barbeau J, Bardos J, Cornell L, Griffin RJ, Menear K, Slade A, Thommes P, Martin NM, Newell DR, Smith GC, Curtin NJ. Chemosensitization of cancer cells by KU-0060648, a dual inhibitor of DNA-PK and PI-3K. Mol Cancer Ther 2012;11(8):1789-1798.

278. Zhao Y, Thomas HD, Batey MA, Cowell IG, Richardson CJ, Griffin RJ, Calvert AH, Newell DR, Smith GC, Curtin NJ. Preclinical evaluation of a potent novel DNA-dependent protein kinase inhibitor NU7441. Cancer Res 2006;66(10):5354-5362.

279. Hardcastle IR, Cockcroft X, Curtin NJ, El-Murr MD, Leahy JJ, Stockley M, Golding BT, Rigoreau L, Richardson C, Smith GC, Griffin RJ. Discovery of potent chromen-4-one inhibitors of the DNA-dependent protein kinase (DNA-PK) using a small-molecule library approach. J Med Chem 2005;48(24):7829-7846.

280. Shinohara ET, Geng L, Tan J, Chen H, Shir Y, Edwards E, Halbrook J, Kesicki EA, Kashishian A, Hallahan DE. DNA-dependent protein kinase is a molecular target for the development of noncytotoxic radiation-sensitizing drugs. Cancer Res 2005;65(12):4987-4992.

281. Ismail IH, Martensson S, Moshinsky D, Rice A, Tang C, Howlett A, McMahon G, Hammarsten O. SU11752 inhibits the DNA-dependent protein kinase and DNA double-strand break repair resulting in ionizing radiation sensitization. Oncogene 2004;23(4):873-882.

282. Willmore E, de Caux S, Sunter NJ, Tilby MJ, Jackson GH, Austin CA, Durkacz BW. A novel DNA-dependent protein kinase inhibitor, NU7026, potentiates the cytotoxicity of topoisomerase II poisons used in the treatment of leukemia. Blood 2004;103(12):4659-4665.

283. Kashishian A, Douangpanya H, Clark D, Schlachter ST, Eary CT, Schiro JG, Huang HM, Burgess LE, Kesicki EA, Halbrook J. DNA-dependent protein kinase

inhibitors as drug candidates for the treatment of cancer. Mol Cancer Ther 2003;2(12):1257-1264.

284. Grawunder U, Zimmer D, Kulesza P, Lieber MR. Requirement for an interaction of XRCC4 with DNA ligase IV for wild-type V(D)J recombination and DNA double-strand break repair in vivo. J Biol Chem 1998;273(38):24708-24714.

285. Bryans M, Valenzano MC, Stamato TD. Absence of DNA ligase IV protein in XR-1 cells: evidence for stabilization by XRCC4. Mutation Res 1999;433(1):53-58.

286. Srivastava M, Nambiar M, Sharma S, Karki SS, Goldsmith G, Hegde M, Kumar S, Pandey M, Singh RK, Ray P, Natarajan R, Kelkar M, De A, Choudhary B, Raghavan SC. An inhibitor of nonhomologous end-joining abrogates double-strand break repair and impedes cancer progression. Cell 2012;151(7):1474-1487.

287. Chen X, Zhong SJ, Zhu Y, Dziegielewska B, Ellenberger T, Wilson GM, MacKerell AD, Tomkinson AE. Rational design of human DNA ligase inhibitors that target cellular DNA replication and repair. Cancer Res 2008;68(9):3169-3177.

288. Jones KR, Gewirtz DA, Yannone SM, Zhou S, Schatz DG, Valerie K, Povirk LF. Radiosensitization of MDA-MB-231 breast tumor cells by adenovirus-mediated overexpression of a fragment of the XRCC4 protein. Mol Cancer Ther 2005;4(10):1541-1547.

289. Wu PY, Frit P, Meesala S, Dauvillier S, Modesti M, Andres SN, Huang Y, Sekiguchi J, Calsou P, Salles B, Junop MS. Structural and Functional Interaction

between the Human DNA Repair Proteins DNA Ligase IV and XRCC4. Mol Cell Biol 2009;29(11):3163-3172.

290. Modesti M, Junop MS, Ghirlando R, van de Rakt M, Gellert M, Yang W, Kanaar R. Tetramerization and DNA ligase IV interaction of the DNA double-strand break repair protein XRCC4 are mutually exclusive. J Mol Biol 2003;334(2):215-228.

291. Critchlow SE, Bowater RP, Jackson SP. Mammalian DNA double-strand break repair protein XRCC4 interacts with DNA ligase IV. Curr Biol 1997;7(8):588-598.

292. Grawunder U, Wilm M, Wu XT, Kulesza P, Wilson TE, Mann M, Lieber MR. Activity of DNA ligase IV stimulated by complex formation with XRCC4 protein in mammalian cells. Nature 1997;388(6641):492-495.

293. Sibanda BL, Critchlow SE, Begun J, Pei XY, Jackson SP, Blundell TL, Pellegrini L. Crystal structure of an Xrcc4-DNA ligase IV complex. Nat Struct Biol 2001;8(12):1015-1019.

294. Smith MC, Gestwicki JE. Features of protein-protein interactions that translate into potent inhibitors: topology, surface area and affinity. Expert Rev Mol Med 2012;14:e16.

295. Grawunder U, Zimmer D, Lieber MR. DNA ligase IV binds to XRCC4 via a motif located between rather than within its BRCT domains. Curr Biol 1998;8(15):873-876.

296. Modesti M, Hesse JE, Gellert M. DNA binding of Xrcc4 protein is associated with V(D)J recombination but not with stimulation of DNA ligase IV activity. Embo J 1999;18(7):2008-2018.

4.8 Appendix

Supporting Information – Materials and Methods

Samples were prepared containing XIR fragment (100 nM) in 1% acetic acid in 1:1 (v/v) methanol/water in the presence of XRCC4 (100 nM), or BSA (100 nM) as a control, and incubated at room temperature for 15 minutes. A control peptide, melittin (Mel) was also used as a control. Samples were then analyzed by ESI-MS/MS and the total signal for each fragment (Bh, $[M+H]^{1+}$: 1413 m/z to 1404, 1346, 1296, and 1172 m/z; H1, $[M+2H]^{2+}$: 586 m/z to 972, 825, and 559 m/z; L, $[M+2H]^{2+}$: 580 m/z to 915, 814, 571, and 245 m/z; H2, $[M+2H]^{2+}$: 788 m/z to 697 and 688 m/z; Mel, $[M+4H]^{4+}$: 713 m/z to 893.5, 813, and 542 m/z) was monitored over time. The total integrated peak area of each sample injection was normalized by letting the peak area for the peptide in the absence of protein represent 100% MS/MS signal.

Supporting Information – Results

To determine if the small peptides corresponding to the secondary structures of XIR could bind to free XRCC4, the MS/MS signal for the free peptide was measured in the presence and absence of XRCC4 and a control protein, BSA. The signal for each of the four XIR fragments decreases significantly upon the addition of one molar equivalent

of XRCC4, but not of BSA (Figure S4.1). All four XIR fragments appear to bind XRCC4, indicated by 62%, 84%, 78%, and 88% loss of MS/MS signal for Bh, H1, L, and H2, respectively. In contrast, the presence of a non-binding protein, BSA, resulted in a maximum loss of signal of 30% for any of the XIR fragments. Furthermore, the signal for the Mel control peptide was not significantly affected by either protein, suggesting that the observed loss of signal for the XIR fragments in the presence of XRCC4 is not due to interferences in peptide ionization. Although conclusions cannot be made regarding the folding of each peptide into secondary structures, these findings suggest the XIR peptides retain the ability to form specific interactions with free XRCC4.

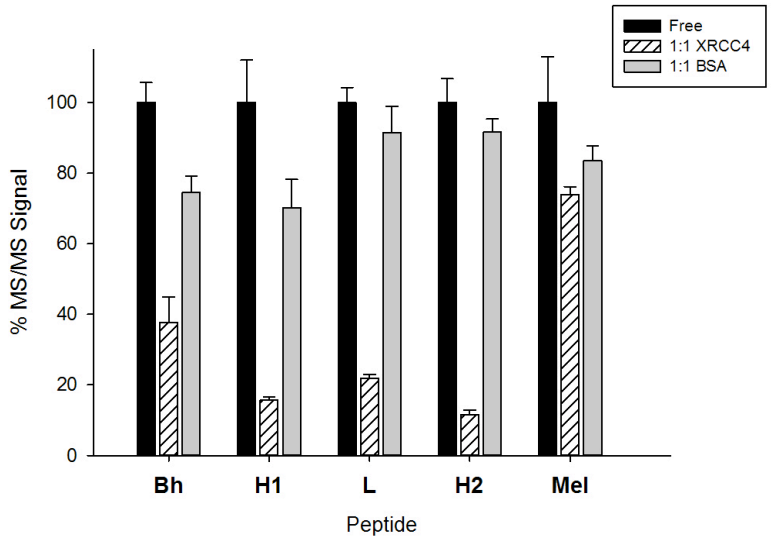

Figure S4.1: Binding study of XIR fragments. Relative MS/MS signal for XIR fragments, β-hairpin (Bh), helix 1 (H1), loop (L), helix 2 (H2), and a control peptide melittin (Mel), measured in the presence of one molar equivalent of XRCC4 or a non-binding protein, BSA. The signal for each sample was normalized by letting a control sample of peptide in the absence of protein represent 100% MS/MS signal.

Chapter Five: Conclusions and Future Outlook

5.1 Thesis Summary

The research presented in this thesis is intended to address a need for functional assays of PPI, which would bring the field of drug discovery closer to fully exploiting these interactions as therapeutic targets.[297-303] There are a number of challenges to identifying small molecule modulators of PPI, but a lack of appropriate screening approaches is one of the most significant obstacles in the search for these elusive compounds.[297-301] A review of current approaches to identify PPI modulators (Table 1.1) reveals a number of advantages and limitations to these methods that can help guide the development of novel assays, including a need for rapid, sensitive, and label-free detection, in addition to a desire to incorporate analytical separation for the purpose of mixture deconvolution in HTS applications. All of these characteristics can be found in MS-based strategies for affinity-based screening of protein-ligand interactions,[304, 305] however there are still two key areas for improvement. The discovery of compounds that modulate an interaction is profoundly more difficult than the identification of those that simply bind to the large surface area of an interface, thus functional assays have increased value over affinity-based approaches. Furthermore, MS detection typically requires sample enrichment to remove bioassay components that can interfere with the ionization of analytes, and regardless of the method of separation used for mixture deconvolution, most of these affinity-based assays rely on LC/MS for automated analyses. Chromatography steps are time-consuming and rely on continuous solvent flow, and incorporation of magnetic separation in place of LC provides an efficient method for

both mixture screening and sample enrichment. This collective work expands the use of MS from affinity-based to function-based assays, and develops two novel approaches to monitor biomolecular interactions. A magnetic "fishing" assay and an MS-based competitive displacement assay are presented as efficient and versatile tools to assist in the difficult process of identifying modulators of PPI.

In chapter two, magnetic separation is combined with MS into a novel magnetic "fishing" assay to monitor the formation of protein complexes in solution. The efficient design is capable of both qualitative and quantitative assessment of PPI and their disruption by small molecule modulators. For drug discovery applications, the value of an HTS platform significantly increases with greater throughput, and the ability of magnetic fishing to functionally screen small molecule mixtures and provide simultaneous mixture deconvolution is a valuable achievement. The validation process involving a screen of 1000 bioactive compounds also identified a novel antagonist of CaM/Mel, methylbenzethonium, which may prove useful in modulating other more relevant CaM-based interactions.

The work presented in chapter three extends to use of the magnetic "fishing" assay to study the nature of the interaction between CaM and transcription factor SOX9. Given the structural similarities of the CaM-binding domain of SOX9 (SOX-CAL) and Mel, which was a model protein for assay development, magnetic fishing is an efficient approach to characterize this interaction and its modulation by CaM antagonists. In addition to determining a binding constant for the high-affinity interaction of CaM/SOX-CAL, magnetic fishing also identified the formation of a low-affinity CaM/SOX-CAL

complex. Although further investigation is required to validate the novel low-affinity site *in vivo*, this discovery has potential to be a missing piece of information for understanding CaM-mediated nuclear import of SOX9. The versatility of the magnetic "fishing" assay is clearly demonstrated in this chapter, however it also emphasizes that the type of information available by this method is highly dependent on the identity of the "bait" protein and the setup of the assay.

Chapter four moves away from the magnetic fishing assay, and introduces an MS-based competitive displacement assay that addresses an important concern when targeting large flat protein interfaces with small molecules. Knowledge regarding the location of vulnerable 'hot-spots'[306, 307] within a large flat interface is extremely valuable for targeted inhibitor design and directing HTS, and this simple assay identifies minimal inhibitory fragments of a protein as indicators of these small regions that are more prone to disruption. The technique is applied to the high-affinity complex of XRCC4/LigIV, and identifies a short helix capable of disrupting this unusually strong interaction. Although the unique resistance of XRCC4/LigIV to denaturing conditions allows the assay to be carried out directly in MS-compatible solvents, the approach can easily be adapted for use with volatile buffers to extend the method to other anti-cancer targets, such as XRCC4/XRCC4-like factor (XRCC4/XLF).[308-313]

Less than a percent of the human interactome has been targeted with small molecule modulators,[300, 314] and a deficiency in appropriate technologies to probe PPI is a significant limiting factor. This thesis takes a considerable step towards overcoming this obstacle, and its achievements contribute in a number of ways to the study of PPI.

Chapter two presents the first MB-based high-throughput approach to identify small molecule modulators of PPI, and chapter three adapts this same assay platform to conduct the first quantitative *in vitro* study of CaM/SOX9 and its modulation by known CaM antagonists. The work in chapter four is the first inhibition study of XRCC4/LigIV, and through the design of a simple MS-based approach, has delineated the key interface of this interaction to facilitate future inhibitor screening to identify small molecules as potential anti-cancer agents. The functional mass spectrometric assays developed herein will assist in characterizing novel complexes, defining optimal target surfaces, and performing HTS of compound libraries to identify modulators as leads for pharmaceuticals. These MS-based approaches are highly adaptable and this body of work will ideally lead to similar discoveries for many other important PPI.

5.2 Future Outlook

The conclusion of this thesis marks the starting point for exciting future endeavors using MB and MS to study modulation of PPI and other biomolecular interactions. From a methods perspective, the magnetic "fishing" assay requires further optimization to reach its full potential. An obvious and desirable enhancement would be automation of the screening platform, and integration of robotic handling systems would greatly increase throughput and labour efficiency. In addition to convenience, automation may also help with the issue of nonspecific binding. The incorporation of magnetic liquid handlers would improve the ease and complexity of wash steps, allowing multiple buffers and temperature gradients to be used to help remove nonspecific contaminants. MS can

monitor multiple targets simultaneously, therefore multiplexed magnetic fishing with two or more bait proteins should also be investigated. To broaden the scope of the assay, magnetic beads are available with a variety of surface modifications to accommodate many different protein affinity tags. A valuable improvement in detection would be the use of alternative mass spectrometers, such as time-of-flight (TOF) or Orbitrap systems, which can offer enhanced sensitivity and wider mass ranges to study complexes of varying size and affinity. With a theoretically unlimited mass range, TOF-MS would permit assays of full-length proteins, and eliminate the need to use truncations for the secondary target in both the magnetic "fishing" and competitive displacement assays. Automation and multiplexing will also benefit the competitive displacement assay, along with the use of volatile buffers that better mimic physiological conditions. Although more extensive optimization of both assays is needed to maximize their utility, they are clear demonstrations of the many advantages of MS for functional studies of PPI, and will hopefully inspire other powerful strategies based on this technology.

A major advantage of magnetic separation is the ability to isolate targets directly from complex matrices, thus magnetic fishing has potential to be applied for screening natural products for modulators of PPI. MB can be added directly to viscous plant extracts and impure cell lysates containing solid particulates, and provides sample enrichment that could allow detection of dilute low-affinity ligands from what is inevitably a varied mixture of biomolecules. Natural products remain consistent but difficult sources of bioactive compounds for drug discovery,[315-318] and magnetic fishing

combined with MS detection is inherently well suited for assays of these extremely complex mixtures.

In addition to PPI, biomolecular interactions involving nucleic acids are involved in many important biological pathways, and a natural extension of magnetic fishing will be to study protein complexes with deoxyribonucleic acid (DNA) and ribonucleic acid (RNA). Small molecule modulation of complexes that regulate DNA transcription, replication, and repair is a promising strategy for the treatment of cancer and many other diseases,[319-322] but recently, some of the most attractive nucleic acid interactions are artificial. Aptamers are synthetic strands of DNA or RNA that selectively bind a protein or small molecule target, and have gained popularity as molecular recognition elements for innovative clinical, bioanalytical, and biosensor applications.[323-327] Like proteins and small molecules, highly charged nucleic acids are also ideal analytes for MS, thus magnetic aptamer fishing has potential to be a convenient approach for target identification, and a way to provide signal enhancement through concentration of dilute ligands from biological samples.

The work within this thesis is a starting point for function-based magnetic fishing assays to probe the diverse biomolecular interactions that occur in a living cell. Although PPI were the focus of assay development, the simplicity and versatility of magnetic fishing creates numerous possibilities to target protein, nucleic acid, and ligand interactions relevant for the field of drug discovery, diagnostic testing, and fundamental biochemical studies.

5.3 References

297. Makley, L.; Gestwicki, J., *Chem. Biol. Drug Des.* **2013,** *81* (1), 22-32.

298. Mullard, A., *Nat. Rev. Drug Discov.* **2012,** *11* (3), 173-175.

299. Smith, M.; Gestwicki, J., *Expert Rev. Mol. Med.* **2012,** *14*, e16.

300. Thompson, A.; Dugan, A.; Gestwicki, J.; Mapp, A., *ACS Chem. Biol.* **2012,** *7* (8), 1311-20.

301. White, A.; Westwell, A.; Brahemi, G., *Expert Rev. Mol. Med.* **2008,** *10*, e8.

302. Wells, J.; McClendon, C., *Nature* **2007,** *450* (7172), 1001-9.

303. Arkin, M.; Wells, J., *Nat. Rev. Drug Discov.* **2004,** *3* (4), 301-17.

304. Jonker, N.; Kool, J.; Irth, H.; Niessen, W., *Anal. Bioanal. Chem.* **2011,** *399* (8), 2669-81.

305. Annis, D. A.; Nickbarg, E.; Yang, X.; Ziebell, M.; Whitehurst, C., *Curr. Opin. Chem. Biol.* **2007,** *11* (5), 518-26.

306. DeLano, W., *Curr. Opin. Struct. Biol.* **2002,** *12* (1), 14-20.

307. Bogan, A. A.; Thorn, K., *J. Mol. Biol.* **1998,** *280* (1), 1-9.

308. Andres, S. N.; Vergnes, A.; Ristic, D.; Wyman, C.; Modesti, M.; Junop, M., *Nucleic Acids Res.* **2012,** *40* (4), 1868-78.

309. Roy, S.; Andres, S. N.; Vergnes, A.; Neal, J. A.; Xu, Y.; Yu, Y.; Lees-Miller, S. P.; Junop, M.; Modesti, M.; Meek, K., *Nucleic Acids Res.* **2012,** *40* (4), 1684-94.

310. Andres, S. N.; Junop, M. S., *Acta Crystallogr. Sect. F Struct. Biol. Cryst. Commun.* **2011,** *67* (Pt 11), 1399-402.

311. Hammel, M.; Rey, M.; Yu, Y.; Mani, R. S.; Classen, S.; Liu, M.; Pique, M. E.; Fang, S.; Mahaney, B. L.; Weinfeld, M.; Schriemer, D. C.; Lees-Miller, S. P.; Tainer, J. A., *J. Biol. Chem.* **2011,** *286* (37), 32638-50.

312. Andres, S. N.; Modesti, M.; Tsai, C. J.; Chu, G.; Junop, M. S., *Mol. Cell* **2007,** *28* (6), 1093-101.

313. Ahnesorg, P.; Smith, P.; Jackson, S. P., *Cell* **2006,** *124* (2), 301-13.

314. Stumpf, M. P.; Thorne, T.; de Silva, E.; Stewart, R.; An, H.; Lappe, M.; Wiuf, C., *PNAS* **2008,** *105* (19), 6959-64.

315. Kirst, H. A., *Expert Opin. Drug Discov.* **2013,** *8* (5), 479-93.

316. Lewis, K., *Nat. Rev. Drug Discov.* **2013,** *12* (5), 371-87.

317. Harvey, A. L.; Clark, R. L.; Mackay, S. P.; Johnston, B. F., *Expert Opin. Drug Discov.* **2010,** *5* (6), 559-68.

318. Li, J. W.; Vederas, J. C., *Science* **2009,** *325* (5937), 161-5.

319. Leung, C. H.; Chan, D.; Ma, V. P.; Ma, D. L., *Med. Res. Rev.* **2013,** *33* (4), 823-46.

320. Curtin, N., *Nat. Rev. Cancer* **2012,** *12* (12), 801-817.

321. Darnell, J. E., *Nat. Rev. Cancer* **2002,** *2* (10), 740-9.

322. Hurley, L., *Nat. Rev. Cancer* **2002,** *2* (3), 188-200.

323. Janssen, K. P.; Knez, K.; Spasic, D.; Lammertyn, J., *Sensors* **2013,** *13* (1), 1353-84.

324. Song, K. M.; Lee, S.; Ban, C., *Sensors* **2012,** *12* (1), 612-31.

325. Wang, T.; Ray, J., *Protein Cell* **2012,** *3* (10), 739-54.

326. Iliuk, A. B.; Hu, L.; Tao, W. A., *Anal. Chem.* **2011,** *83* (12), 4440-52.

327. Strehlitz, B.; Nikolaus, N.; Stoltenburg, R., *Sensors* **2008,** *8*, 4296-4307.